同濟大學
TONGJI UNIVERSITY

Achievements of TMEP

Jun Xu

Content

1. Introduction of nuclear EOS and transport approaches
2. Representative studies on constraining EOS with HICs
3. Transport Model Evaluation Project (TMEP)

Intermediate-energy heavy-ion collisions

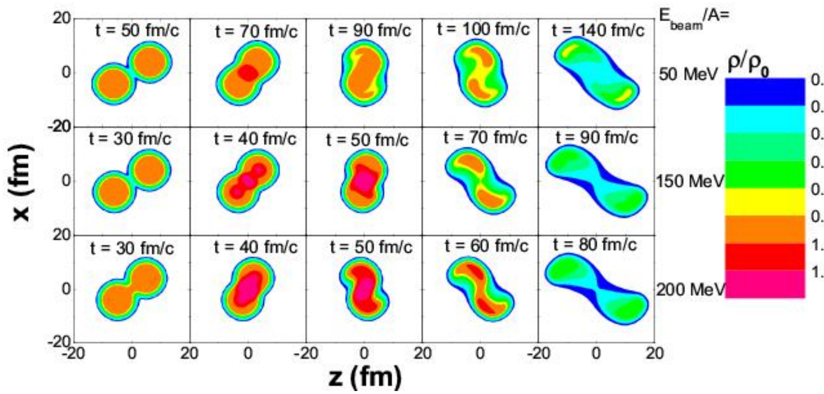

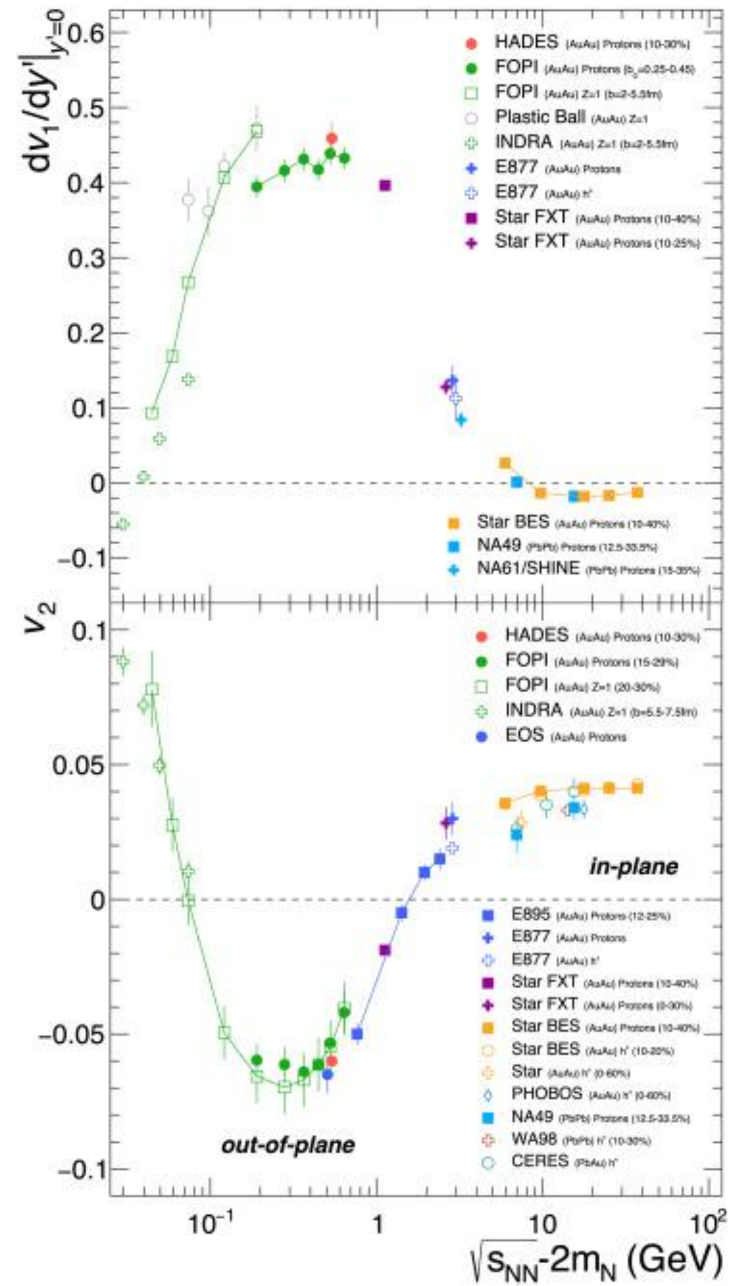

Energy regime: 50 A MeV ~ 2 A GeV
Maximum density reached: 1.2~3 ρ_0
Produced particles: pions, kaons, hyperons, Δ

dynamics dominated by
nucleon degree of freedom

Relevant experiments:

China	HIRFL/IMP, HIAF/IMP
USA	FRIB/MSU, STAR-FXT/BNL
Germany	SIS/GSI, FAIR/GSI
Russian	NICA/Dubna
Japan	RIBF/RIKEN
Korea	ROAN/IBS

Modified cartoons from Hermann Wolter

Nuclear EOS, E_{sym}

How reliable?

Heavy-ion experiments

Mean-field potential

Transport simulations

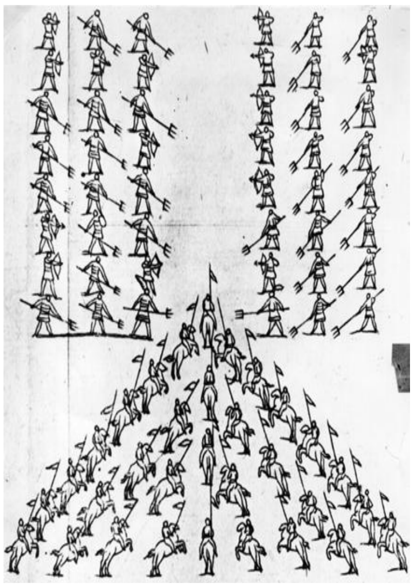

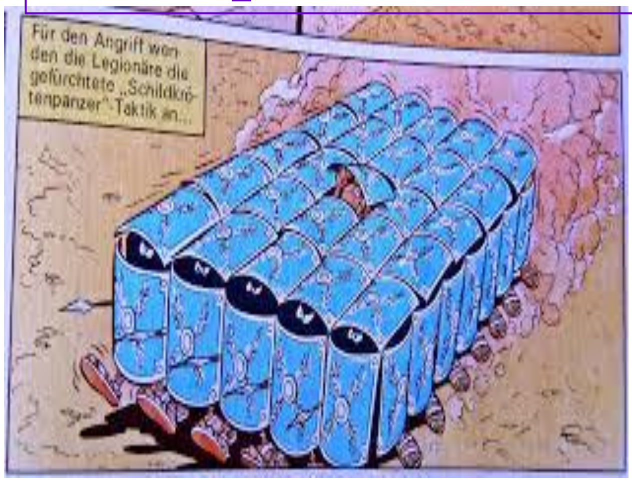

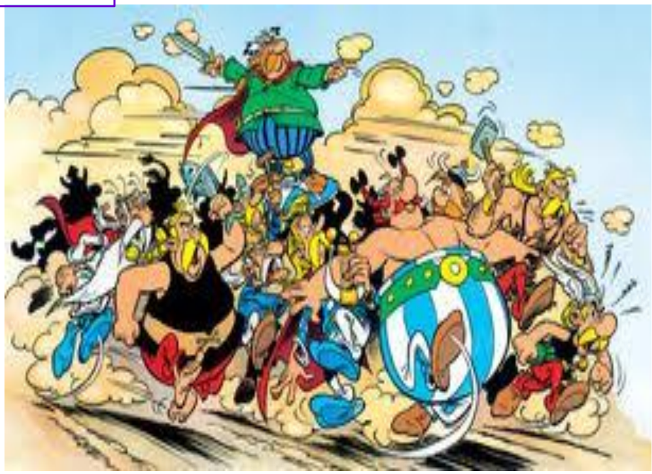

Initialization

Mean Field :
attractive
Low Energy

$$\frac{\partial \vec{P}}{\partial t} = -\nabla_r U(\vec{r}, \vec{p})$$

NN collisions:
repulsive
Pauli Blocking
Particle production
High Energy

Intermediate Energy: competition between mean field and nucleon-nucleon collisions

1. Introduction of nuclear EOS and transport approaches

Equation of State (EOS) of nuclear matter

Asymmetric nuclear matter

$$E(\rho,\delta) = E_0(\rho) + E_{\text{sym}}(\rho)\delta^2 + E_{\text{sym},4}(\rho)\delta^4 + O(\delta^6)$$

Symmetric nuclear matter

$$E_0(\rho) = E_0(\rho_0) + L_0\chi + \frac{K_0}{2!}\chi^2 + \frac{J_0}{3!}\chi^3 + \frac{I_0}{4!}\chi^4 + O(\chi^5)$$

isospin asymmetry $\delta = (\rho_n - \rho_p)/\rho$ $\qquad \chi = \dfrac{\rho - \rho_0}{3\rho_0}$

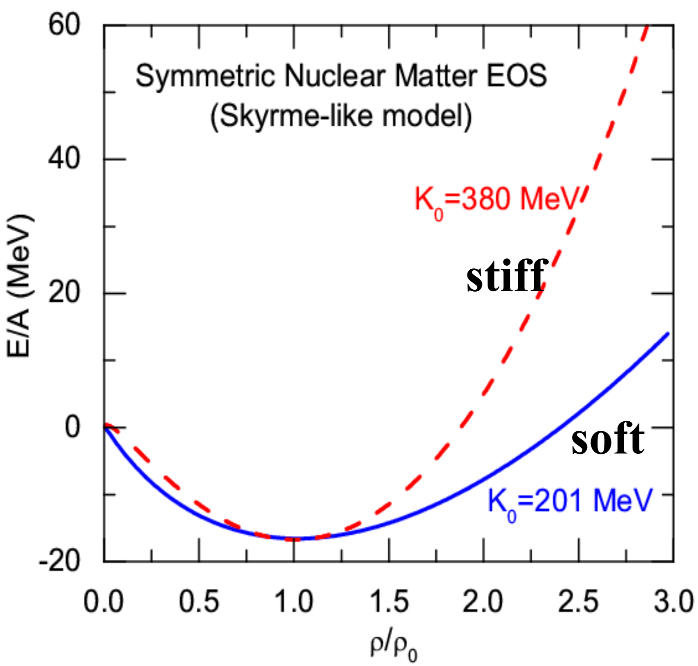

$$L_0 = 3\rho_0 \left.\frac{dE_0(\rho)}{d\rho}\right|_{\rho=\rho_0},$$

$$K_0 = 9\rho_0^2 \left.\frac{d^2E_0(\rho)}{d\rho^2}\right|_{\rho=\rho_0},$$

$$J_0 = 27\rho_0^3 \left.\frac{d^3E_0(\rho)}{d\rho^3}\right|_{\rho=\rho_0},$$

$$I_0 = 81\rho_0^4 \left.\frac{d^4E_0(\rho)}{d\rho^4}\right|_{\rho=\rho_0}.$$

$\rho_0 \sim 0.16 fm^{-3}$

$E_0(\rho_0) \sim -16 MeV$

$L_0 = 0$

GMR:

$K_0 = 230 \pm 30 MeV$

Symmetry energy

$$E_{\rm sym}(\rho) = E_{\rm sym}(\rho_0) + L\chi + \frac{K_{\rm sym}}{2!}\chi^2 + \frac{J_{\rm sym}}{3!}\chi^3 + \frac{I_{\rm sym}}{4!}\chi^4 + O(\chi^5)$$

$$L = 3\rho_0 \left.\frac{dE_{\rm sym}(\rho)}{\partial\rho}\right|_{\rho=\rho_0},$$

$$K_{\rm sym} = 9\rho_0^2 \left.\frac{d^2E_{\rm sym}(\rho)}{\partial\rho^2}\right|_{\rho=\rho_0},$$

$$J_{\rm sym} = 27\rho_0^3 \left.\frac{d^3E_{\rm sym}(\rho)}{\partial\rho^3}\right|_{\rho=\rho_0}$$

$$I_{\rm sym} = 81\rho_0^4 \left.\frac{d^4E_{\rm sym}(\rho)}{\partial\rho^4}\right|_{\rho=\rho_0}$$

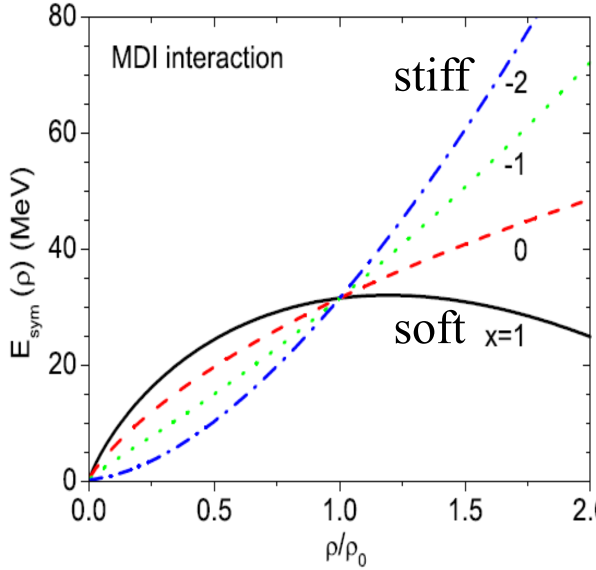

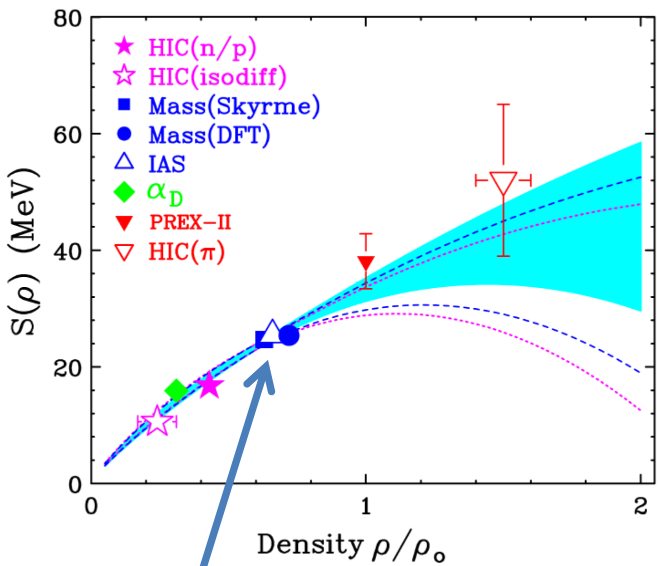

or better constrained around $2\rho_0/3$

Liquid-drop model

$$E_B = a_V A - a_S A^{2/3} - a_C \frac{Z^2}{A^{1/3}} - \boxed{a_A \frac{(A-2Z)^2}{A}} - \delta(A,Z)$$

bulk

surface

$$E_{sym}(\rho_0) \sim 30MeV \quad L = ?\, K_{sym} = ?$$

Mean-field potential

Isospin-dependent BUU equation

$$\frac{\partial f_\tau(\vec{r},\vec{p},t)}{\partial t} + \frac{\vec{p}}{m}\cdot\frac{\partial f_\tau(\vec{r},\vec{p},t)}{\partial \vec{r}} - \boxed{\frac{\partial U_\tau}{\partial \vec{r}}}\cdot\frac{\partial f_\tau(\vec{r},\vec{p},t)}{\partial \vec{p}} = I(\vec{r},\vec{p},t)$$

Collision term

τ is the isospin index for neutrons or protons.

Mean-field potential $U_\tau = \left(\frac{\partial \varepsilon_p}{\partial \rho_\tau}\right)_{\rho_{-\tau}}$

Binding energy per nucleon $E = \frac{\varepsilon_k + \varepsilon_p}{\rho}$

Kinetic energy density $\varepsilon_k = \sum_\tau 2\int \frac{d^3k}{(2\pi)^3}\frac{k^2}{2m}n_\tau(k)$

Potential energy density ε_p

neutron $U_n \approx U_0 + U_{sym}\delta + U_{sym,2}\delta^2$ **repulsive**

proton $U_p \approx U_0 - U_{sym}\delta + U_{sym,2}\delta^2$ **attractive**

Symmetry potential $U_{sym} \approx \frac{U_n - U_p}{2\delta}$

Effective/phenomenological nuclear interaction

An improved momentum-dependent interaction (ImMDI)

Effective two-body force

$$v(\vec{r}_1,\vec{r}_2) = \frac{1}{6}t_3(1+x_3P_\sigma)\rho^\gamma\left(\frac{\vec{r}_1+\vec{r}_2}{2}\right)\delta(\vec{r}_1-\vec{r}_2)$$

$$+(W+GP_\sigma-HP_\tau-MP_\sigma P_\tau)\frac{e^{-\mu|\vec{r}_1-\vec{r}_2|}}{|\vec{r}_1-\vec{r}_2|}$$

$$\boxed{t_3, x_3, \gamma, W, G, H, M, \mu}$$

$$\Updownarrow$$

$$\boxed{A_u, A_l, \sigma, B, x, C_{\tau,\tau}, C_{\tau,-\tau}, \Lambda}$$

Potential energy density

$$V(\rho,\delta) = \frac{A_u\rho_n\rho_p}{\rho_0} + \frac{A_l}{2\rho_0}(\rho_n^2+\rho_p^2) + \frac{B}{\sigma+1}\frac{\rho^{\sigma+1}}{\rho_0^\sigma}$$

$$\times(1-x\delta^2) + \frac{1}{\rho_0}\sum_{\tau,\tau'}C_{\tau,\tau'}$$

$$\times\iint d^3p\,d^3p'\frac{f_\tau(\vec{r},\vec{p})f_{\tau'}(\vec{r},\vec{p}\,')}{1+(\vec{p}-\vec{p}\,')^2/\Lambda^2}.$$

Mean-field potential

$$U_\tau(\rho,\delta,\vec{p}) = A_u\frac{\rho_{-\tau}}{\rho_0} + A_l\frac{\rho_\tau}{\rho_0}$$

$$+B\left(\frac{\rho}{\rho_0}\right)^\sigma(1-x\delta^2) - 4\tau x\frac{B}{\sigma+1}\frac{\rho^{\sigma-1}}{\rho_0^\sigma}\delta\rho_{-\tau}$$

$$+\frac{2C_l}{\rho_0}\int d^3p'\frac{f_\tau(\vec{r},\vec{p}\,')}{1+(\vec{p}-\vec{p}\,')^2/\Lambda^2}$$

$$+\frac{2C_u}{\rho_0}\int d^3p'\frac{f_{-\tau}(\vec{r},\vec{p}\,')}{1+(\vec{p}-\vec{p}\,')^2/\Lambda^2}.$$

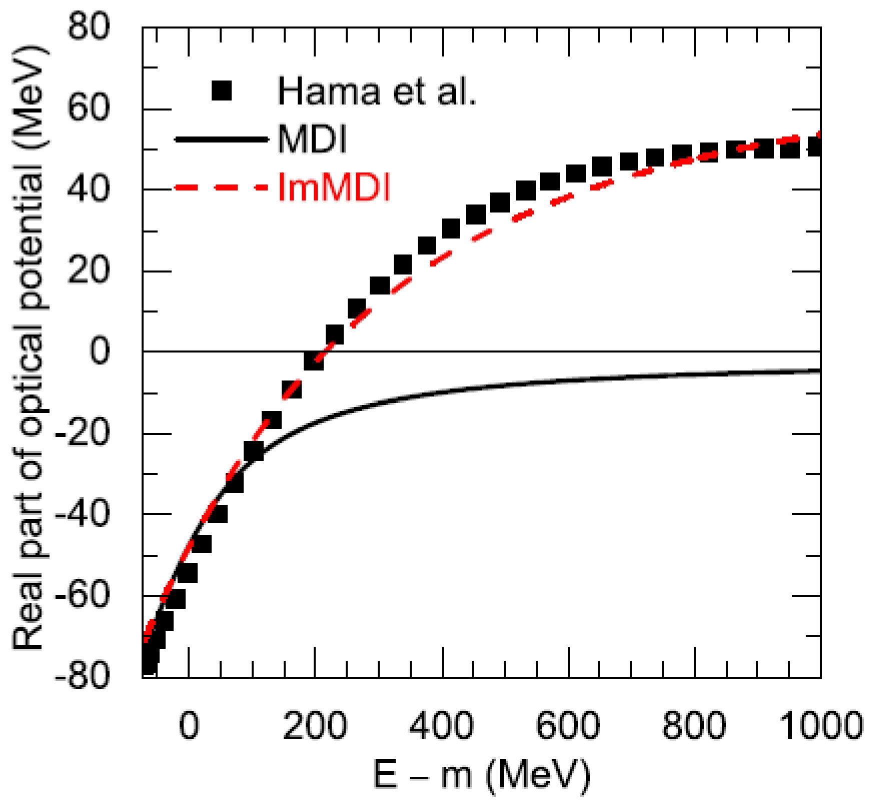

Nucleon effective mass

Electron effective mass:

dispersion relation different from free electrons near the energy gap

$$\frac{1}{m^*} = \frac{1}{\hbar^2}\frac{\mathrm{d}^2\epsilon}{\mathrm{d}k^2}$$

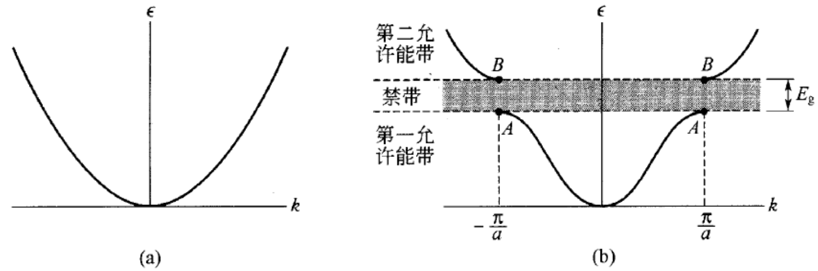

Nucleon effective mass:

in-medium interaction lowers the nucleon mass

P-mass: $$\frac{\tilde{m}^*_\tau}{m} = \left[1 + \frac{m}{p}\frac{\partial U_\tau(p,\varepsilon_\tau(p))}{\partial p}\right]^{-1}$$

E-mass: $$\frac{\bar{m}^*_\tau}{m} = 1 - \frac{\partial U_\tau(p,\varepsilon_\tau(p))}{\partial \varepsilon_\tau}$$

$\tau = n, p$

Dirac mass: $m^*_{Dirac,\tau} = m + \Sigma^s_\tau$ $\qquad$ Σ^s_τ: scalar self-energy

Skyrme-Hartree-Fock: **non-relativistic, momentum-dependent potential**

Relativistic mean-field: **relativistic, meson exchange**

Comparison between non-relativistic mass with relativistic mass

Lorentz effective mass:

$$m^*_{Lorentz,\tau} = m\left(1 - \frac{dU_{SEP,\tau}}{dE_\tau}\right) = (E_\tau - \Sigma^0_\tau)\left(1 - \frac{d\Sigma^0_\tau}{dE_\tau}\right) - (m + \Sigma^s_\tau)\frac{d\Sigma^s_\tau}{dE_\tau} + m - E_\tau$$

M. Jaminon and C. Mahaux, PRC (1989); B.A. Li, L.W. Chen, and C.M. Ko, Phys. Rep. (2008); Z.X. Li, Nucl. Phys. Rev. (2014); B.A. Li, B.J. Cai, L.W. Chen, and J. Xu, Prog. Part. Nucl. Phys. (2018)

Hugenholtz–Van Hove theorem

$$E_{\rm sym}(\rho) = \frac{1}{3}\frac{\hbar^2 k^2}{2m_0^*}\bigg|_{k_F} + \frac{1}{2}U_{\rm sym,1}(\rho, k_F)$$

$$L(\rho) = \frac{2}{3}\frac{\hbar^2 k^2}{2m_0^*}\bigg|_{k_F} - \frac{1}{6}\left(\frac{\hbar^2 k^3}{m_0^{*2}}\frac{\partial m_0^*}{\partial k}\right)\bigg|_{k_F} + \frac{3}{2}U_{\rm sym,1}(\rho, k_F) + \frac{\partial U_{\rm sym,1}}{\partial k}\bigg|_{k_F} \cdot k_F + 3U_{\rm sym,2}(\rho, k_F)$$

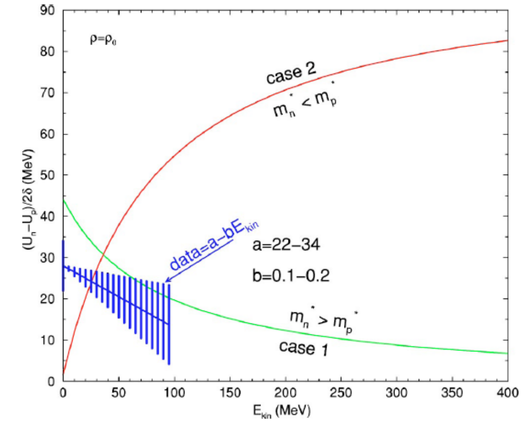

C. Xu, B.A. Li, and L.W. Chen, PRC (2010);
R. Chen, B.J. Cai, L.W. Chen, B.A. Li, X.H. Li, and C. Xu, PRC (2012)

$$m^*_{n-p}(\rho_0, \delta) \approx \delta \cdot \left[3E_{\rm sym}(\rho_0) - L(\rho_0) - \frac{1}{3}\frac{m}{m_0^*}E_F(\rho_0)\right] \Big/ \left[E_F(\rho_0)\cdot(m/m_0^*)^2\right]$$

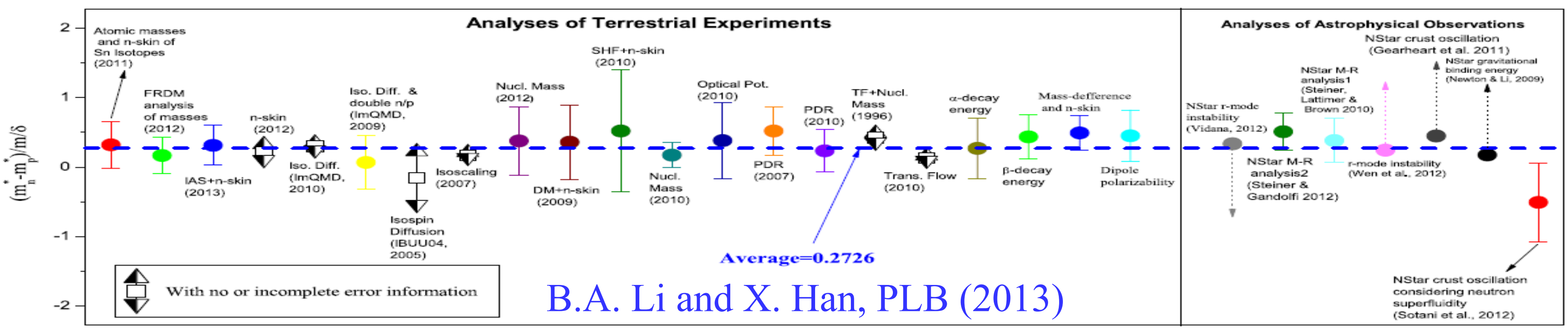

B.A. Li and X. Han, PLB (2013)

BUU transport approach

Boltzmann-Uehling-Uhlenbeck equation:

$$\left(\frac{\partial}{\partial t} + \frac{\vec{p}}{m}\cdot\nabla_r - \nabla_r U \cdot \nabla_p\right) f(\vec{r},\vec{p};t) = I_{coll}[f;\sigma_{12}]$$

Collision term with quantum statistics

$$\begin{aligned} I_{coll} &= \frac{1}{(2\pi)^6}\int dp_2 dp_3 d\Omega |v - v_2| \frac{d\sigma_{12}^{med}}{d\Omega}(2\pi)^3\delta(p + p_2 - p_3 - p_4) \\ &\times \; [f_3 f_4 (1-f)(1-f_2) - f f_2 (1-f_3)(1-f_4)] \end{aligned}$$

Derivation: real-time Green's function formulism; von-Neumann equation with density matrix; higher-order cutoff from TDHF; …

test-particle (TP) method: parallel events

C.Y. Wong, PRC 25, 1460 (1982); G.F. Bertsch and S. Das Gupta, Phys. Rep. 160, 189 (1988).

Point particle or finite size (triangular, Gaussian)

$$f(\vec{r},\vec{p};t) = \frac{1}{N_{TP}}\sum_{i=1}^{N_{TP}A} g(\vec{r}-\vec{r}_i(t))\tilde{g}(\vec{p}-\vec{p}_i(t))$$

Equations of motion from pseudoparticle method:

$$d\vec{r}_i/dt = \nabla_{\vec{p}_i} H; \qquad d\vec{p}_i/dt = -\nabla_{\vec{r}_i} H.$$

QMD transport approach

single-particle wave function:

$$\phi_i(\vec{r};t) = \frac{1}{(2\pi L)^{4/3}} \exp\left[-\frac{(\vec{r}-\vec{r}_i(t))^2}{4L} + \frac{i\vec{p}_i(t)\cdot\vec{r}}{\hbar}\right]$$

Many-body wave function $\Phi(\vec{r};t) = \Pi_i \phi(\vec{r},\vec{r}_i,\vec{p}_i;t)$ **Except AMD and FMD**

Wigner function (phase-space distribution):

$$\begin{aligned} f_i(\vec{r},\vec{p}) &= \frac{1}{(2\pi\hbar)^3}\int \phi_i^*(\vec{r}-\vec{s}/2)\phi_i(\vec{r}+\vec{s}/2)\exp(-i\vec{p}\cdot\vec{s})d^3s \\ &= \frac{1}{(\pi\hbar)^3}\exp\left[-\frac{(\vec{r}-\vec{r}_i)^2}{2L} - \frac{2L(\vec{p}-\vec{p}_i)^2}{\hbar^2}\right], \end{aligned}$$

$\langle\ldots\rangle \sim \int f_i \ldots f_j \, dr_i dp_i dr_j dp_j$

Many-body Hamiltonian $$H = \sum_i T_i + \frac{1}{2}\sum_{i\neq j} V_{ij}$$

$\langle V_{ij}\rangle$ **from Hartree calculation**

$\langle\rho^\gamma\rangle \approx \langle\rho\rangle^\gamma$

Equations of motion

$$\frac{d\vec{r}_i}{dt} = \frac{\vec{p}_i}{m} + \frac{1}{2}\sum_{j,j\neq i}\frac{\partial\langle V_{ij}\rangle}{\partial\vec{p}_i} = \frac{\partial\langle H\rangle}{\partial\vec{p}_i},$$

$$\frac{d\vec{p}_i}{dt} = -\frac{1}{2}\sum_{j,j\neq i}\frac{\partial\langle V_{ij}\rangle}{\partial\vec{r}_i} = -\frac{\partial\langle H\rangle}{\partial\vec{r}_i}.$$

Ch. Hartnack et al., PRC 495, 303 (1989); J. Aichelin, Phys. Rep. 202, 233 (1988).

NN scattering cross section

In free space:

$$\sigma_{np}^{\text{free}} = -70.67 - 18.18\beta^{-1} + 25.26\beta^{-2} + 113.85\beta \text{ (mb)},$$

$$\sigma_{pp}^{\text{free}} = 13.73 - 15.04\beta^{-1} + 8.76\beta^{-2} + 68.67\beta^{4} \text{ (mb)},$$

$$\beta \equiv v/c$$

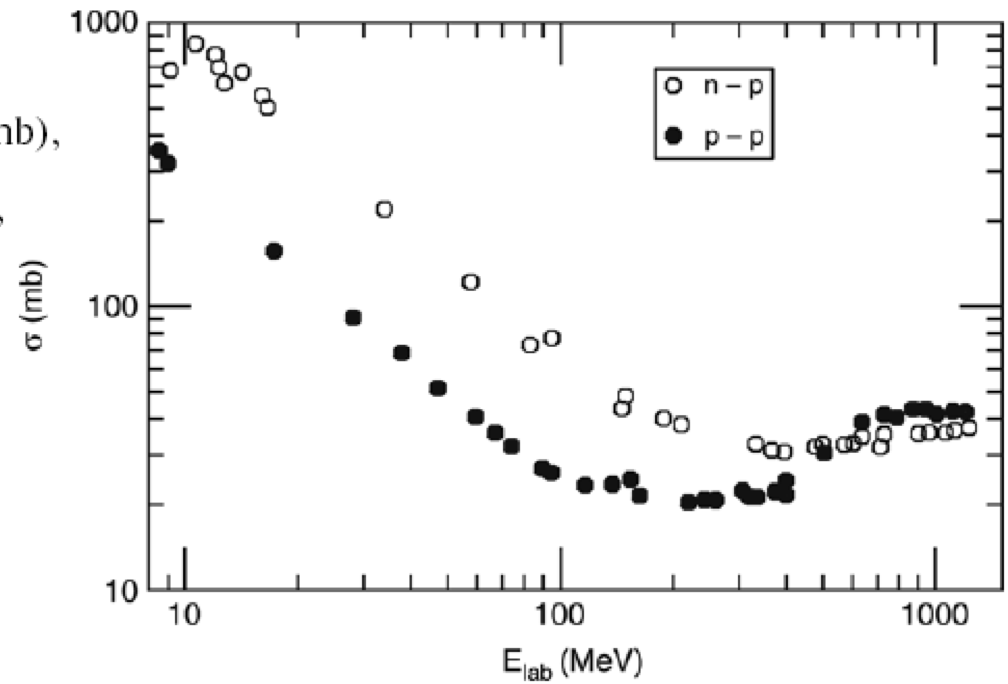

In-medium cross section is uncertain, with various parameterizations/approximations.

In symmetric nuclear matter:

$$\sigma_{np}^{\text{medium}} = \left[31.5 + 0.092\,abs(20.2 - E_{\text{lab}}^{0.53})^{2.9}\right] \cdot \frac{1.0 + 0.0034E_{\text{lab}}^{1.51}\rho^{2}}{1.0 + 21.55\rho^{1.34}} \text{ (mb)},$$

$$\sigma_{pp}^{\text{medium}} = \left[23.5 + 0.0256(18.2 - E_{\text{lab}}^{0.5})^{4}\right] \cdot \frac{1.0 + 0.1667E_{\text{lab}}^{1.05}\rho^{3}}{1.0 + 9.704\rho^{1.2}} \text{ (mb)}.$$

or

$$\sigma_{NN}^{\text{medium}} = \left(1 + \alpha\frac{\rho}{\rho_0}\right)\sigma_{NN}^{\text{free}}$$

$$\alpha \approx -0.2$$

Effective mass scaling of NN cross section

The cross section for the scattering of two nucleons in vacuum, from momentum states $\mathbf{k}_1$ and $\mathbf{k}_2$ to states $\mathbf{k}_3$ and $\mathbf{k}_4$ is given by

$$\frac{d\sigma}{d\Omega}=\frac{L^3}{v_{\mathrm{rel}}}\frac{2\pi}{\hbar}|t|^2 D_f \ , \qquad (2.1)$$

where L^3 is the normalization volume, v_{rel} the relative velocity,

$$v_{\mathrm{rel}}=\hbar|\mathbf{k}_1-\mathbf{k}_2|/m \ ,$$

and the density of final states

$$D_f=L^3 m|\mathbf{k}_3-\mathbf{k}_4|/32\pi^3\hbar^2 \ .$$

$$\frac{1}{\hbar}\frac{de(k,\rho)}{dk}=\frac{\hbar k}{m}+\frac{1}{\hbar}\frac{d}{dk}U(k,\rho)\equiv\frac{\hbar k}{m^*(k,\rho)}$$

$$D_f'=D_f\frac{m^*[\sqrt{\tfrac{1}{2}(k_3^2+k_4^2)},\rho]}{m}$$

the present context. Using $t'\approx t$ we obtain

$$\frac{d\sigma'}{d\Omega}=\frac{v_{\mathrm{rel}}}{v_{\mathrm{rel}}'}\frac{D_f'}{D_f}\frac{d\sigma}{d\Omega} \qquad (2.8)$$

$$=\frac{|\mathbf{k}_1-\mathbf{k}_2|}{m}\left[\left|\frac{\mathbf{k}_1}{m^*(k_1,\rho)}-\frac{\mathbf{k}_2}{m^*(k_2,\rho)}\right|\right]^{-1}$$

$$\times\frac{m^*[\sqrt{(k_3^2+k_4^2)/2},\rho]}{m}\frac{d\sigma}{d\Omega} \ . \qquad (2.9)$$

$$R_{\mathrm{medium}}\equiv\sigma_{NN}^{\mathrm{medium}}/\sigma_{NN}^{\mathrm{free}}=(\mu_{NN}^*/\mu_{NN})^2$$

reduced mass

$\mu^*_{NN}=m^*_1 m^*_2/(m^*_1+m^*_2)$

Pandharipande and Peiper, PRC (1992)

Initialization

- Woods-Saxon distribution
- Skyrme-Hartree-Fock or Thomas-Fermi calculation
- Frictional cooling
- Binding energy and charge radius

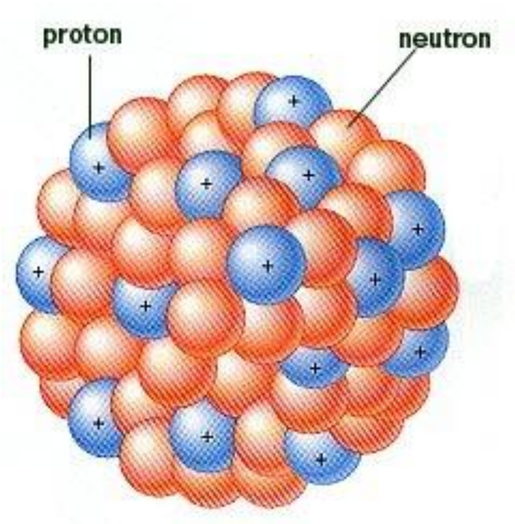

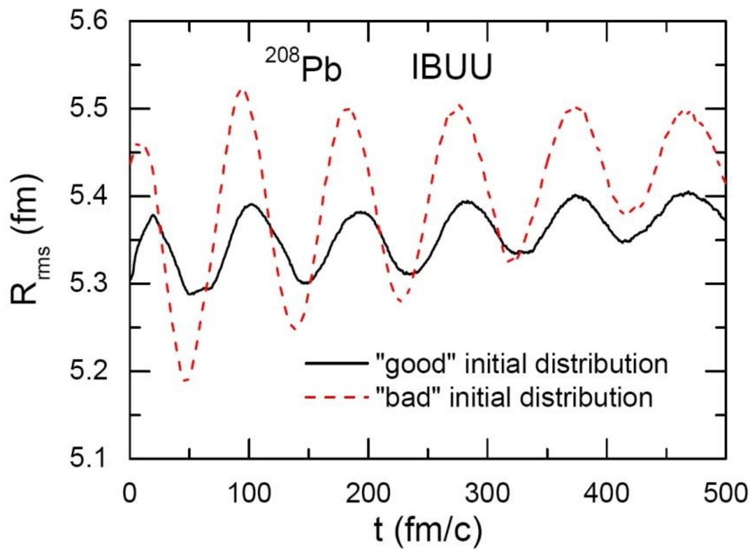

Mean-field calculation

$$\vec{p}_i(t+\Delta t) = \vec{p}(t) - \nabla U[f(\vec{r},\vec{p};t)]$$

Lattice Hamiltonian: $\rho_L(\vec{r}_\alpha) = \sum_{i \epsilon V_\alpha}^{AN} S(\vec{r}_\alpha - \vec{r}_i)$

$$S(\vec{r}_\alpha - \vec{r}_i) = \frac{1}{N(nl)^6} g(x)g(y)g(z)$$

$$g(q) = (nl-|q|)\Theta(nl-|q|)$$

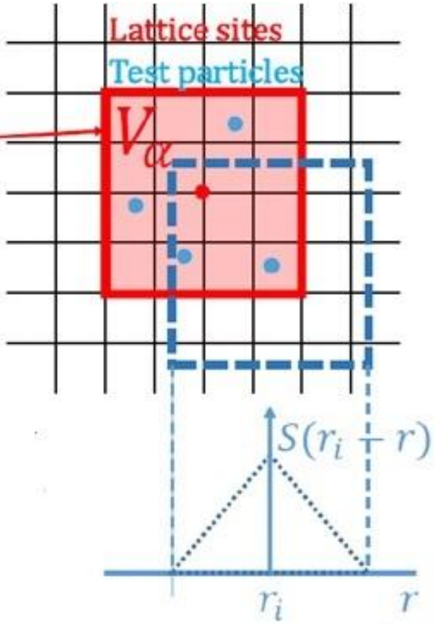

R. J. Lenk and V. R. Pandharipande, PRC 39, 2242 (1989)

BUU: Size and shape of the test particle (point, Gaussian, triangular)
QMD: width of the Gaussian wave packet

Nucleon-nucleon collisions
(in most transport models)

- **Bertsch's approach (Phys. Rep. 160, 189 (1988))**
  - Go into the C.M. frame of the two nucleons $\quad \delta t = \alpha \Delta t$
  - Collision can happen if $\quad \alpha \approx 1/\gamma$

$$b = \sqrt{(\Delta \boldsymbol{r})^2 - (\Delta \boldsymbol{r} \cdot \boldsymbol{p}/p)^2} < \sqrt{\sigma/\pi} \quad \text{and} \quad \left| \frac{\Delta \boldsymbol{r} \cdot \boldsymbol{p}}{p} \right| < \left(\frac{p}{\sqrt{p^2 + m_1^2}} + \frac{p}{\sqrt{p^2 + m_2^2}} \right) \boxed{\delta t}/2$$

  - If collision happen, change the direction of P_{cm} in the C.M. frame
  - Boost the momenta of the two nucleons to lab frame
  - Check phase space density; if Pauli blocked, return to the initial momenta
- **Stochastic method**

Møller velocity $v_{\text{mol}} = \frac{\sqrt{[s-(m_1+m_2)^2][s-(m_1-m_2)^2]}}{2E_1E_2}$

Collision probability proportional to $v_{mol}\sigma \frac{\Delta t}{(\Delta x)^3}$

	Distance condition	Time condition	Collision order
BUU type			
BUU-VM	$\pi d_\perp^{*2} < \sigma$	$\lvert t_{\text{coll}}^* - t_0^* \rvert < \frac{1}{2}\Delta t$	Fixed order
GiBUU	$\pi d_\perp^{*2} < \sigma / N_{\text{TP}}$	$\lvert t_{\text{coll}}^* - t_0^* \rvert < \frac{1}{2}\Delta t$	Fixed order
IBUU	$\pi d_\perp^{*2} < \sigma$	$\lvert t_{\text{coll}}^* - t_0^* \rvert < \frac{1}{2}\Delta t$	Fixed order
pBUU	$i, j \in$ the same V_{cell} volume	$P = \frac{\sigma}{N_{\text{TP}}} \frac{1}{\gamma V_{\text{cell}}} v_{ij}^* \alpha \Delta t$	Randomly nominate (i, j) pairs
RVUU	$\pi d_\perp^{*2} < \sigma_{\max} / N_{\text{TP}}$, $P = \sigma / \sigma_{\max}$	$\lvert t_{\text{coll}}^* - t_0^* \rvert < \frac{1}{2}\Delta t$	Fixed order
SMASH	$\pi d_\perp^{*2} < \sigma / N_{\text{TP}}$	$t_{\text{coll}}^{(\text{ref})} \in [t_0, t_0 + \Delta t]$	Ordered by $t_{\text{coll}}^{(\text{ref})}$
SMF	$j =$ closest to i in same ensemble	$P = \frac{1}{2}\sigma v_{ij} \rho_i \Delta t$	Cyclic with random starting for i
QMD type			
CoMD	$j =$ closest to i, $j > i$ [a]	$P = 1 - e^{-\sigma v_{ij} \rho_i \Delta t}$	Cyclic with random starting for i
ImQMD	$\pi d_\perp^{*2} < \sigma$	$\lvert t_{\text{coll}}^* - t_0^* \rvert < \frac{1}{2}\gamma \Delta t$	Fixed order
IQMD-BNU	$\pi d_\perp^{*2} < \sigma$	$\lvert t_{\text{coll}}^* - t_0^* \rvert < \frac{1}{2}\Delta t$	Fixed order
IQMD-IMP	$\pi d_\perp^{*2} < \sigma$	$\lvert t_{\text{coll}}^* - t_0^* \rvert < \frac{1}{2}\gamma \Delta t$	Fixed order
JAM	$\pi d_\perp^{*2} < \sigma$	$\bar{t}_{\text{coll}} \in [t_0, t_0 + \Delta t]$	Ordered by $\bar{t}_{\text{coll}}$
JQMD	$d_\perp^* < b_{\max}$, $P = \sigma / \pi b_{\max}^2$	$\lvert \bar{t}_{\text{coll}} - t_0 \rvert < \frac{1}{2}\Delta t$	Fixed order
TuQMD	$\pi d_\perp^{*2} < \sigma$	$t_{1-}^*, t_{2-}^* < t_{\text{coll}}^* < t_{1+}^*, t_{2+}^*$	Randomly ordered
UrQMD	$\pi d_\perp^{*2} < \sigma$	$t_{\text{coll}}^{(\text{ref})} \in [t_0, t_0 + \Delta t]$	Ordered by $t_{\text{coll}}^{(\text{ref})}$
Basic cascade			
Rel. ($\delta t = \alpha \Delta t$)	$\pi d_\perp^{*2} < \sigma$	$\lvert t_{\text{coll}}^* - t_0^* \rvert < \frac{1}{2}\alpha \Delta t$	Fixed order
Rel. ($\delta t = \Delta t$)	$\pi d_\perp^{*2} < \sigma$	$\lvert t_{\text{coll}}^* - t_0^* \rvert < \frac{1}{2}\Delta t$	Fixed order
Quasirelativistic	$\pi d_\perp^{(\text{ref})2} < \sigma$	$\lvert t_{\text{coll}}^{(\text{ref})} - t_0 \rvert < \frac{1}{2}\Delta t$	Fixed order

Y.X. Zhang et al., PRC 97, 034625 (2018)

How is Pauli blocking realized?
(in most transport models)

- Update the occupation probability n_i at each time step (n_i is calculated differently for each code, and can be different for BUU and QMD)

BUU: **counting local phase-space cell** **fit with a superposition of two FD distributions**

$$n_i = \frac{(2\pi\hbar)^3}{g_N V_r V_p} \int_{i \in V_r, V_p} f(\vec{r}, \vec{p}) d^3r d^3p \qquad n_i(\bar{p}) = \frac{A'}{\exp[(\sqrt{m^2 + p'^2} - \mu')/T'] + 1} + \frac{A''}{\exp[(\sqrt{m^2 + p''^2} - \mu'')/T''] + 1}$$

QMD: **overlap of wavepackets** **hard sphere overlap**

$$n_i = \frac{(2\pi\hbar)^3}{g_N} \frac{1}{(\pi\hbar)^3} \sum_{j, j \neq i} \exp\left[-\frac{(\vec{r}_j - \vec{r}_i)^2}{2\mathrm{L}} - \frac{2\mathrm{L}(\vec{p}_j - \vec{p}_i)^2}{\hbar^2} \right] \qquad n_i = \sum_{j, j \neq i} \frac{O_{ij}^{(r)}}{\frac{4}{3}\pi(\Delta r)^3} \frac{O_{ij}^{(p)}}{\frac{4}{3}\pi(\Delta p)^3}$$

- When a collision is attempted, check the Pauli blocking probability $1\text{-}(1\text{-}n_i)(1\text{-}n_j)$
- Additional constraint if any (phase-space constraint, surface correction, …)

TABLE III: Pauli-blocking treatment used in various codes in homework calculations.

Code name	Occupation probability f_i	Blocking probability[a]	Additional constraints
AMD	antisymmetrized wavepackets[b]	physical wavepacket[b]	no
IQMD-BNU	f_i in h^3	$1-(1-f_i)(1-f_j)$	yes[c]
IQMD	f_i in h^3	$1-(1-f_i)(1-f_j)$	yes[d]
CoMD	f_i in h^3	$f_i', f_j' < f_{\max} = 1.05-1.1$	yes[e]
ImQMD-CIAE	f_i in h^3	$1-(1-f_i)(1-f_j)$	no
IQMD-IMP	f_i in phase-space cell with $dx = 3.367$ fm, $dp = 89.3$ MeV/c	$1-(1-f_i)(1-f_j)$	no
IQMD-SINAP	$f_i = \sum_k e^{-(\vec{r}_k-\vec{r}_i)^2/[2(\Delta x)^2]} e^{-(\vec{p}_k-\vec{p}_i)^2 \cdot 2(\Delta x)^2/\hbar^2}$	$1-(1-f_i)(1-f_j)$	no
TuQMD	f_i in spherical phase-space cell with $dx = 3.0$ fm, $dp = 240$ MeV/c[f]	$1-(1-f_i)(1-f_j)$	yes[g]
UrQMD	$f_i = \sum_k e^{-(\vec{r}_k-\vec{r}_i)^2/[2(\Delta x)^2]} e^{-(\vec{p}_k-\vec{p}_i)^2 \cdot 2(\Delta x)^2/\hbar^2}$	$1-(1-f_i)(1-f_j)$	yes[h]
BLOB	f_i in sphere with radius 3.5 fm with Gaussian weight in momentum space[i]	$1-(1-f_i)(1-f_j)$	yes[j]
GIBUU-RMF	f_i in phase-space cell with $dx = 1.4$ fm, $dp = 68$ MeV/c	$1-(1-f_i)(1-f_j)$	no
GIBUU-Skyrme	f_i in phase-space cell with $dx = 1.4$ fm, $dp = 68$ MeV/c	$1-(1-f_i)(1-f_j)$	no
IBL	f_i in h^3	$1-(1-f_i)(1-f_j)$	yes[k]
IBUU	f_i in phase-space cell with $dx = 2.73$ fm, $dp = 187$ MeV/c	$1-(1-f_i)(1-f_j)$	no
pBUU	f_i in same and neighboring spatial cell[l]	$1-(1-f_i)(1-f_j)$	no
RBUU	f_i in phase-space cell with $dx = 1.4$ fm, $dp = 64$ MeV/c	$1-(1-f_i)(1-f_j)$	no
RVUU	f_i in phase-space cell with $dx = 1.14$ fm, $dp = 331$ MeV/c[m]	$1-(1-f_i)(1-f_j)$	no
SMF	f_i in sphere with radius 2.53 fm with Gaussian weight in momentum space[n]	$1-(1-f_i)(1-f_j)$	no

[a] Occupation probability f_i is replaced by $\min[f_i, 1]$ if f_i is larger than 1.
[b] See Ref. [27] for details.
[c] Phase-space constraint, see Ref. [28] for details.
[d] Isospin average, see Ref. [29] for details.
[e] Phase-space constraint, see Ref. [41] for details.
[f] In TuQMD the Pauli Blocking is implemented by computing the wave function overlap using the method described in Ref. [30].
[g] Surface modification, see Ref. [42] for details.
[h] Phase-space constraint: $\frac{4\pi}{3} r_{ik}^3 \frac{4\pi}{3} p_{ik}^3 \geq \left(\frac{h}{2}\right)^3/4$.
[i] Width of the Gaussian from definition of test-particle agglomerates, see Ref. [19] for details.
[j] Wavepacket modulation (shape, widths) to ensure strict Pauli blocking.
[k] Fermi constraint, see Ref. [21] for details.
[l] See Ref. [23] for details.
[m] Obtained using $dx = [3/(4\pi\rho_0)]^{1/3}$ and $dp = [6\pi^2\rho_0/(2s+1)]^{1/3}$, see Ref. [25] for details.
[n] The width of the Gaussian is 29 MeV/c.

J .Xu et al.,
PRC 93, 044609 (2016)

TABLE V. Pauli-blocking treatments used by different codes in the box calculation comparison.

Code name	Occupation probability f_i	Blocking probability[a]	Additional constraints
BUU-VM	In sphere,[b] $R_x = 2.76$ fm, $R_p = 59.04$ MeV/c	$1-(1-f_i)(1-f_j)$	No
GiBUU	In cube,[b] $\Delta x = 1.4$ fm, $\Delta p = 68$ MeV/c	$1-(1-f_i)(1-f_j)$	No
IBUU	In cube,[b] $\Delta x = 2.0$ fm, $\Delta p = 100$ MeV/c [c]	$1-(1-f_i)(1-f_j)$	No
pBUU	In same and adjacent spatial cells[d]	$1-(1-f_i)(1-f_j)$	No
RVUU	In cube,[b] $\Delta x = 2$ fm, $\Delta p = 100$ MeV/c	$1-(1-f_i)(1-f_j)$	No
SMASH	In sphere,[b] $R_x = 2.2$ fm, $R_p = 80$ MeV/c [e]	$1-(1-f_i)(1-f_j)$	No
SMF	In sphere,[b] $R_x = 2.53$ fm, $R_p = 29$ MeV/c [f]	$1-(1-f_i)(1-f_j)$	No
CoMD	Overlap of hard spheres[g]	$f_i', f_j' < f_{\max} = 1.08$[j]	No
ImQMD	Overlap of wave packets,[h] $(\Delta x)^2 = 2\ \text{fm}^2$	$1-(1-f_i)(1-f_j)$	No
IQMD-BNU	Overlap of wave packets,[h] $(\Delta x)^2 = 2\ \text{fm}^2$	$1-(1-f_i)(1-f_j)$	No
IQMD-IMP	Overlap of hard spheres,[i] $R_x = 3.367$ fm, $R_p = 112.5$ MeV/c	$1-(1-f_i)(1-f_j)$	No
JAM	Overlap of wave packets,[h] $(\Delta x)^2 = 2\ \text{fm}^2$	$1-(1-f_i)(1-f_j)$	No
JQMD	Overlap of wave packets,[h] $(\Delta x)^2 = 2\ \text{fm}^2$	$1-(1-f_i)(1-f_j)$	No
TuQMD	Overlap of hard spheres,[k] $R_x = 3.0$ fm, $R_p = 240$ MeV/c	$1-(1-f_i)(1-f_j)$	Yes
UrQMD	Overlap of wave packets,[h] $(\Delta x)^2 = 2\ \text{fm}^2$	$1-(1-f_i)(1-f_j)$	Yes[l]

[a]Occupation probability f_i replaced by 1 if $f_i > 1$.
[b]Occupation in spherical or cubic phase space cell with given dimensions.
[c]Interpolation among neighboring phase-space cells.
[d]See Ref. [20] for details.
[e]With weighting in coordinate space; see Ref. [22].
[f]Gaussian weight in momentum space.
[g]See explanation of hard sphere overlap in the text below Eq. (14).
[h]Overlap of wave packets, Eq. (14), with given width $(\Delta x)^2$.
[i] $f_i' = \frac{2}{h^3}\sum_{k\in\tau(k\neq i)} O_{ik}^{(x)} O_{ik}^{(p)}$; see explanation of hard sphere overlap in the text below Eq. (14).
[j] f_i' is the occupation of the final cell, including the scattered particle; see Ref. [25] for details.
[k] $f_i' = \sum_{k\in\tau(k\neq i)}(O_{ik}^{(x)}/\frac{4}{3}\pi R_x^3)(O_{ik}^{(p)}/\frac{4}{3}\pi R_p^3)$ with a surface correction is applied; see Refs. [41,42] for details.
[l]Phase-space constraint: $\frac{4\pi}{3} r_{ik}^3 \frac{4\pi}{3} p_{ik}^3 \geqslant (\frac{h}{2})^3/4$.

Y.X. Zhang et al., PRC 97, 034625 (2018)

Implementation of Coulomb force

- Important for isovector observables
- Retarded electromagnetic field

BUU: point particle with cut-off

$$\vec{F}_i^{cou} = \frac{Z_i e^2}{N_m} \sum_{j(\neq i), r_{ij} > r_c} Z_j \frac{\vec{r}_{ij}}{r_{ij}^3}$$

Poisson equation approach

$$\nabla^2 \phi(\vec{r}) = -4\pi e \rho^c(\vec{r})$$

lattice Hamiltonian framework

$$\vec{F}_i^{cou} = -l^3 Z_i \sum_{\alpha} \frac{\partial \epsilon_\alpha^{cou}}{\partial \vec{r}_i}$$

$$\epsilon_\alpha^{\mathrm{cou}} = \frac{l^3}{2} e^2 \sum_{\alpha'(\neq\alpha)} \frac{\rho_L^c(\vec{r}_\alpha)\rho_L^c(\vec{r}_{\alpha'})}{|\vec{r}_\alpha - \vec{r}_{\alpha'}|} - \frac{3}{4} e^2 \left[\frac{3\rho_L^c(\vec{r}_\alpha)}{\pi}\right]^{4/3}$$

QMD: treat Coulomb interaction as an effective interaction

$$V^{cou} = \frac{Z_i Z_j e^2}{|\vec{r} - \vec{r}'|}$$

$$\vec{F}_i^{cou} = -\frac{\partial}{\partial \vec{r}_i}\left[\frac{e^2}{2} Z_i \sum_{j(\neq i)} \frac{Z_j}{r_{ij}} \mathrm{erf}\left(\frac{r_{ij}}{\sqrt{4\mathrm{L}}}\right)\right] = -\frac{e^2}{2} Z_i \sum_{j(\neq i)} Z_j \left[\frac{\exp(-r_{ij}^2/4\mathrm{L})}{r_{ij}\sqrt{\pi \mathrm{L}}} - \frac{1}{r_{ij}^2}\mathrm{erf}\left(\frac{r_{ij}}{\sqrt{4\mathrm{L}}}\right)\right] \cdot \frac{\vec{r}_{ij}}{r_{ij}}$$

2. Representative studies on constraining EOS with HICs

Probe of symmetric NM EOS: kaon production

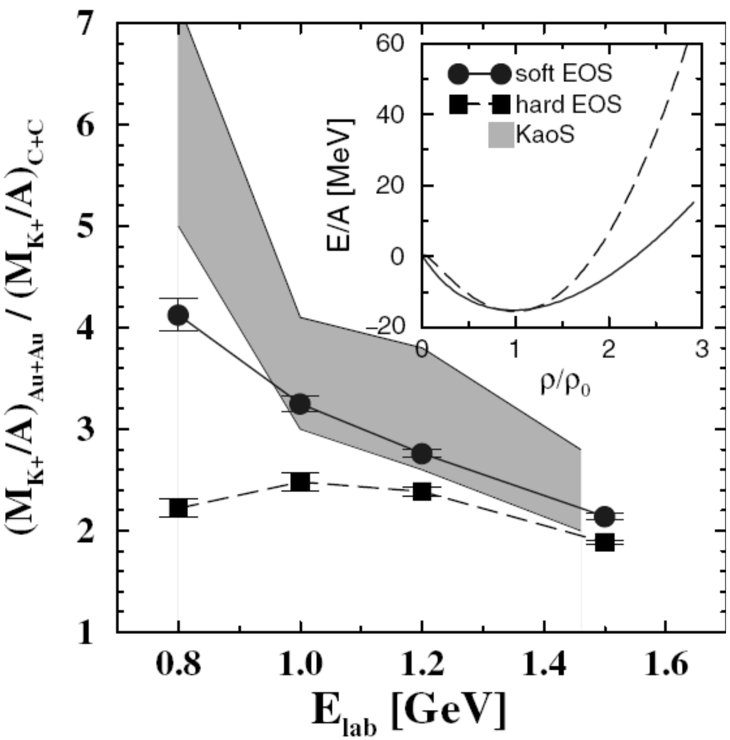

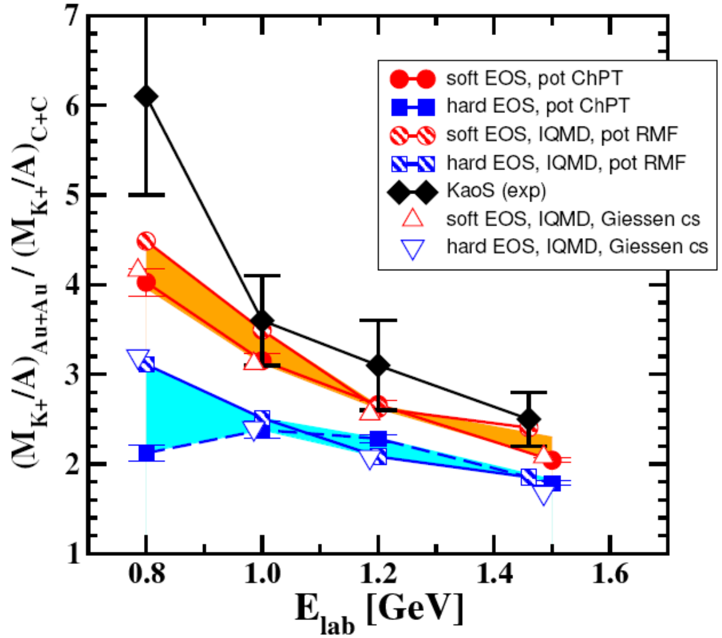

C. Fuchs and H.H. Wolter, EPJA 30, 5 (2006)

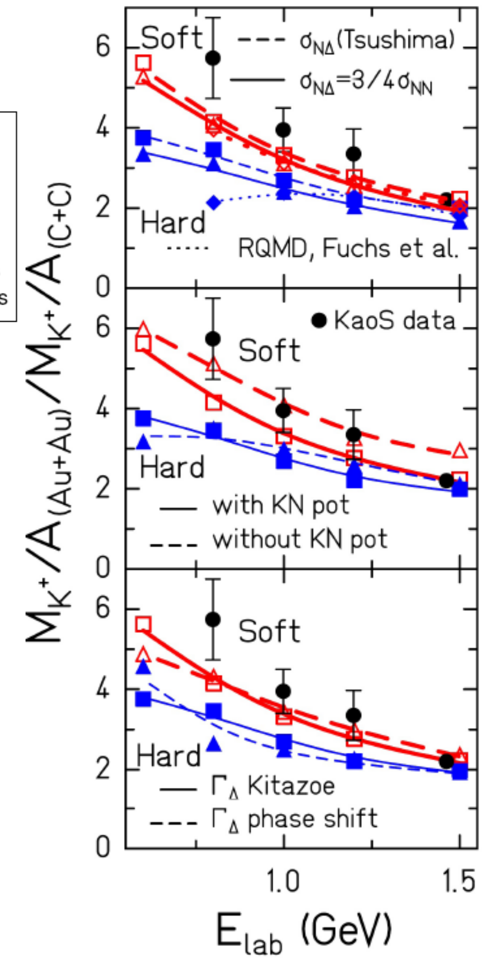

J. Aichelin and C.M. Ko, PRL 55, 2661 (1985)

C. Fuchs et al., PRL 86, 1974 (2001)

Ch. Hartnack, H. Oeschler, and J. Aichelin, PRL 96, 012302 (2006)

$$B + B \to B + Y + K^+ \qquad \pi + B \to Y + K^+$$

$$\Delta + N \to N + K^+ + \Lambda$$

Probes of symmetric NM EOS: collective flows

Slope of Transverse flow/directed flow (v_1)

Elliptic flow(v_2)

$$v_1 = \left\langle \frac{p_x}{p_T} \right\rangle$$

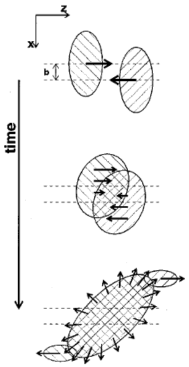

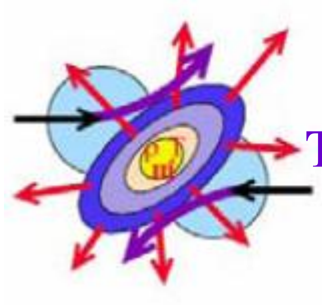

Model dependence?

Theoretical uncertainty?

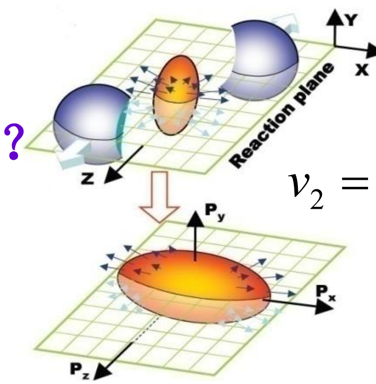

$$v_2 = \left\langle \frac{p_x^2 - p_y^2}{p_T^2} \right\rangle$$

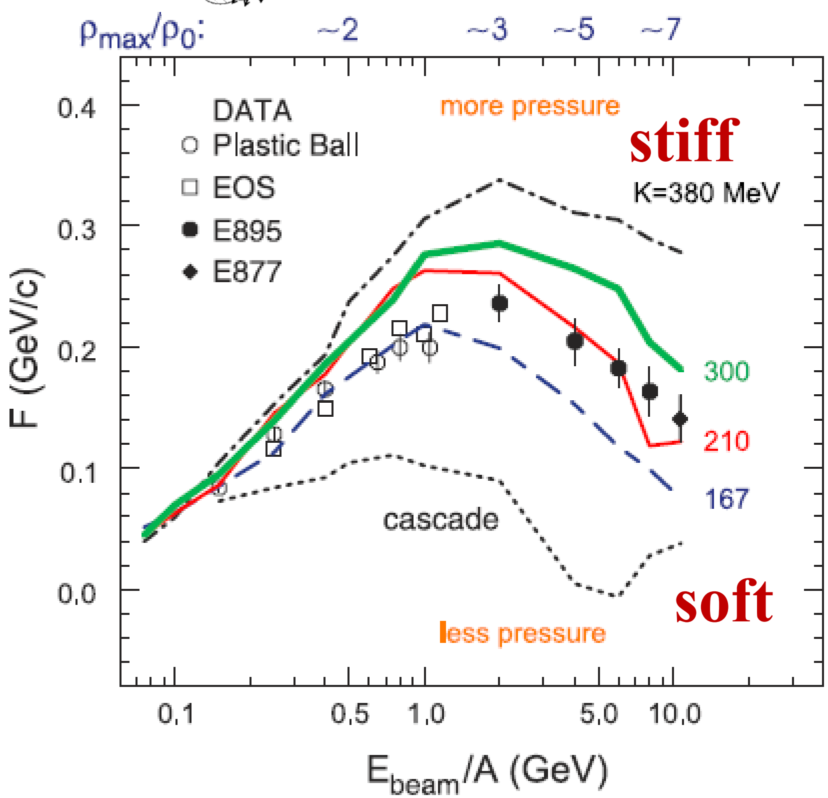

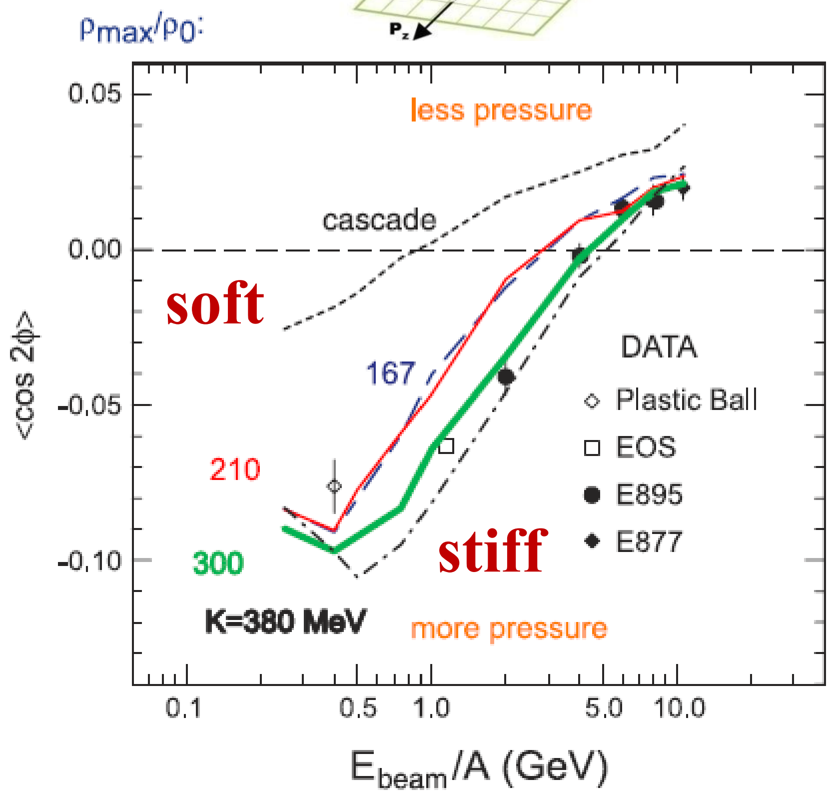

P. Danielewicz, R. Lacey, and W.G. Lynch, Science (2002)

Probes of symmetric NM EOS: collective flows

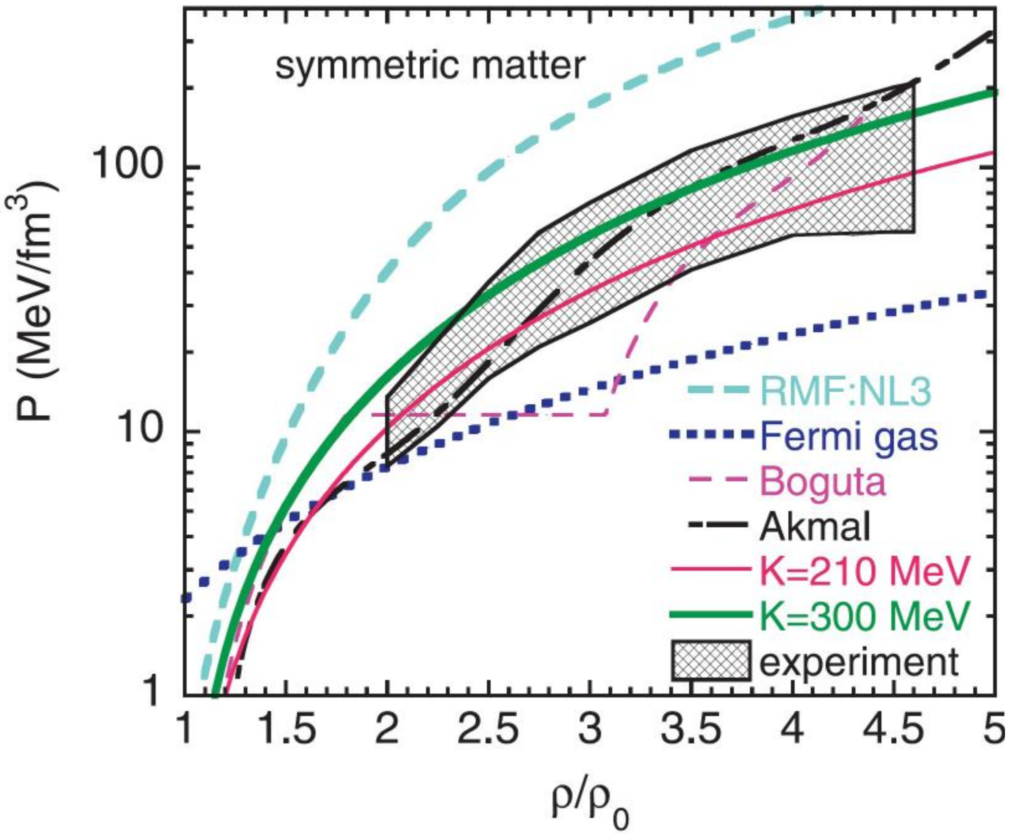

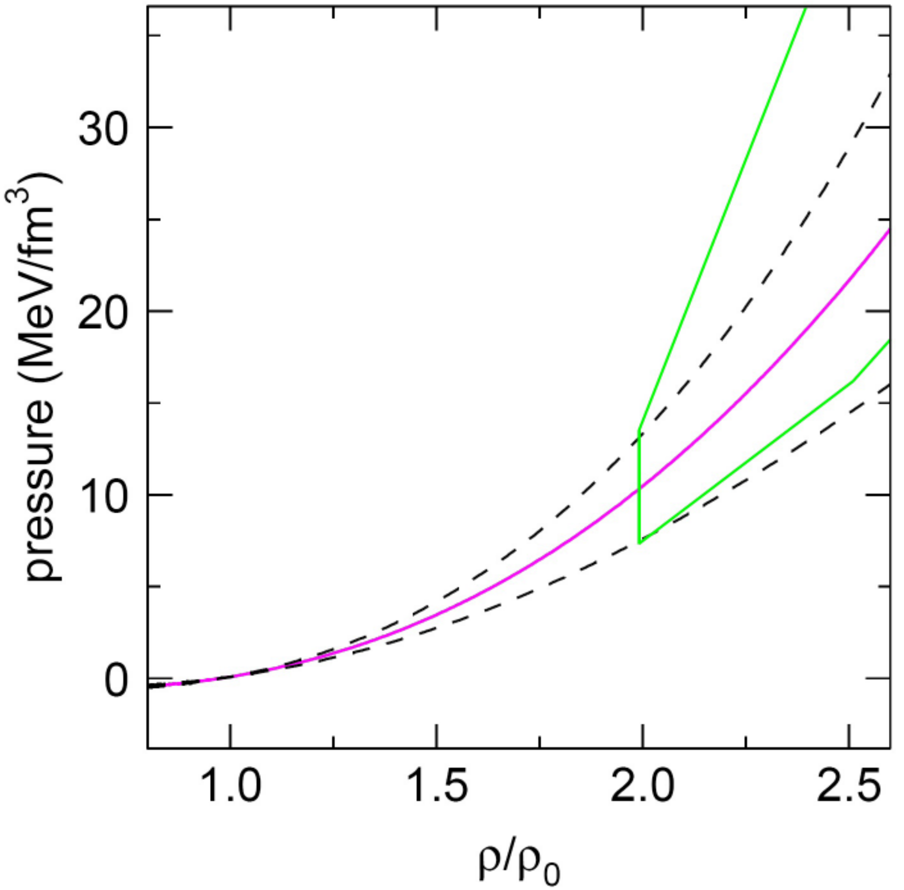

P. Danielewicz, R. Lacey,
and W.G. Lynch, Science (2002)

More latest constraint from IQMD-FOPI:
A. LeFèvre, Y. Leifels, W. Reisdorf, J. Aichelin,
and Ch. Hartnack, NPA 945, 112 (2016).

Probes of Esym at subsaturation densities: n/p

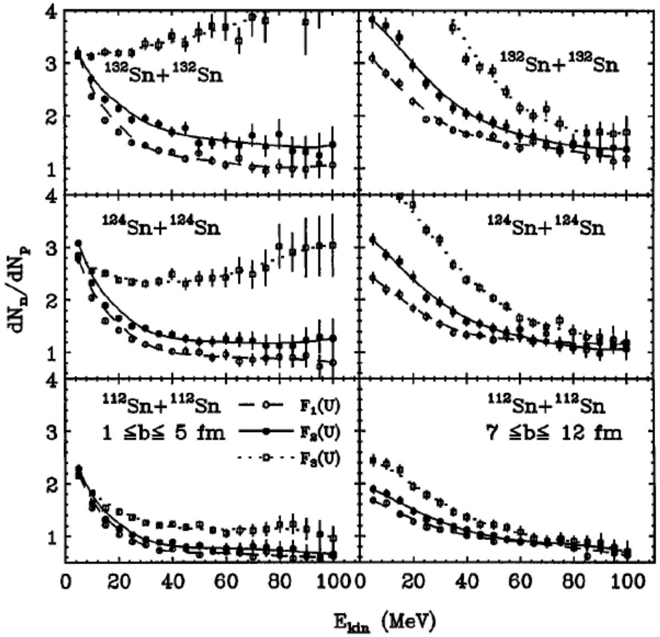

$$F_1(u) = 2u^2/(1+u)$$

$$F_2(u) = u$$

$$F_3(u) = u^{1/2}$$

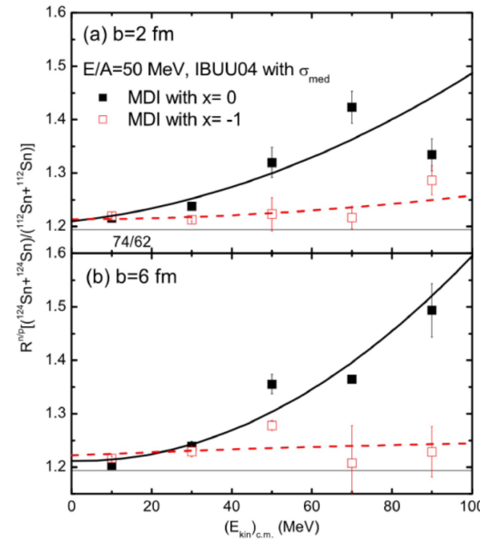

B. A. Li, L. W. Chen, G. C. Yong, W. Zuo, PLB 634, 378 (2006)

B. A. Li, C. M. Ko, and Z. Z. Ren, PRL 78, 1644 (1997)

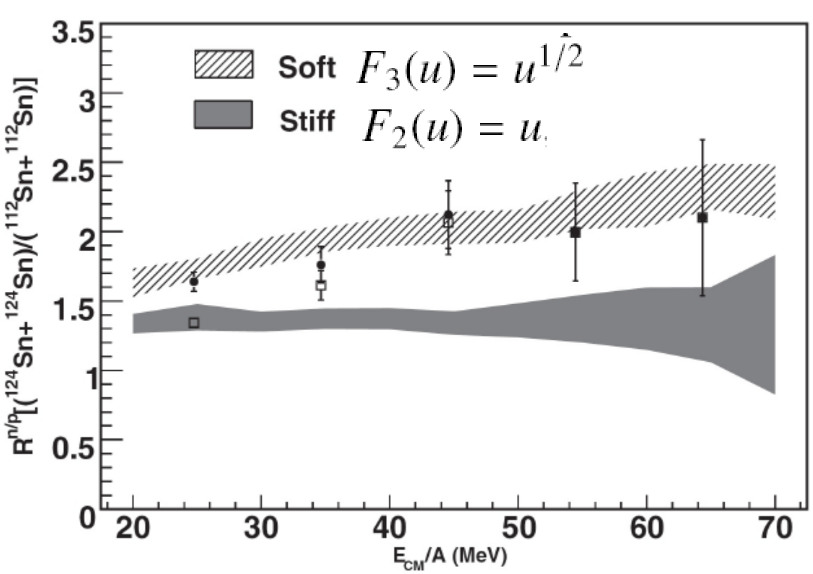

M. A. Famiano et al., PRL 97, 052701 (2006)

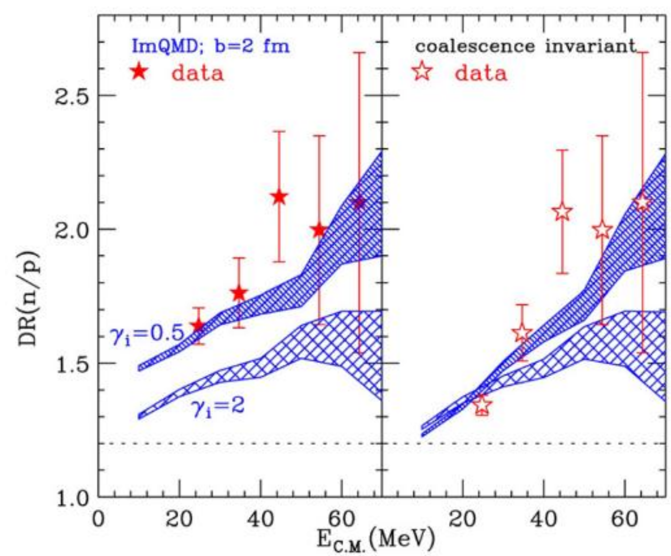

Y. X. Zhang, P. Danielewicz, M. A. Famiano, Z. X. Li, W. G. Lynch, M. B. Tsang, PLB 664, 145 (2008)

Probes of Esym at subsaturation densities: t/^{3}He

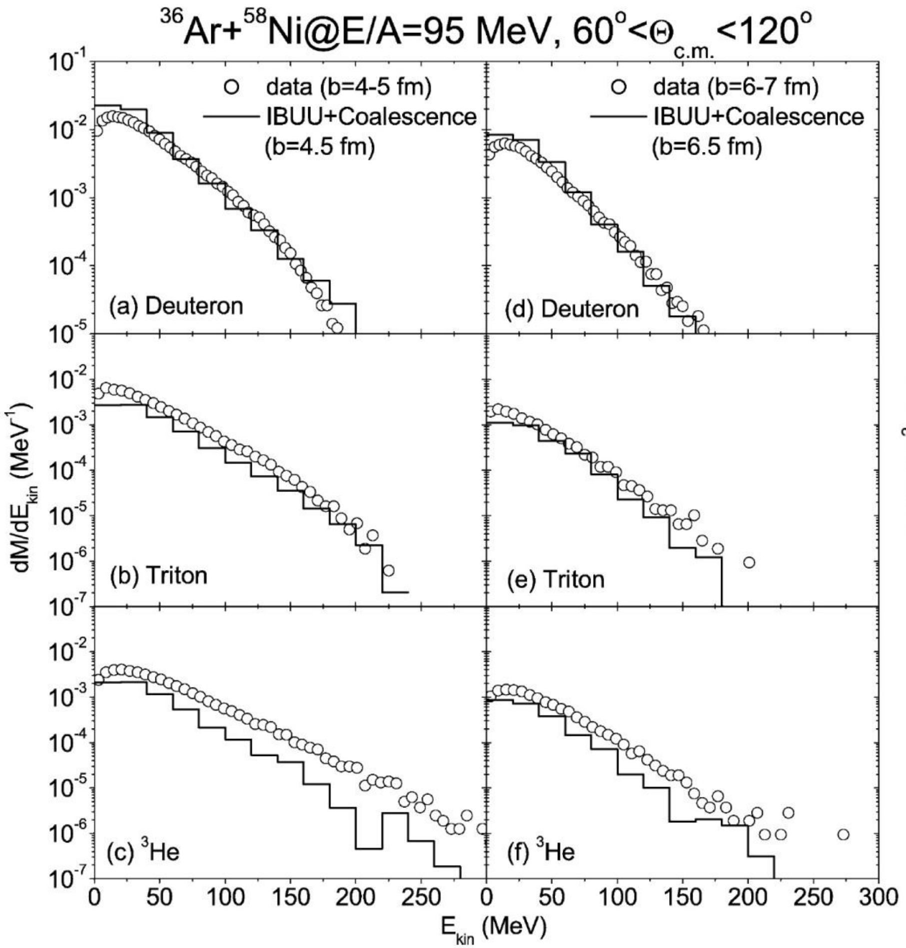

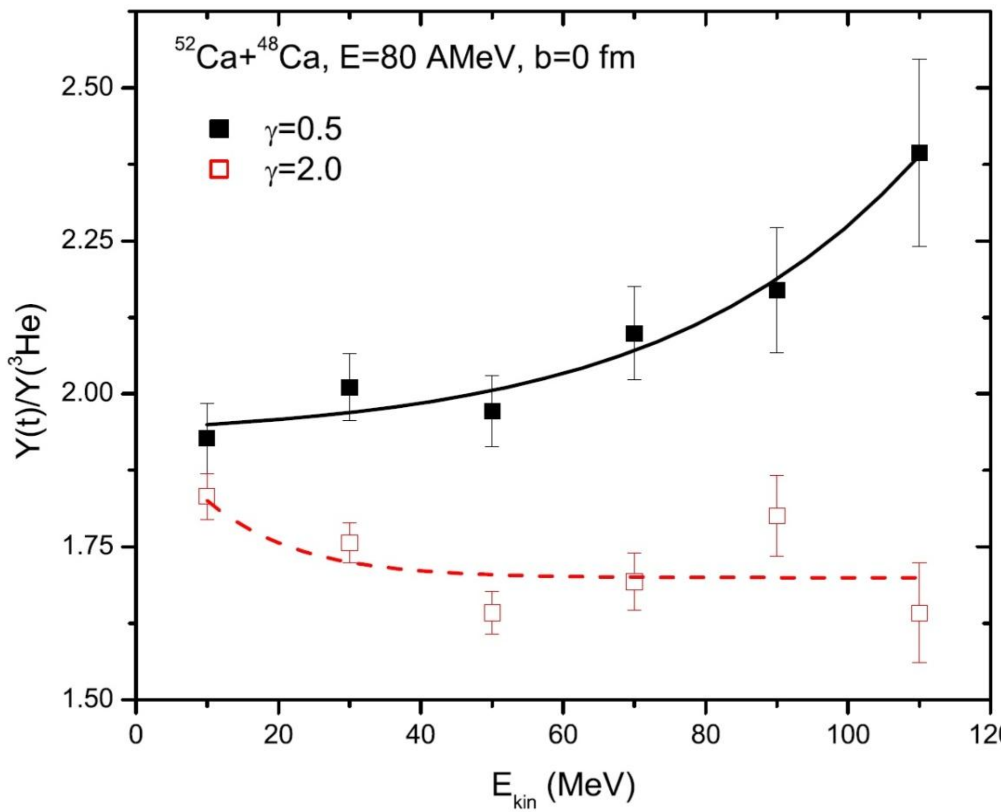

L. W. Chen, C. M. Ko, and B. A. Li, PRC 68, 017601 (2003)

L. W. Chen, C. M. Ko, and B. A. Li, NPA 729, 809 (2003)

$$\rho^{W}_{t(^3\mathrm{He})}(\rho, \lambda, \mathbf{k}_\rho, \mathbf{k}_\lambda) = 8^2 \exp\left(-\frac{\rho^2+\lambda^2}{b^2}\right) \exp(-(\mathbf{k}_\rho^2 + \mathbf{k}_\lambda^2) b^2)$$

Probes of Esym at subsaturation densities: collective flows

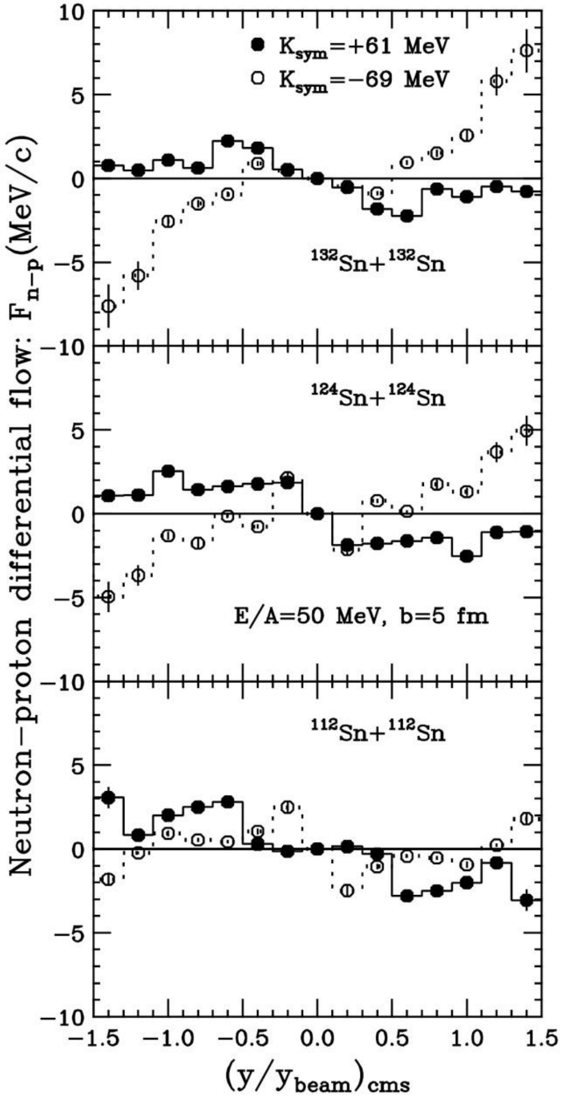

B.A. Li, PRL 85, 4421 (2000)

$$F_{n-p}(y) = \frac{1}{N(y)} \sum_i (p_x)_i \tau_i$$

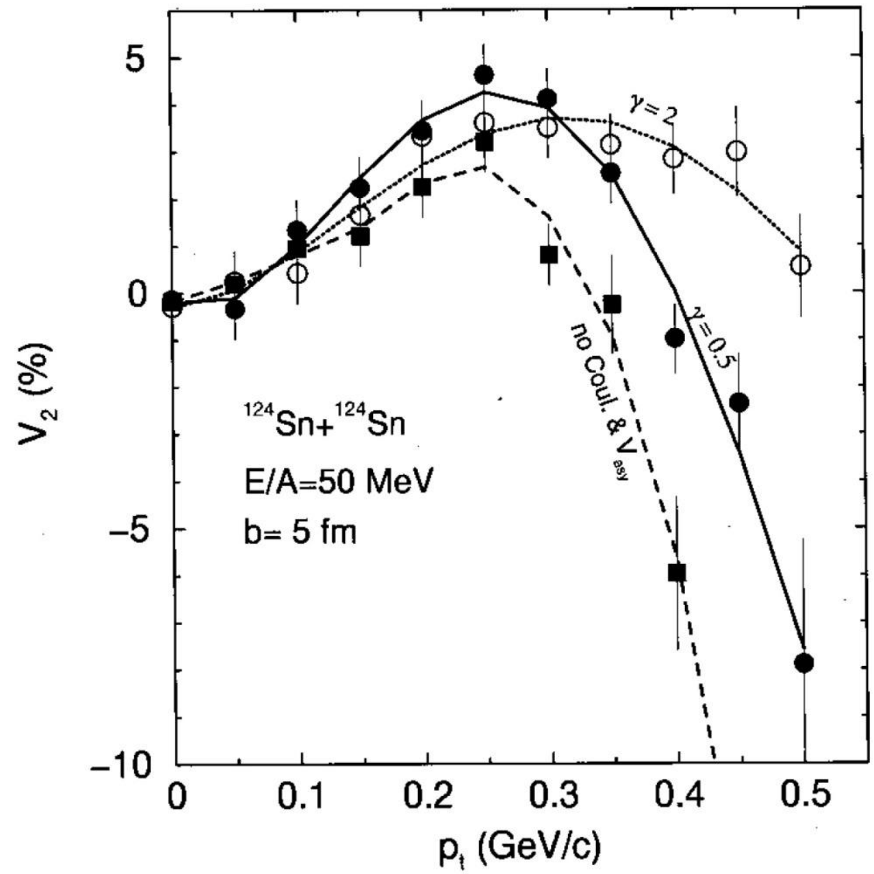

B. A. Li, A. T. Sustich, and B. Zhang, PRC 64, 054604 (2001)

Probes of Esym at subsaturation densities: isoscaling of produced isotopes

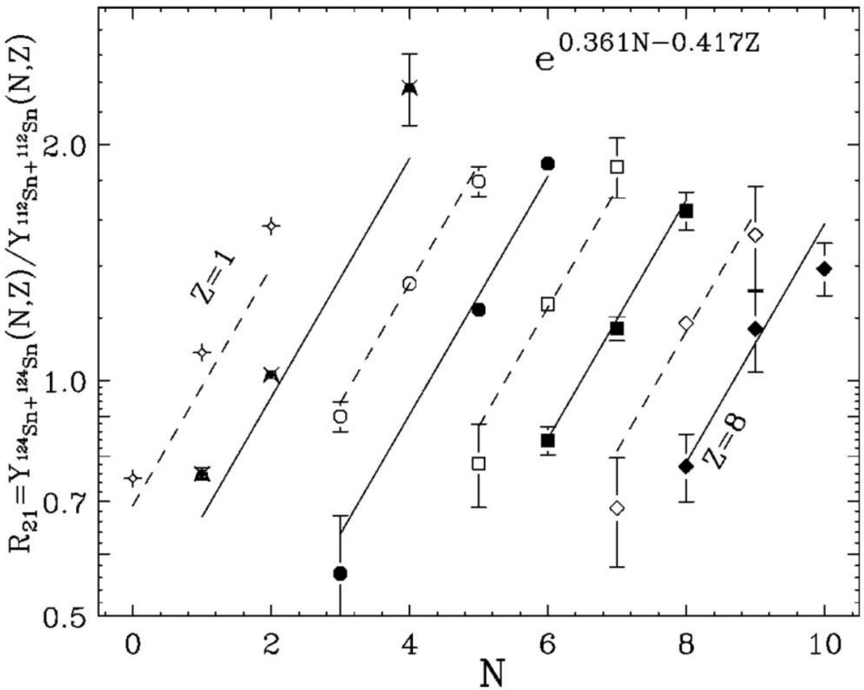

M. B. Tsang et al., PRL 86, 5023 (2001)

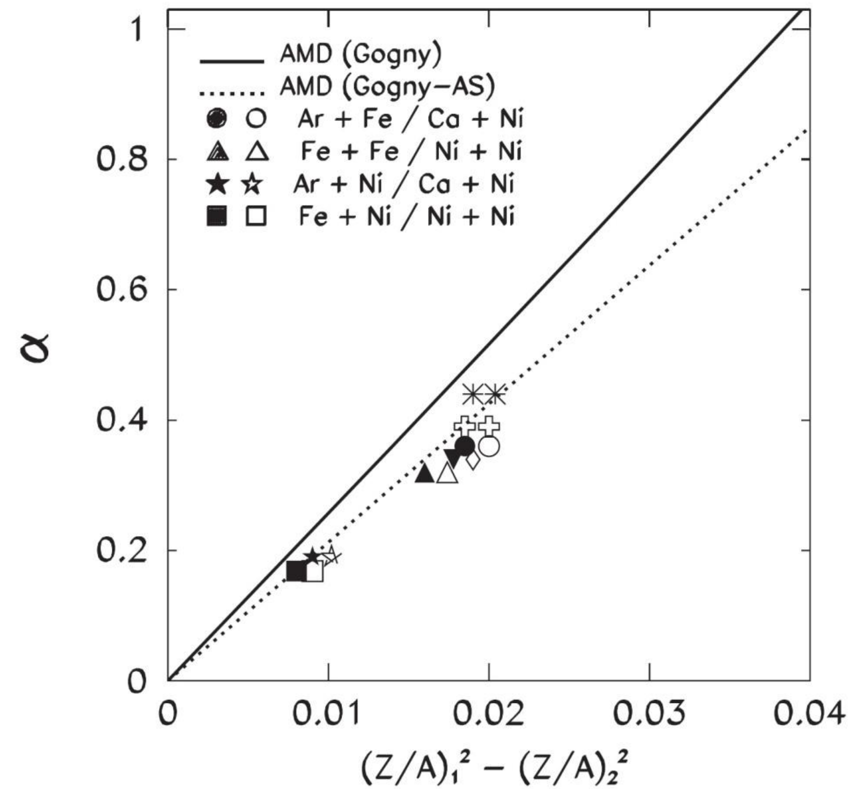

D. V. Shetty, S. J. Yennello, and G. A. Souliotis, PRC 75, 034602 (2007)

$$R_{12}(N,Z) = Y_2(N,Z)/Y_1(N,Z) = C\exp(\alpha N + \beta Z)$$

$$\alpha = 4C_{sym}[(Z_1/A_1)^2 - (Z_2/A_2)^2]/T$$

Probes of Esym at subsaturation densities: isospin diffusion

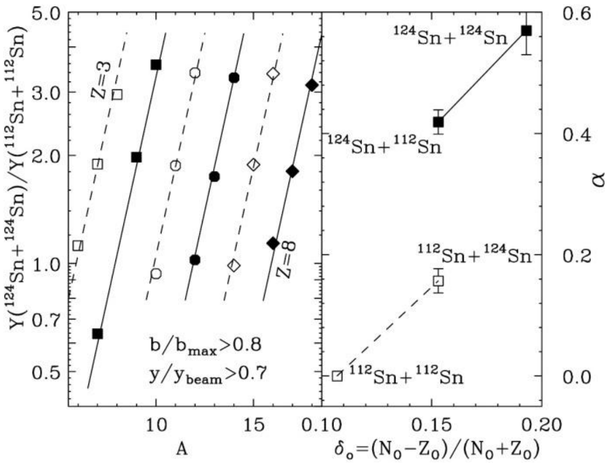

$$R_i = \frac{2x - x_{124+124} - x_{112+112}}{x_{124+124} - x_{112+112}}$$

M.B. Tsang et al., PRL 92, 062701 (2004)

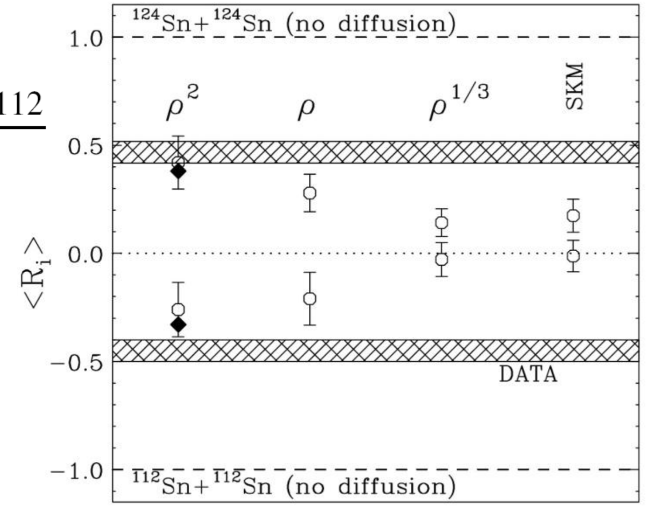

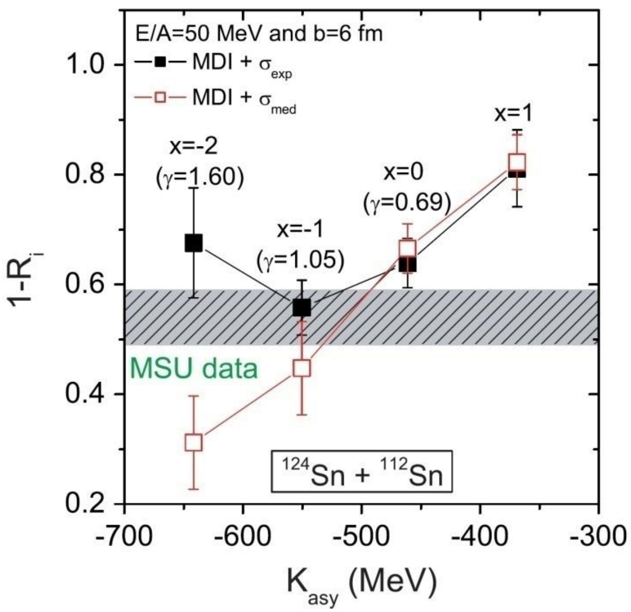

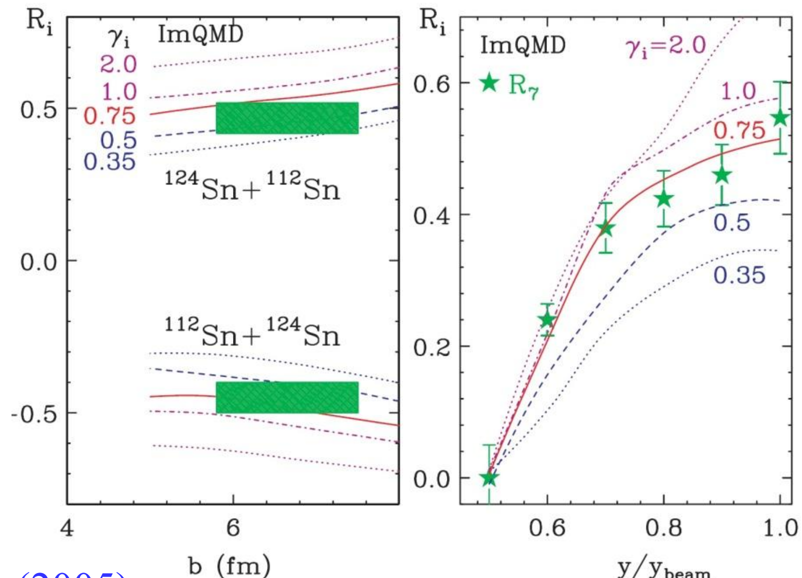

L.W. Chen, B.A. Li, and C.M. Ko, PRL 94, 032701 (2005)
B.A. Li and L.W. Chen, PRC 72, 064611 (2005)

M.B. Tsang et al., PRL 102, 122701 (2009)

Probes of Esym at subsaturation densities: Hanbury-Brown Twiss correlation

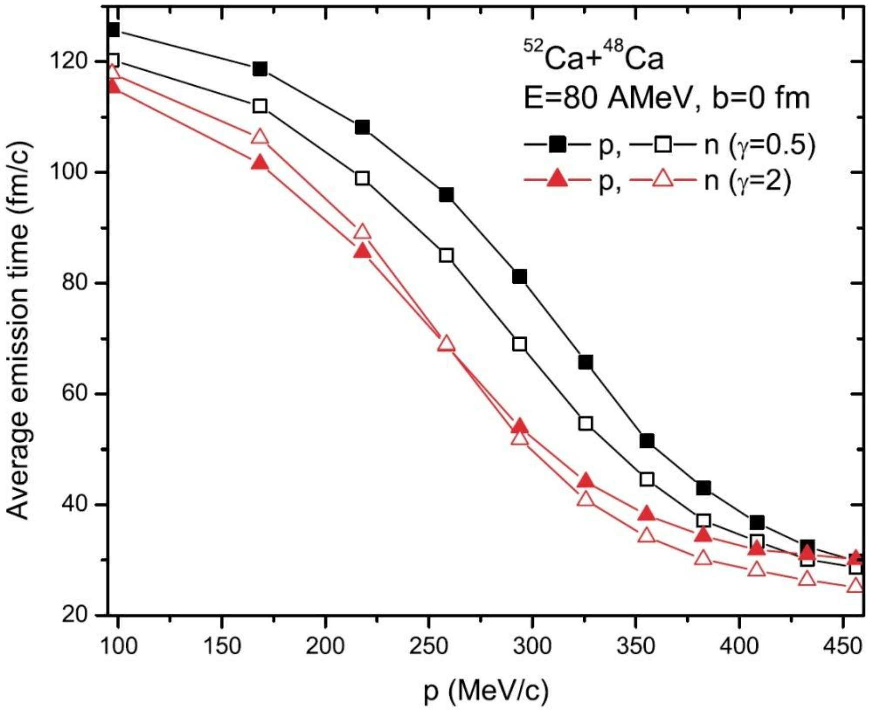

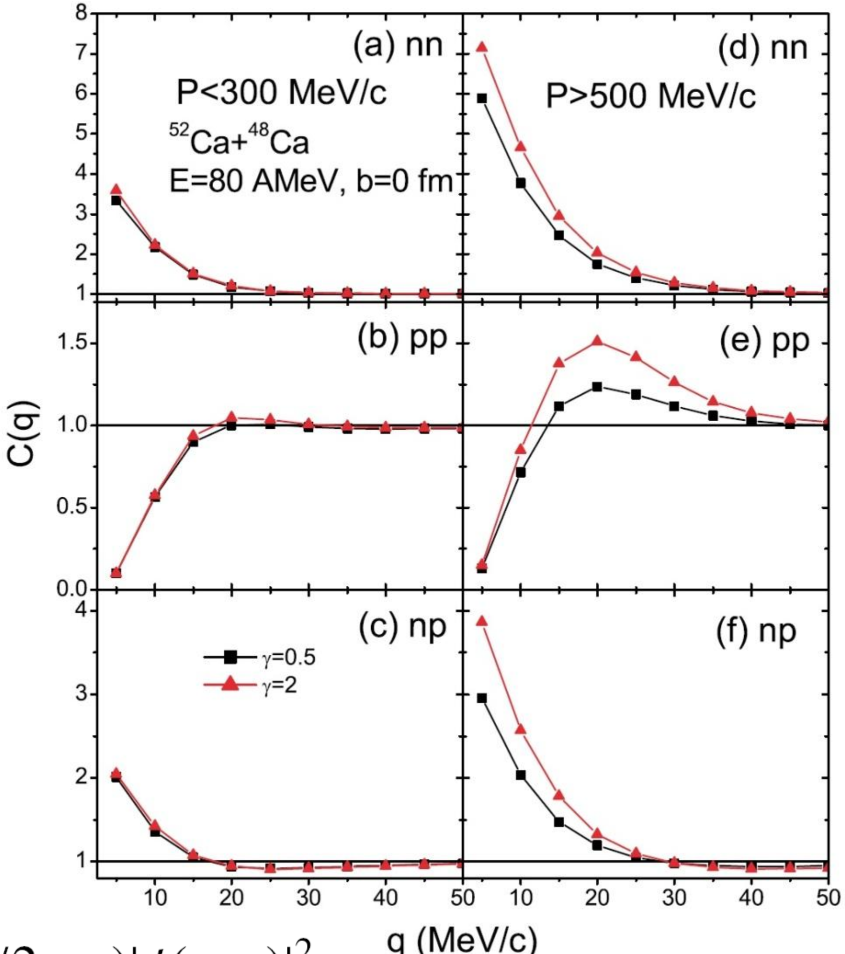

L.W. Chen, V. Greco, C.M. Ko, and B.A. Li, PRL 90, 162701 (2003)

$$C(\mathbf{P},\mathbf{q}) = \frac{\int d^4x_1 d^4x_2 g(\mathbf{P}/2, x_1) g(\mathbf{P}/2, x_2) |\phi(\mathbf{q},\mathbf{r})|^2}{\int d^4x_1 g(\mathbf{P}/2, x_1) \int d^4x_2 g(\mathbf{P}/2, x_2)}$$

Probes of Esym at subsaturation densities: np correlation angle

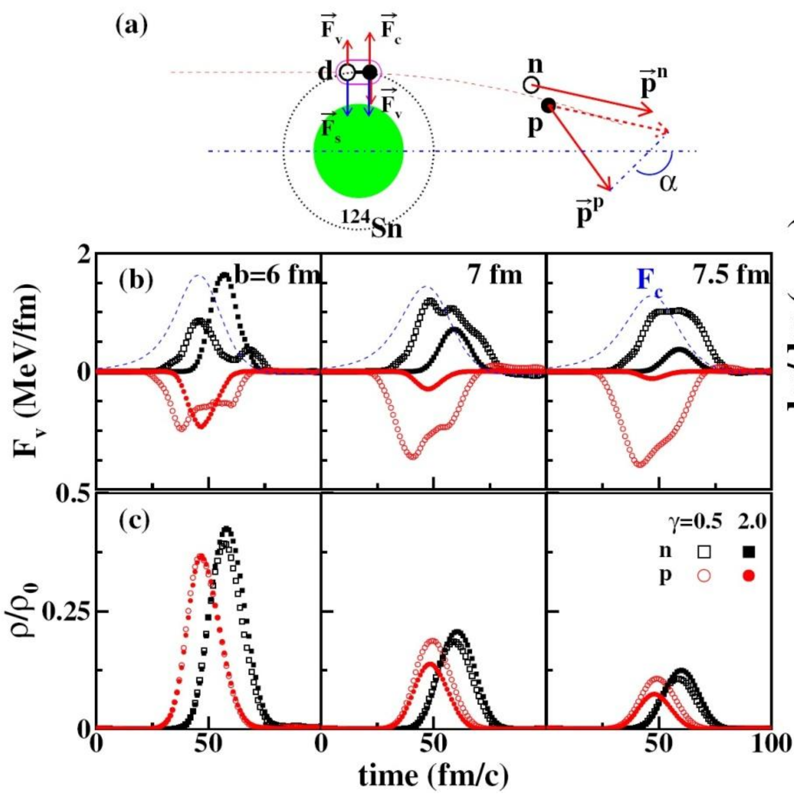

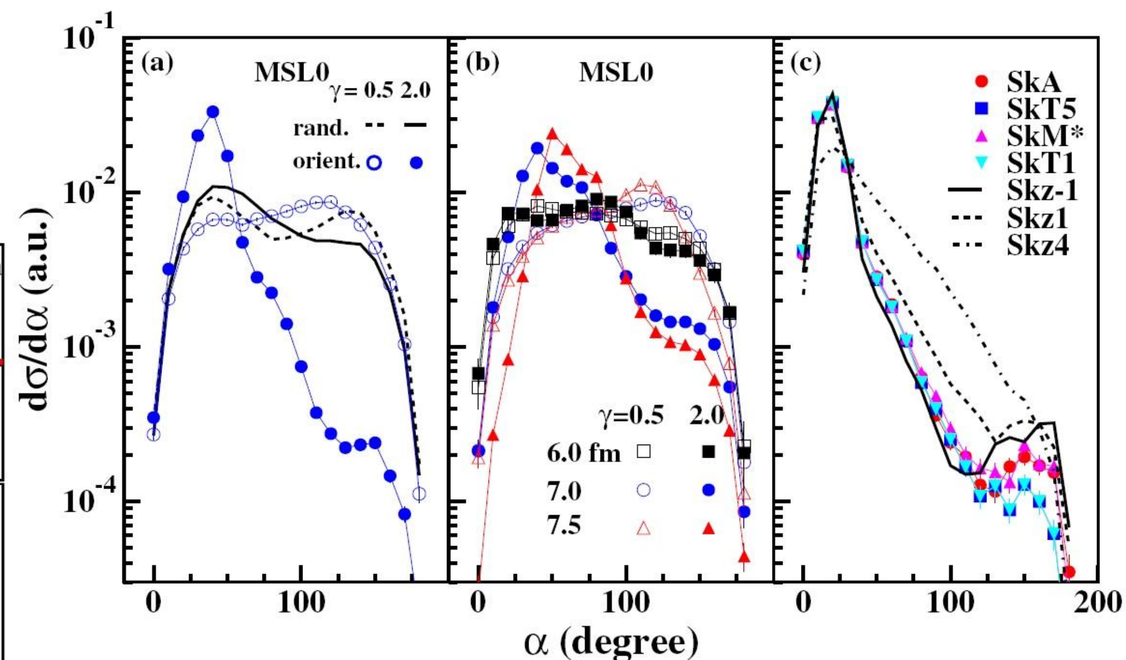

L. Ou, Z. G. Xiao, H. Yi, N. Wang, M. Liu, and J. L. Tian, PRL 115, 212501 (2015)

Probes of Esym at suprasaturation densities: differential flow

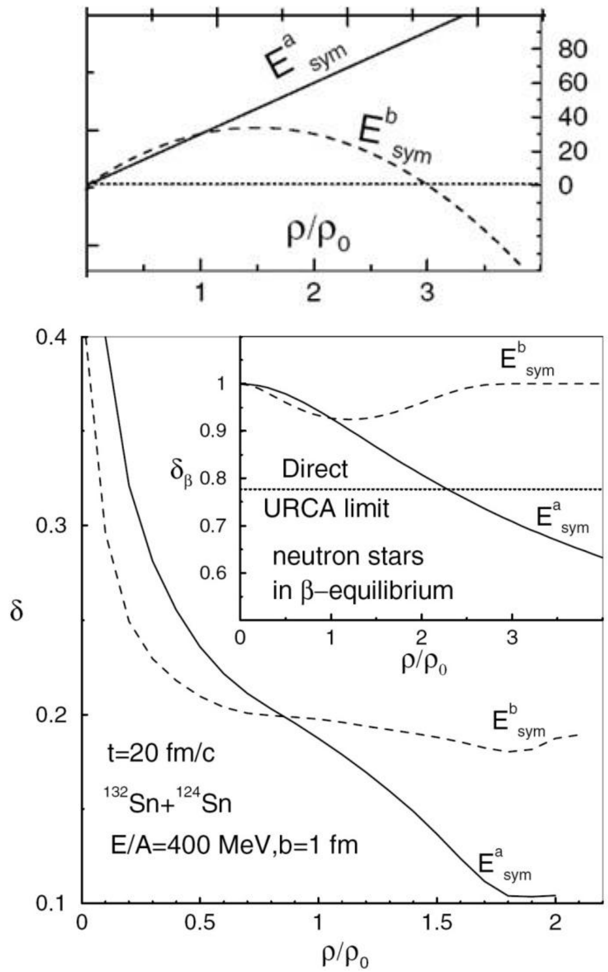

B.A. Li, PRL 88, 192701 (2002)

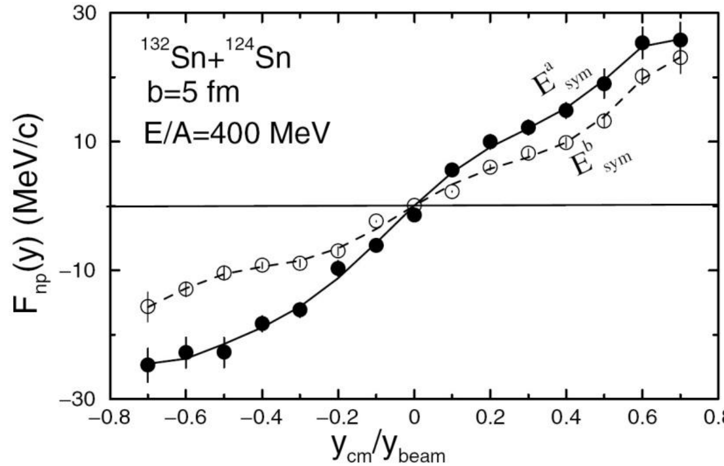

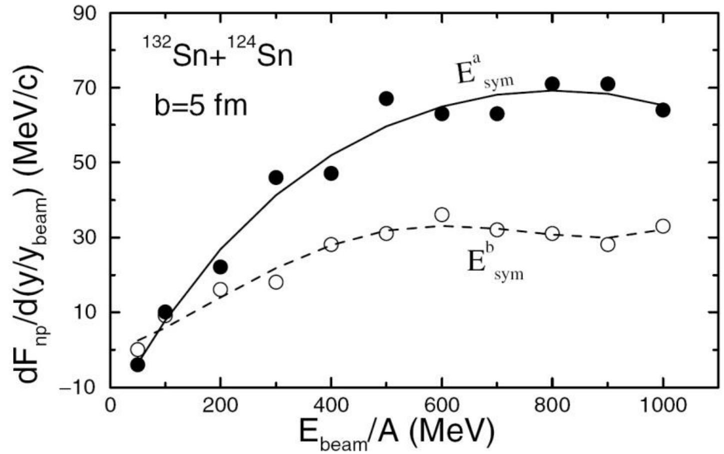

$$F_{n-p}(y) = \frac{1}{N(y)} \sum_i (p_x)_i \tau_i$$

Probes of Esym at suprasaturation densities: elliptic flow

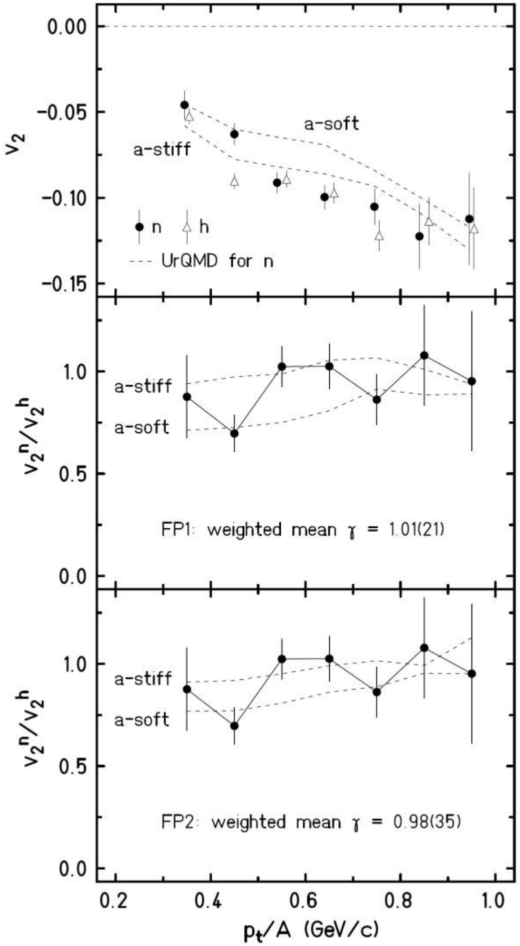

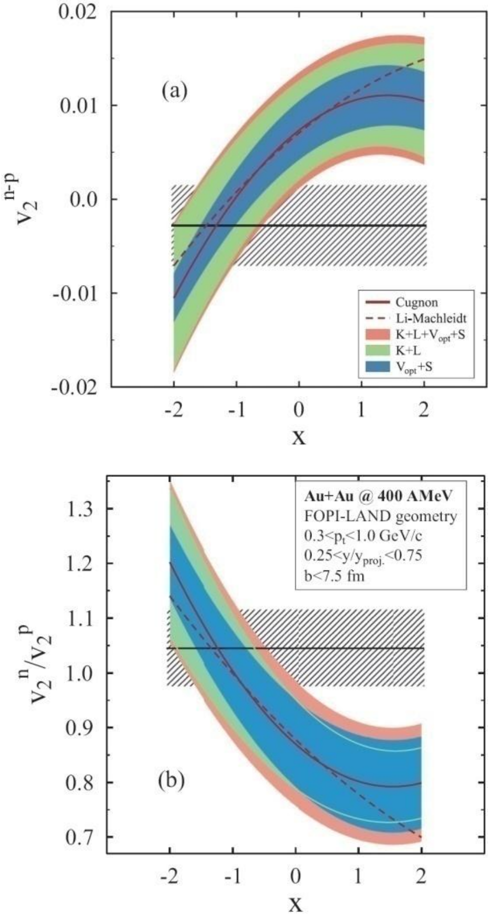

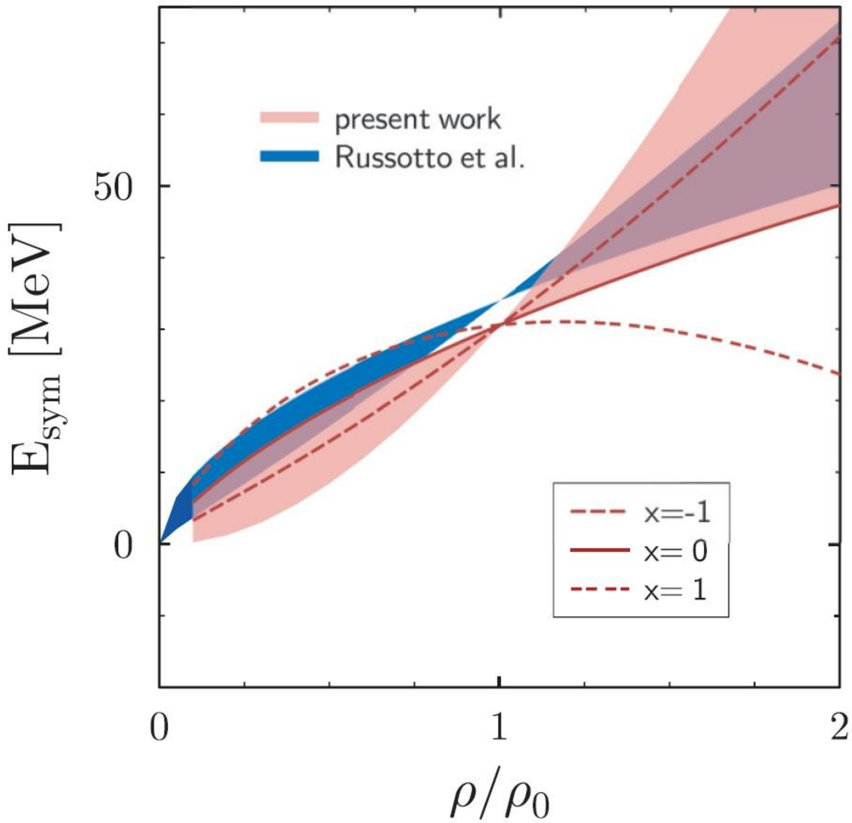

P. Russotto et al., PLB 697, 471 (2011)

M.D. Cozma, Y. Leifels, W. Trautmann, and Q. Li, and P. Russotto, PRC 88, 044912 (2013)

Probes of Esym at suprasaturation densities: charged pion yield ratio

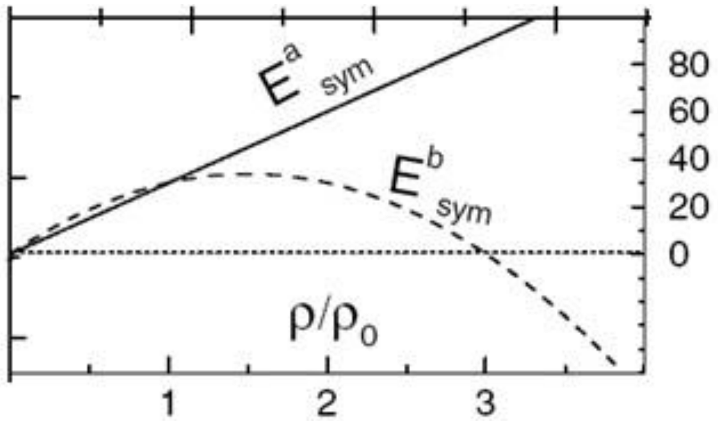

B.A. Li, PRL 88, 192701 (2002)

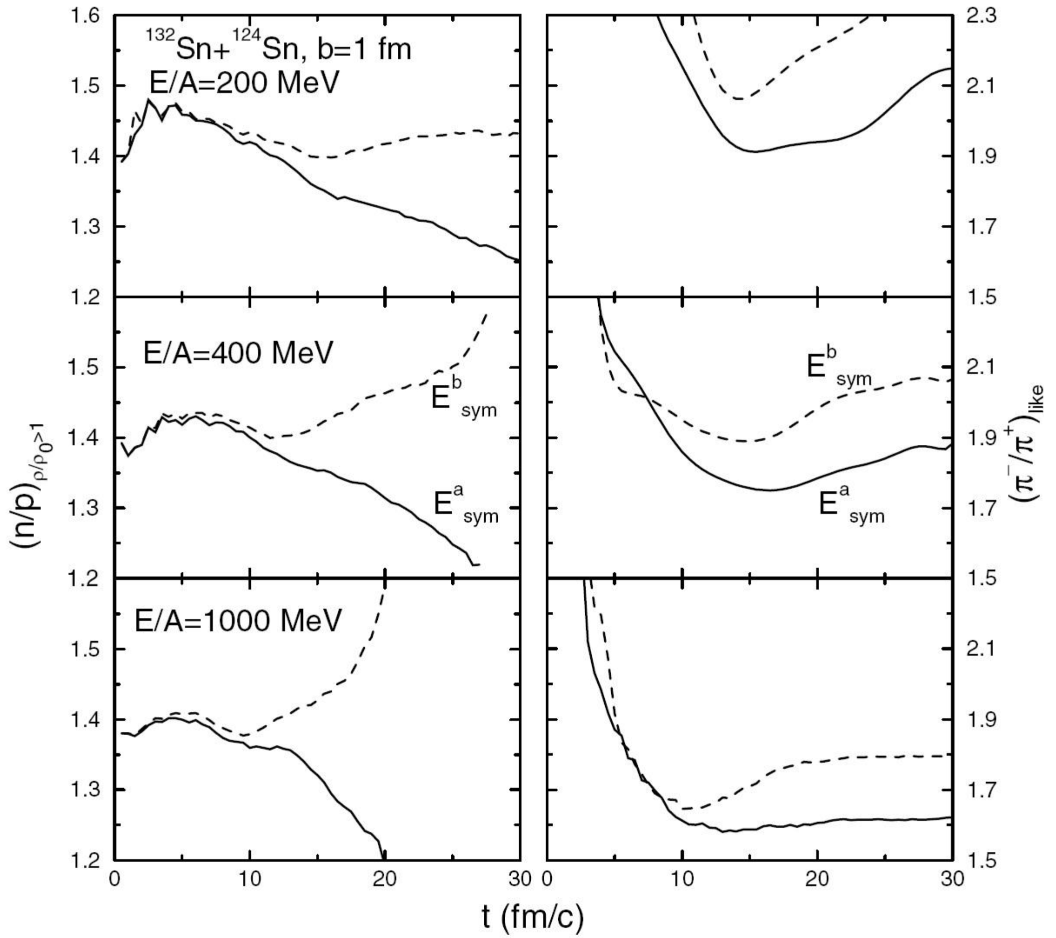

$$n + n \rightarrow \Delta^- + p,\ \Delta^- \rightarrow n + \pi^- \quad p + p \rightarrow \Delta^{++} + n,\ \Delta^{++} \rightarrow p + \pi^+$$

Probes of Esym at suprasaturation densities: charged pion yield ratio

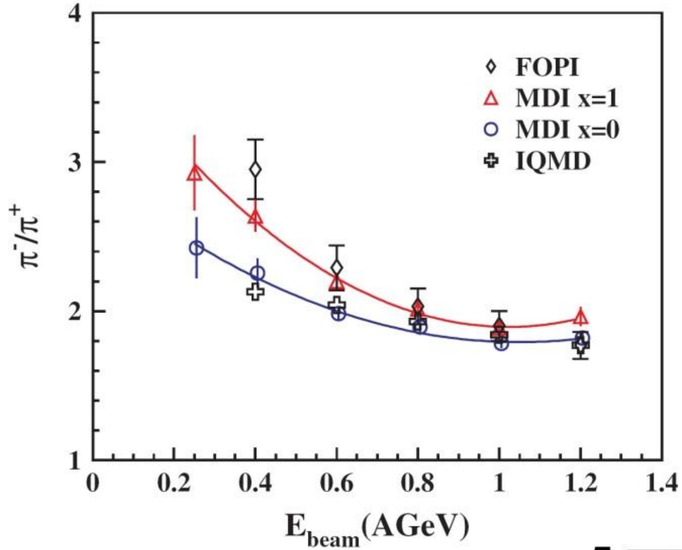

Z.G. Xiao et al.,
PRL 102, 062502 (2009)

Z.Q. Feng and G.M. Jin
PLB 683, 104 (2010)

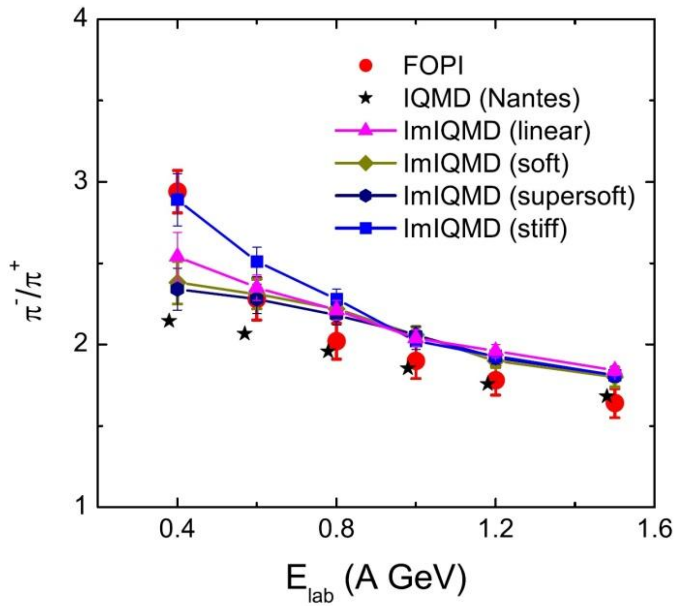

W. J. Xie et al.,
PLB 718, 1510 (2013)

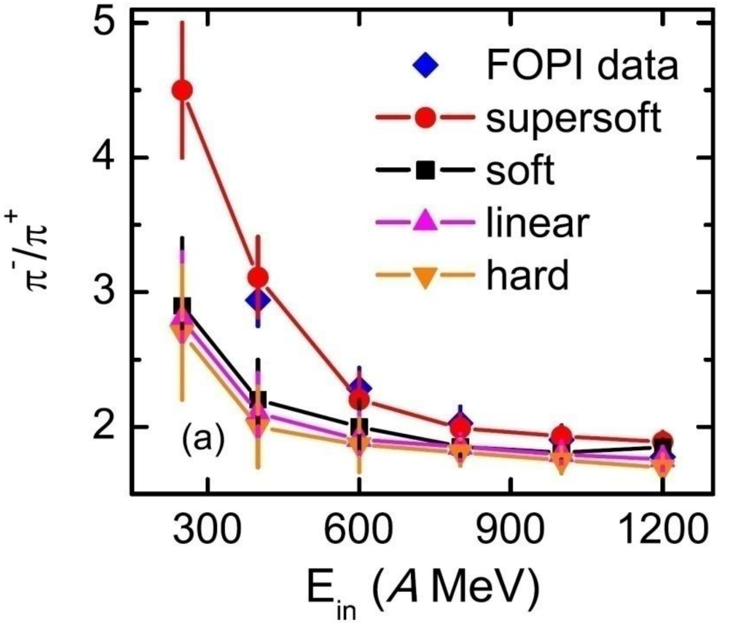

Probes of Esym at suprasaturation densities: charged pion yield ratio

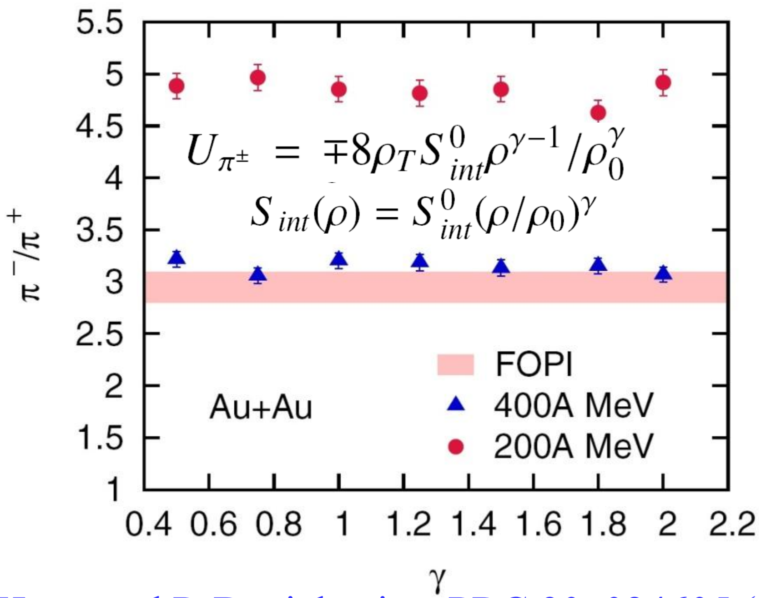

J. Hong and P. Danielewicz, PRC 90, 024605 (2010)

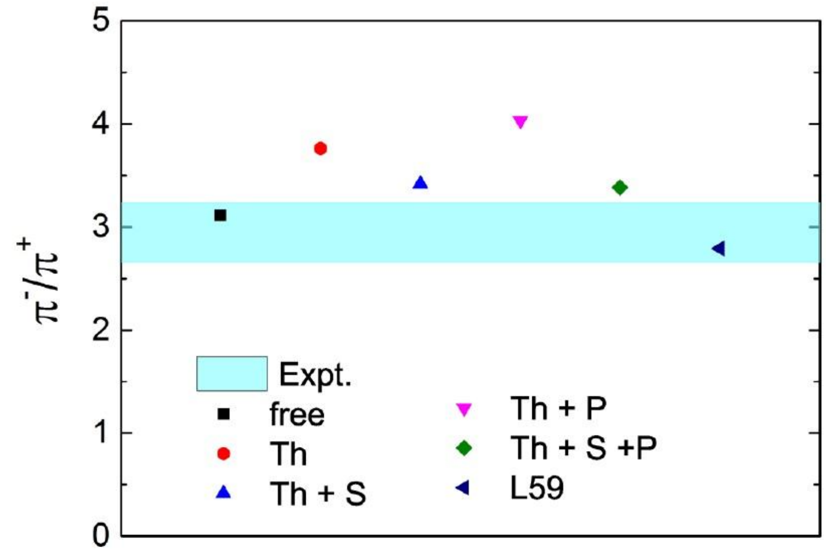

Z. Zhang and C.M. Ko, PRC 95, 064604 (2017)

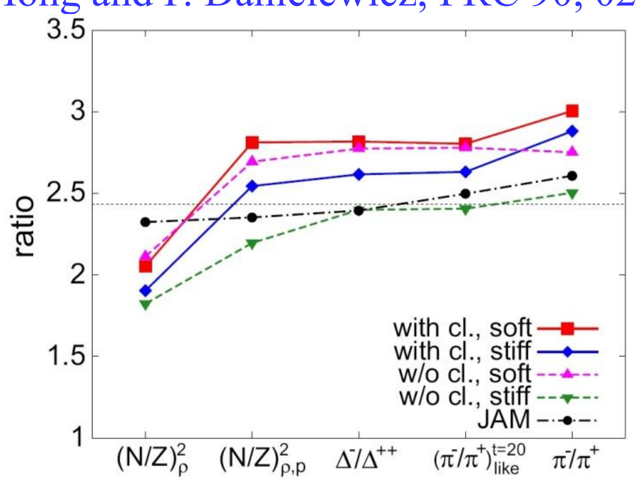

N. Ikeno et al.,
PRC 93, 044612 (2016)

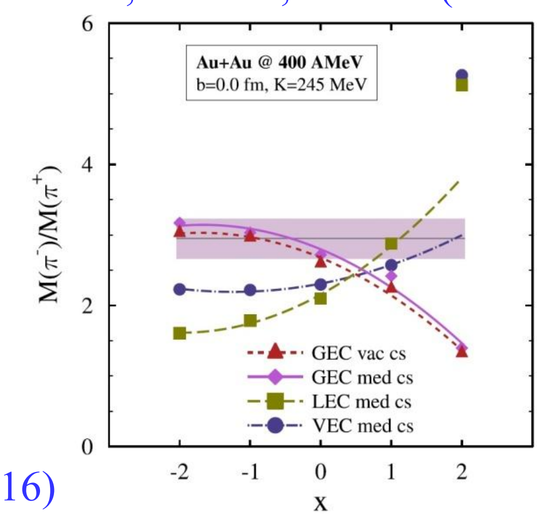

M.D. Cozma,
PLB 753, 166 (2016)

Divergence of Esym from FOPI π^-/π^+ data

LQMD, Feng/Jin, PLB (2010)

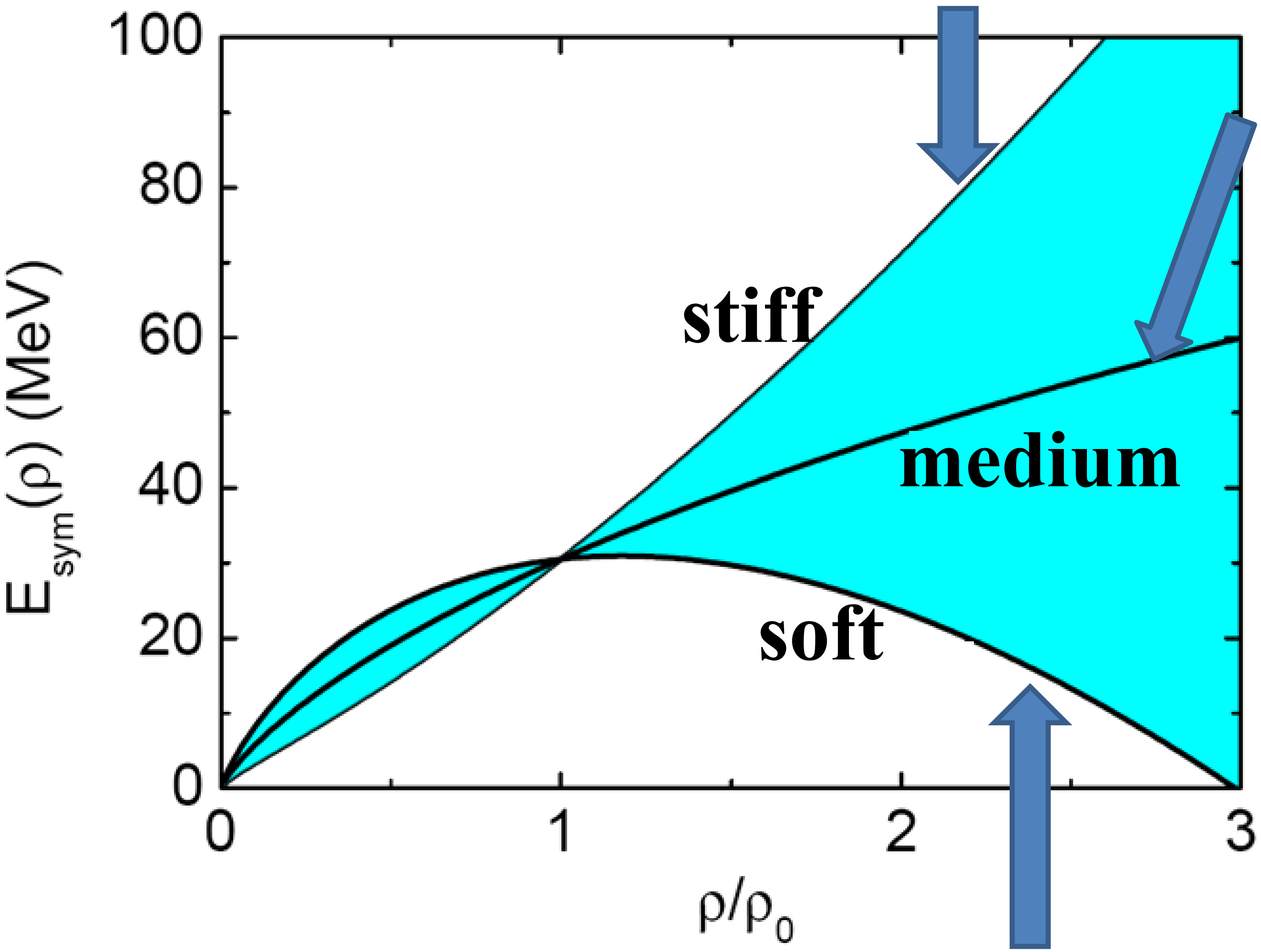

IBUU04, Xiao/Chen/Li/Zhang, PRL, (2009)
IBL, Xie/Su/Zhu/Zhang, PLB, (2013)

TuQMD,
Cozma/Trauntmann/Li, PRC (2013)

Pion s&p-wave from thermal model
Xu/Ko/Oh, PRC (2010)
Xu/Chen/Li/Ko/Ma, PRC (2013)

Pion s-wave from pBUU
Hong/Pawel, PRC (2014)

Pion threshold effect from RVUU
Song/Ko, PRC (2015)

Energy conservation from TuQMD
Cozma, PLB (2016)

Clustering and Pauli Blocking from JAM/AMD
Ikeno/Ono/Nara/Onoshi, PRC (2016,2019)

Pion s&p-wave from RVUU
Zhang/Ko (2017,2018)
...

Probes of Esym at suprasaturation densities: kaon yield ratio

$$n + \pi^- \rightarrow \Sigma^- + K^0 \qquad p + \pi^+ \rightarrow \Sigma^+ + K^+$$

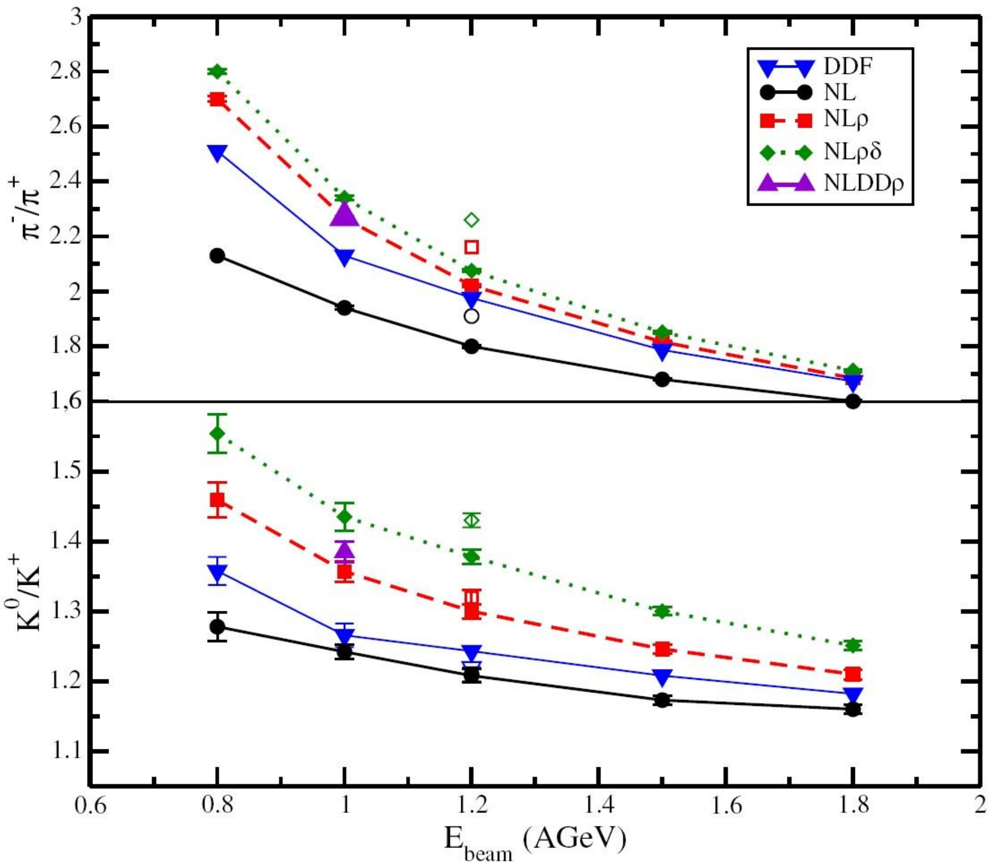

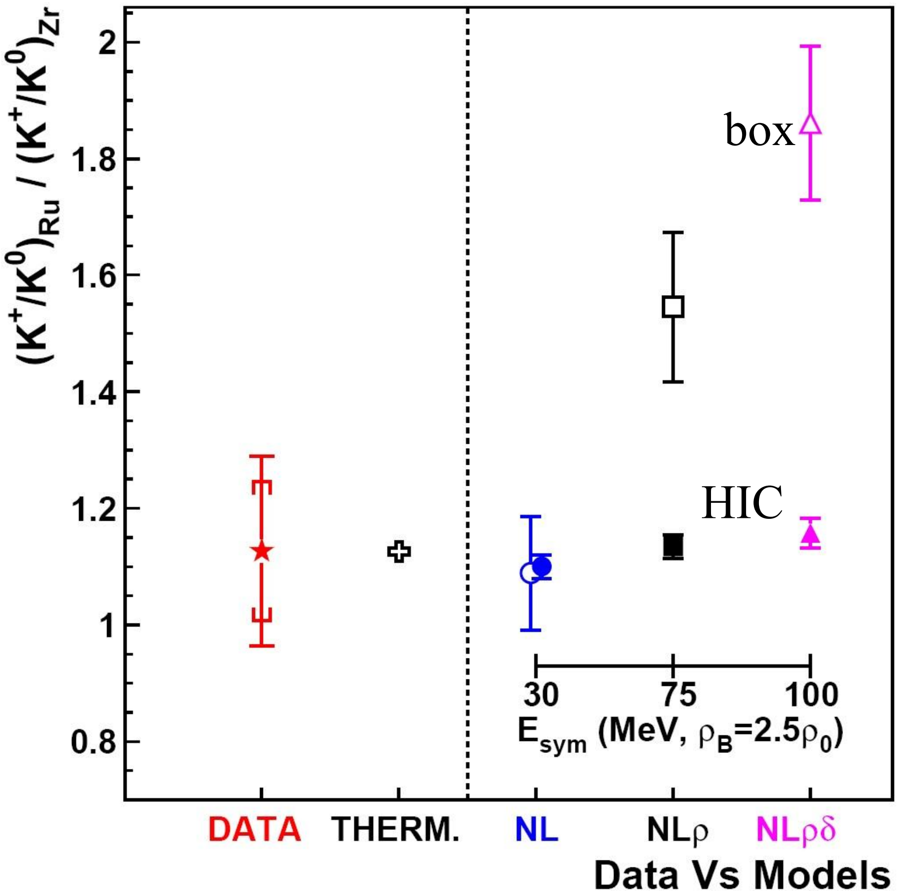

G. Ferini et al., PRL 97, 202301 (2006)

X. Lopez et al., PRC 75, 011901(R) (2007)

Probes of np effective mass splitting: np emission

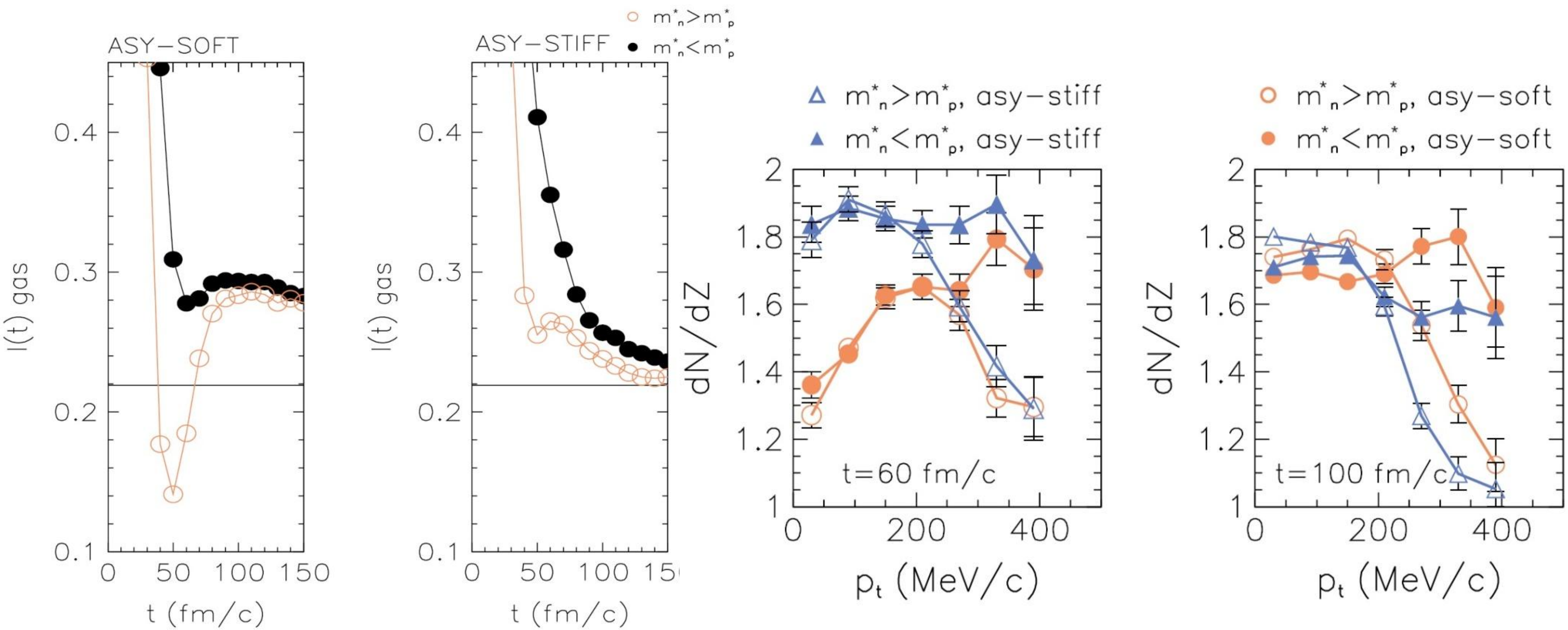

J. Rizzo, M. Colonna, and M. Di Toro, PRC 72, 064609 (2005)

Probes of np effective mass splitting: isospin diffusion

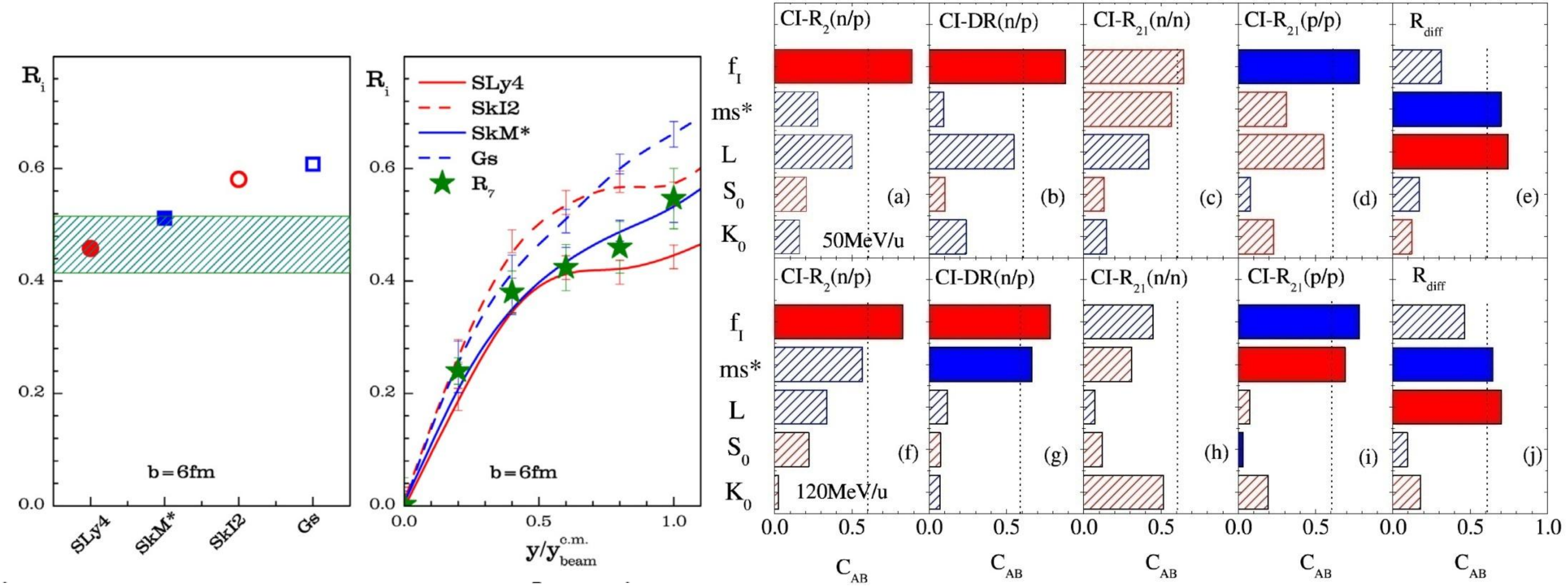

Para.	ρ_0	E_0	K_0	S_0	L	K_{sym}	m^*/m	m_n^*/m	m_p^*/m
SLy4	0.160	-15.97	230	32	46	-120	0.69	0.68	0.71
SkI2	0.158	-15.78	241	33	104	71	0.68	0.66	0.71
SkM*	0.160	-15.77	217	30	46	-156	0.79	0.82	0.76
Gs	0.158	-15.59	237	31	93	14	0.78	0.81	0.76

Y.X. Zhang et al., PLB 732, 186 (2014); Y.X. Zhang et al., PLB 749, 262 (2015)

3. Transport Model Evaluation Project (TMEP)

BUU Type	Code Correspondents	Energy Range [A GeV]	Relativity
BLOB	P. Napolitani, M. Colonna	0.01–0.5	non-rel
BUU-VM	S. Mallik	0.02–1	rel
DJBUU	Y. Kim, S. Jeon, M. Kim, C.-H. Lee, K. Kim	0.05–2	cov
GiBUU	J. Weil, T. Gaitanos, K. Gallmeister, U. Mosel	0.05–40	rel/cov
IBL	W.J. Xie, F.S. Zhang	0.05–2	rel
IBUU	J. Xu, L.W. Chen, B.A. Li	0.05–2	rel
LBUU(LHV)	R. Wang, Z. Zhang, L.-W. Chen	0.01–1.5	rel
pBUU	P. Danielewicz	0.01–12	rel
PHSD	E. Bratkovskaya, W. Cassing	0.1–200	rel/cov
RBUU	T. Gaitanos	0.05–2	cov
RVUU	Z. Zhang, C.M. Ko, T. Song	0.05–2	cov
SMASH	D. Oliinychenko, H. Elfner, A. Sorensen	0.5–200	cov
SMF	M. Colonna, P. Napolitani	0.01–0.5	non-rel
χBUU	Z. Zhang, C.M. Ko	0.01–0.5	non-rel
QMD Type	**Code Corespondents**	**Energy Range [AGeV]**	**Relativity**
AMD	A. Ono	0.01–0.3	non-rel
AMD+JAM	N. Ikeno, A. Ono	0.01–0.3	non-rel+rel
BQMD/IQMD	A. Le Fèvre, J. Aichelin, C. Hartnack, R. Kumar	0.05–2	rel
CoMD	M. Papa	0.01–0.3	non-rel
ImQMD	Y.X. Zhang, N. Wang, Z.X. Li	0.02–0.4	rel
IQMD-BNU	J. Su, F.S. Zhang	0.05–2	rel
IQMD-SINAP	G.Q. Zhang	0.05–2	rel
JAM	A. Ono, N. Ikeno, Y. Nara, A. Ohnishi	1–158	rel
JQMD 2.0	T. Ogawa, K. Niita, S. Hashimoto, T. Sato	0.01–3	rel
LQMD(IQMD-IMP)	Z.Q. Feng, H.G. Cheng	0.01–10	rel
TuQMD/dcQMD	D. Cozma	0.1–2	rel
UrQMD	Y. J. Wang, Q. F. Li, Y. X. Zhang	0.05–200	rel

14 BUU and 12 QMD, which one should be trusted?

H. Wolter, et al., Prog. Part. Nucl. Phys. 125, 103962 (2022)

History of Transport Model Evaluation Project I

Trento I (2003): energy 1-2 AGeV, emphasis on particle production p, π, K

mean field and Pauli blocking not quite so important

Summary Published in J.Phys. G31, 741 (2005)

Improvements from the workshop:

Prog.Part.Nucl.Phys. 56, 1 (2006)

Phys.Rep. 510, 119 (2012)

- **Trento II (2009): energy 100, 400 AMeV**

large differences in flow observables and collision rates

origin was not firmly identified, results not published

Participating codes in Trento workshop

code correspondents	acronyms
Barz/Wolf	
Cassing	HSD
Reiter	UrQMD
Hartnack	IQMD
Larionov	GiBUU
Chen	RVUU
Fuchs	TuQMD
Gaitanos	RBUU
Danielewicz	pBUU

3 QMD codes and 6 BUU codes

protons

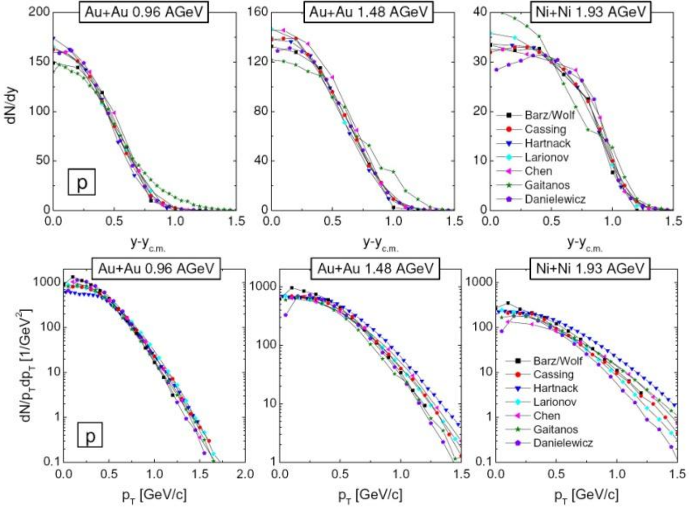

pions

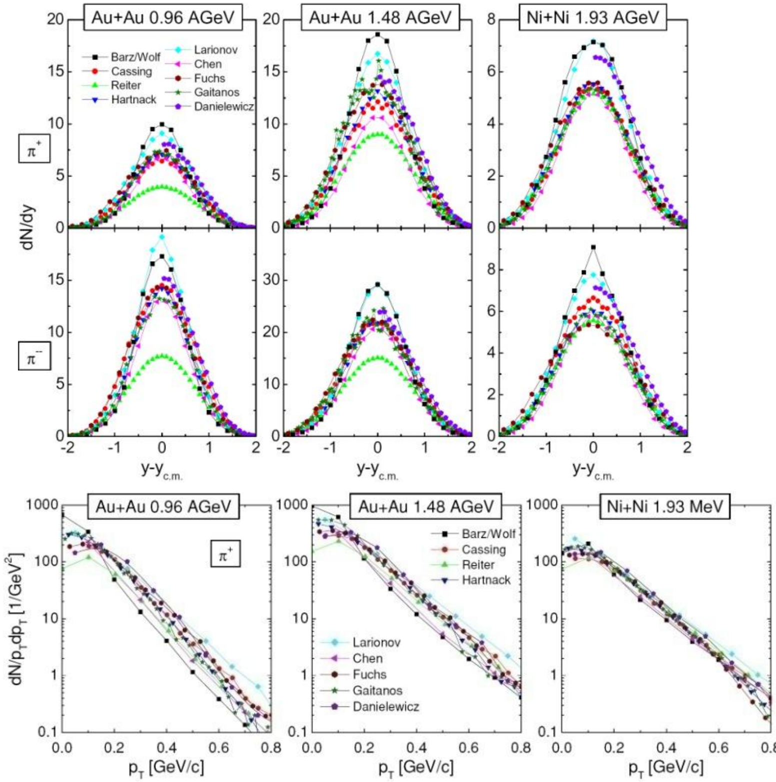

K$^+$

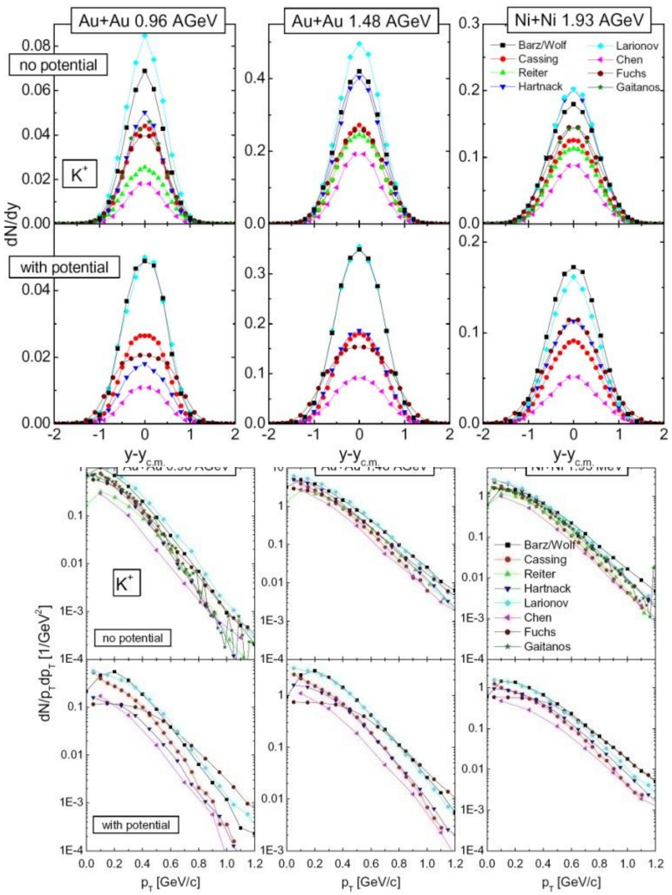

K- $\omega_K(\rho_B, k) = \sqrt{[m_K^*(\rho_B)]^2 + k^2}$ $\quad m_K^*(\rho_B) = m_K^0\left(1 - \alpha\frac{\rho_B}{\rho_0}\right)$

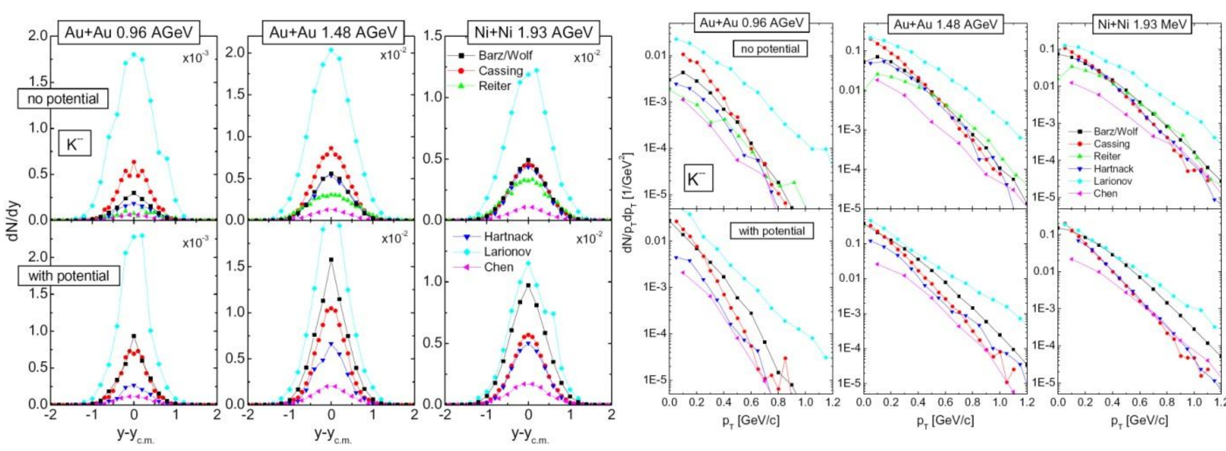

History of Transport Model Evaluation Project II

- Transport2014 (2014): Mainly 100 AMeV, also 400 AMeV. Focus on low-energy dynamics: stability, stopping, and flow

  Results published in Phys.Rev.C 93, 044609 (2016)

- Transport2017 (2017): Box calculation of NN scatterings, mean-field evolution, and production of pion-like particles

  Box-cascade: Phys.Rev.C 97, 034626 (2018)

  Box-pion: Phys.Rev.C 100, 044617 (2019)

  Box-Vlasov: Phys.Rev.C 104, 024603 (2021)

- Transport2019 (2019): production of pion-like particles at 270 AMeV

  HIC-pion: Phys.Rev.C 109, 044609 (2024)

  Box-pion2: Energy conservation effect on pion production

Transport2014 in Shanghai

Participating Codes

Boltzmann-Uehling-Uhlenbeck(BUU)-type models (9)

BUU-type	code correspondents	energy range	reference
BLOB	P.Napolitani,M.Colonna	$0.01 \sim 0.5$	[19]
GIBUU-RMF	J.Weil	$0.05 \sim 40$	[20]
GIBUU-Skyrme	J.Weil	$0.05 \sim 40$	[20]
IBL	W.J.Xie,F.S.Zhang	$0.05 \sim 2$	[21]
IBUU	J.Xu,L.W.Chen,B.A.Li	$0.05 \sim 2$	[11, 22]
pBUU	P.Danielewicz	$0.01 \sim 12$	[23]
RBUU	K. Kim,Y.Kim,T.Gaitanos	$0.05 \sim 2$	[24]
RVUU	T.Song,G.Q.Li,C.M.Ko	$0.05 \sim 2$	[25]
SMF	M.Colonna,P.Napolitani	$0.01 \sim 0.5$	[26]

In GeV

Find representative references for each code in PRC 93, 044609 (2016)

Participating Codes

Quantum-Molecular-Dynamics(QMD)-type models(9)

QMD-type	code correspondents	energy range	reference
AMD	A.Ono	$0.01 \sim 0.3$	[27]
IQMD-BNU	J.Su,F.S.Zhang	$0.05 \sim 2$	[28]
IQMD	C.Hartnack,J.Aichelin	$0.05 \sim 2$	[29, 30]
CoMD	M.Papa	$0.01 \sim 0.3$	[31]
ImQMD-CIAE	Y.X.Zhang,Z.X.Li	$0.02 \sim 0.4$	[32]
IQMD-IMP	Z.Q.Feng	$0.01 \sim 10$	[33]
IQMD-SINAP	G.Q.Zhang	$0.05 \sim 2$	[34]
TuQMD	D.Cozma	$0.1 \sim 2$	[35]
UrQMD	Y.J.Wang,Q.F.Li	$0.05 \sim 200$	[36, 37]

In GeV

ImQMD-GXNU: low-energy fusion reaction

Find representative references for each code in PRC 93, 044609 (2016)

Homework description: Initialization and reaction parameters

2) Reaction:

a) **Au + Au, at 100 AMeV**

Initial coordinate space: Woods-Saxon distribution

b) Initialisation: Initialize your (test)particles to obtain in coordinate space a Fermi function density profile with radius $R=xA^{1/3}$ ($x=1.12$ fm) and diffuseness $a=0.6$ fm. In case you are using finite size (test)particles, use a sphere of the above radius and try to adjust the width in such a way as to approach the diffuseness (if possible).
The momentum of the particles should then be chosen randomly in the local Fermi sphere.

c) impact parameter b= 7. and 20. fm, with initial distance (between the centers of project and target) in z-direction 16 fm

d) number of runs and (test)particles:
  BUU: 10 runs, 100 TP/nucleon (for finite size TP), 500 TP/nucleon (for point TP)
  MD: 1000 runs.

e) time evolution: run until t=140 fm/c. Use the time step you are usually using. For a second order integration method we suggest 0.5 fm/c.

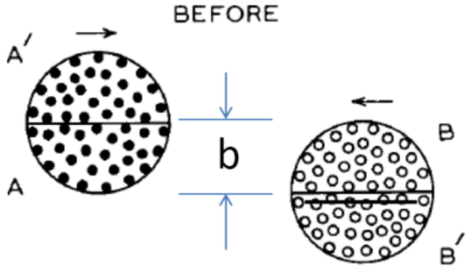

b=7 fm: real collisions
b=20 fm: single nucleus evolution - stability

Homework description:
Mean-field potential and NN scattering

1) Physical input parameters:

a) Equation-of-state:

For non-relativistic transport codes: use a standard *soft Skyrme* parametrization (without momentum dependence) with the following parameters:

a = -209.2 MeV, b = 156.4 MeV, τ=1.35, M=938 MeV

with a symmetry potential energy with linear density dependence $S_{pot}*(\rho/\rho_0)$, S_{pot} =18 MeV.

The total single-particle potential is then:

$U_{n/p}=a(\rho/\rho_0)+b(\rho/\rho_0)^{\tau}$ +/- $2S_{pot}*\rho/\rho_0*\delta$ $\qquad(\delta=(\rho_n-\rho_p)/\rho)$

(Properties of this parameterization: Compression modulus K_0=240 MeV, saturation density ρ_0=0.16 fm^{-3}, binding energy at saturation density E_0= -16 MeV, symmetry energy $S(\rho_0)$~30.3 MeV)

For relativistic transport codes: use a *nonlinear σ-ω-ρ RMF* parameterization *"NLρ"* (see parameter set I in PRC65, 045201, by Liu B et al.)

(properties of this parameterization: K_0=240 MeV, ρ_0=0.16 fm^{-3}, E_0=-16 MeV, $S(\rho_0)$~30.3 MeV)

b) use a constant isotropic elastic cross section of 40 mb.

c) turn off all inelastic collisions.

Homework list for code contributors

Mode A). Homework1

Mode B). Au+Au@100 AMeV

B.1) No Surface Term mode: Turn off the surface term in the mean field (e.g., the Yukawa interaction in the QMD-like models, the gradient term in the BUU-like models). Allow collisions between all nucleons (or TP).

B-Full: both mean field and NN scattering

B.2) Vlasov mode: Turn off all collisions and use mean field as in B.1 (no surface terms)..

B-Vlasov: only mean field

B.3) Cascade mode: Turn off all interaction potentials in B.1 mode

B-Cascade: only NN scattering

Mode C). Common initialization

Mode D). Au+Au@400 AMeV

D-Full: 400AMeV, both mean field and NN scattering

Mode E). Box calculation

Initial density profile

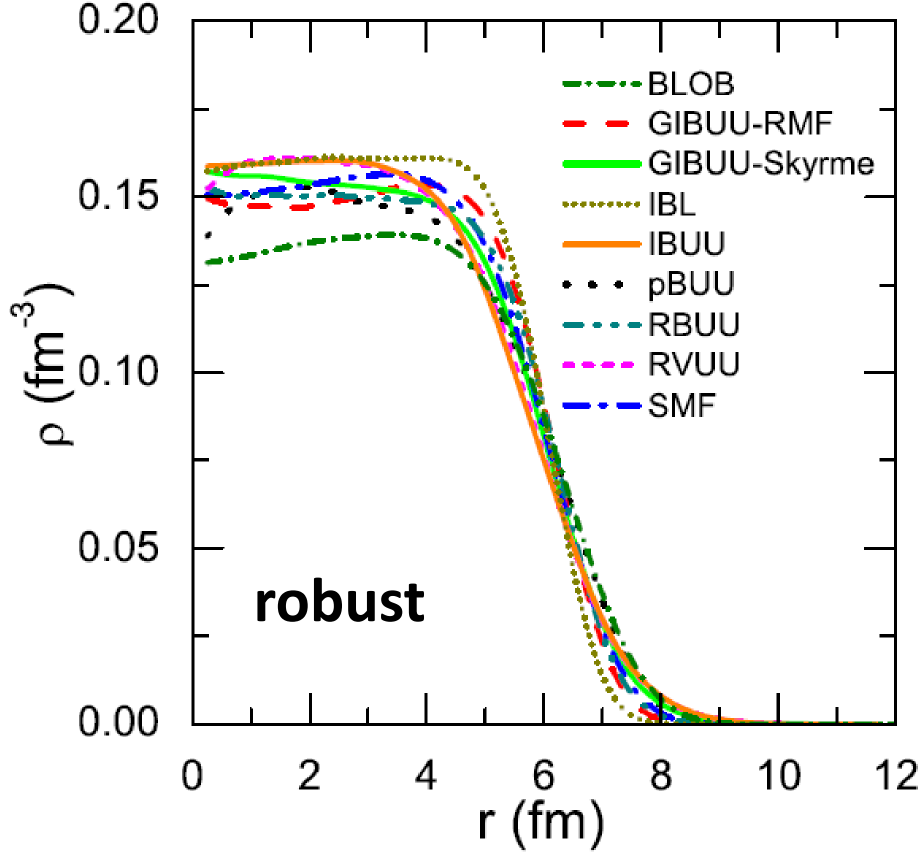

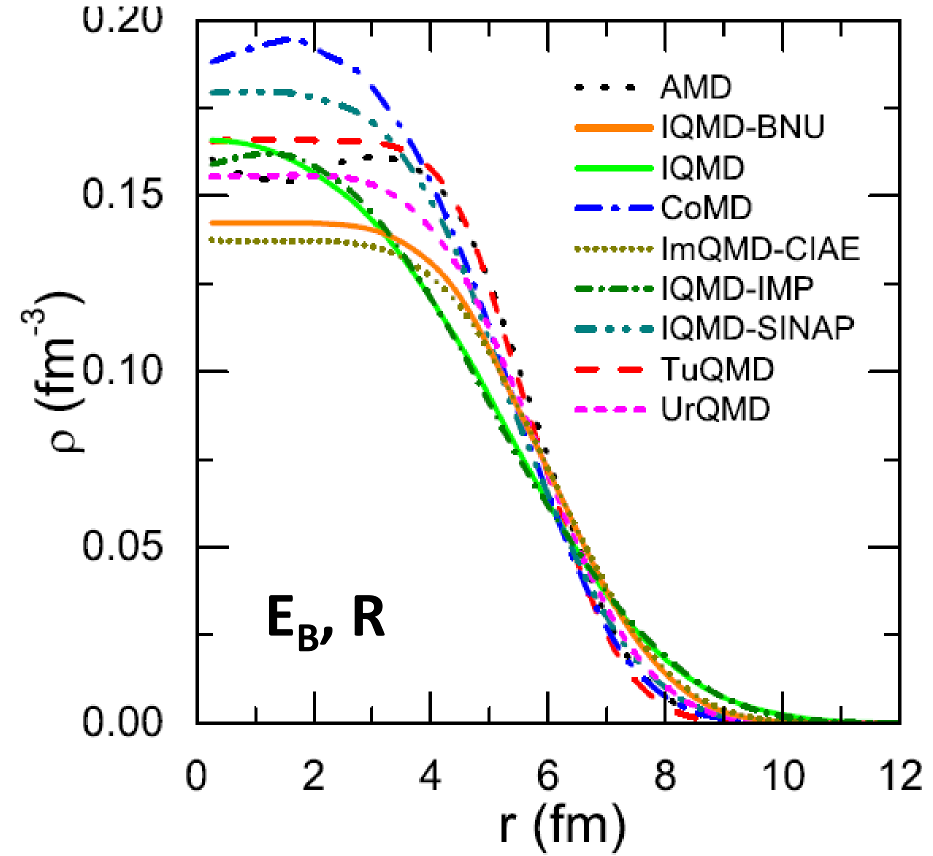

average over 1000 events

BUU: mostly follow the suggested Woods-Saxon distribution, easily stable

QMD: mostly deviate from the suggested Woods-Saxon distribution

ground state? Thomas-Fermi or Hartree-Fock, frictional cooling

Difficult to get a common initialization

TABLE II: Initialization and nucleon-nucleon scattering treatment used in various codes in homework calculations.

Code name	Shape of particles	$(\Delta x)^2$ [fm^2][a]	$\delta < r^2 >^{1/2}$ (fm)[b]	$\delta < r^4 >^{1/4}$ (fm)[c]	Attempted collisions	1st collisions within same nucleus
AMD	Gaussian	1.56	-0.01	0.01	$p = \alpha e^{-\nu R_{ij}^2} v_{ij} \Delta t$	yes
IQMD-BNU	Gaussian	1.97	0.32	0.39	Bertsch approach[d]	no
IQMD	Gaussian	2.16	0.64	0.85	Bertsch approach	yes
CoMD	Gaussian	1.32	-0.11	-0.04	$p = 1 - e^{\Delta t/\tau}$	yes
ImQMD-CIAE	Gaussian	2.02	0.39	0.47	Bertsch approach	yes
IQMD-IMP	Gaussian	1.92	0.61	0.80	Bertsch approach	yes
IQMD-SINAP	Gaussian	2.16	0.03	0.12	Bertsch approach	yes
TuQMD	Gaussian	2.16	-0.17	-0.17	Bertsch approach	yes
UrQMD	Gaussian	2	0.12	0.18	collision time table[e]	yes
	Shape of test particle	$(\Delta x)^2$ [fm^2] or l [fm][f]				
BLOB	triangle	2	0.10	0.07	$p = \sigma^{med} \frac{(\rho_i+\rho_j)}{2} v_{ij} \Delta t$	yes
GIBUU-RMF	Gaussian	1	-0.18	-0.26	Bertsch approach	yes
GIBUU-Skyrme	Gaussian	1	-0.03	-0.03	Bertsch approach	yes
IBL	Gaussian	2	-0.32	-0.42	Bertsch approach	no
IBUU	triangle	1	0.01	0.04	Bertsch approach	yes
pBUU	point	0[g]	0.01	-0.02	cell[h]	yes
RBUU	invar.Gauss	1.4	-0.12	-0.19	Bertsch approach	yes
RVUU	point	0	0.01	0.03	Bertsch approach	yes
SMF	triangle	2	-0.13	-0.18	$p = \sigma^{med} \frac{(\rho_i+\rho_j)}{2} v_{ij} \Delta t$	yes

[a] Δx is the width of the Gaussian wavepacket as in Eq. (6).

[b] $\delta < r^2 >^{1/2} = < r^2 >^{1/2} - < r^2 >_{WS}^{1/2}$ with $< r^2 >_{WS}^{1/2}$ from the required Woods-Saxon distribution.

[c] $\delta < r^4 >^{1/4} = < r^4 >^{1/4} - < r^4 >_{WS}^{1/4}$ with $< r^4 >_{WS}^{1/4}$ from the required Woods-Saxon distribution.

[d] "Bertsch approach" means: $b < \sqrt{\sigma^{med}/\pi}$ and $v_{ij}\gamma\Delta t/2 > |r_{ij} \cdot \vec{p}/p|$ as described in the Appendix B of Ref. [38].

[e] Details about the collision criterion in UrQMD can be found in Ref. [37]

[f] l is the lattice spacing for test particle with triangular shape. See its definition in Ref. [39].

[g] The node separation for the calculation of average quantities is typically 0.92 fm, but can decrease with increasing energy. See Ref. [23] for details.

Stability (b=20 fm)

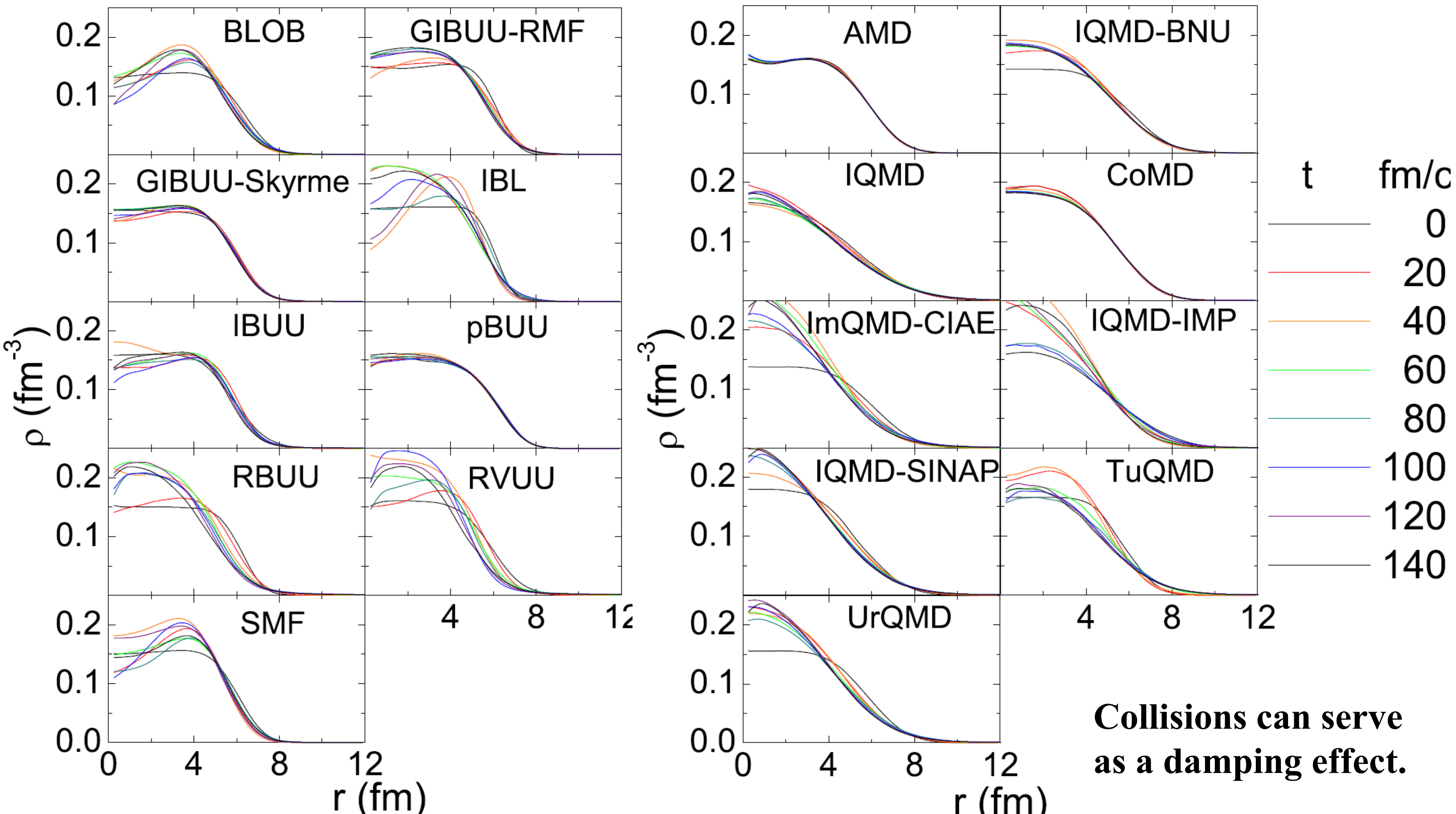

Collisions can serve as a damping effect.

Stable: GIBUU-Skyrme, pBUU, AMD, CoMD

GMR: IBUU, SMF, RVUU, TuQMD, IQMD-IMP

Bubble: IBL, BLOB

evolve to another stable configuration: IQMD-BNU, IQMD-SINAP, UrQMD

Density evolution at b = 7 fm - BUU

average over 1000 events

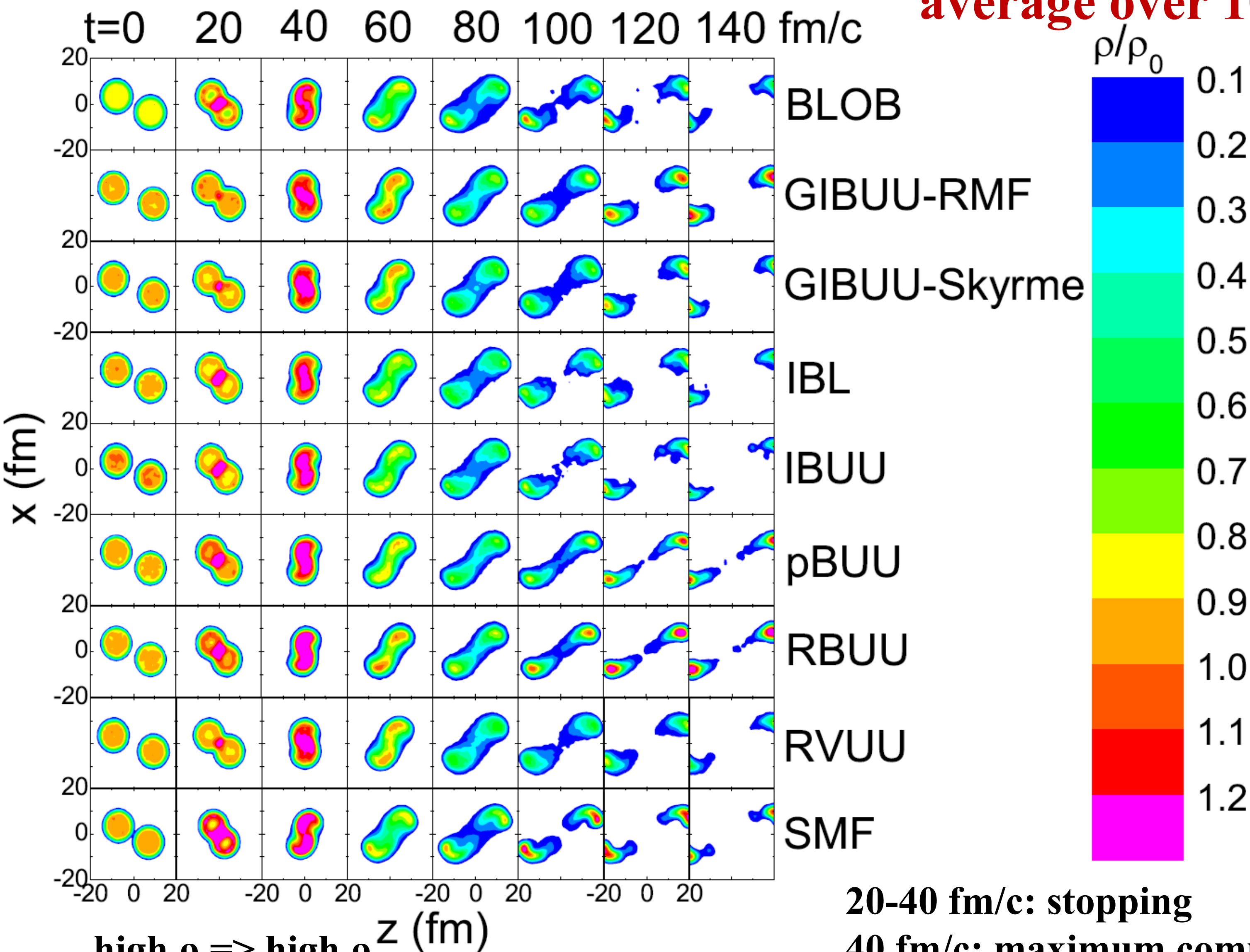

high ρ => high ρ

20-40 fm/c: stopping
40 fm/c: maximum compression
60-80 fm/c: sideward flow developed
Around 100 fm/c: neck

Density evolution at b = 7 fm - QMD

average over 1000 events

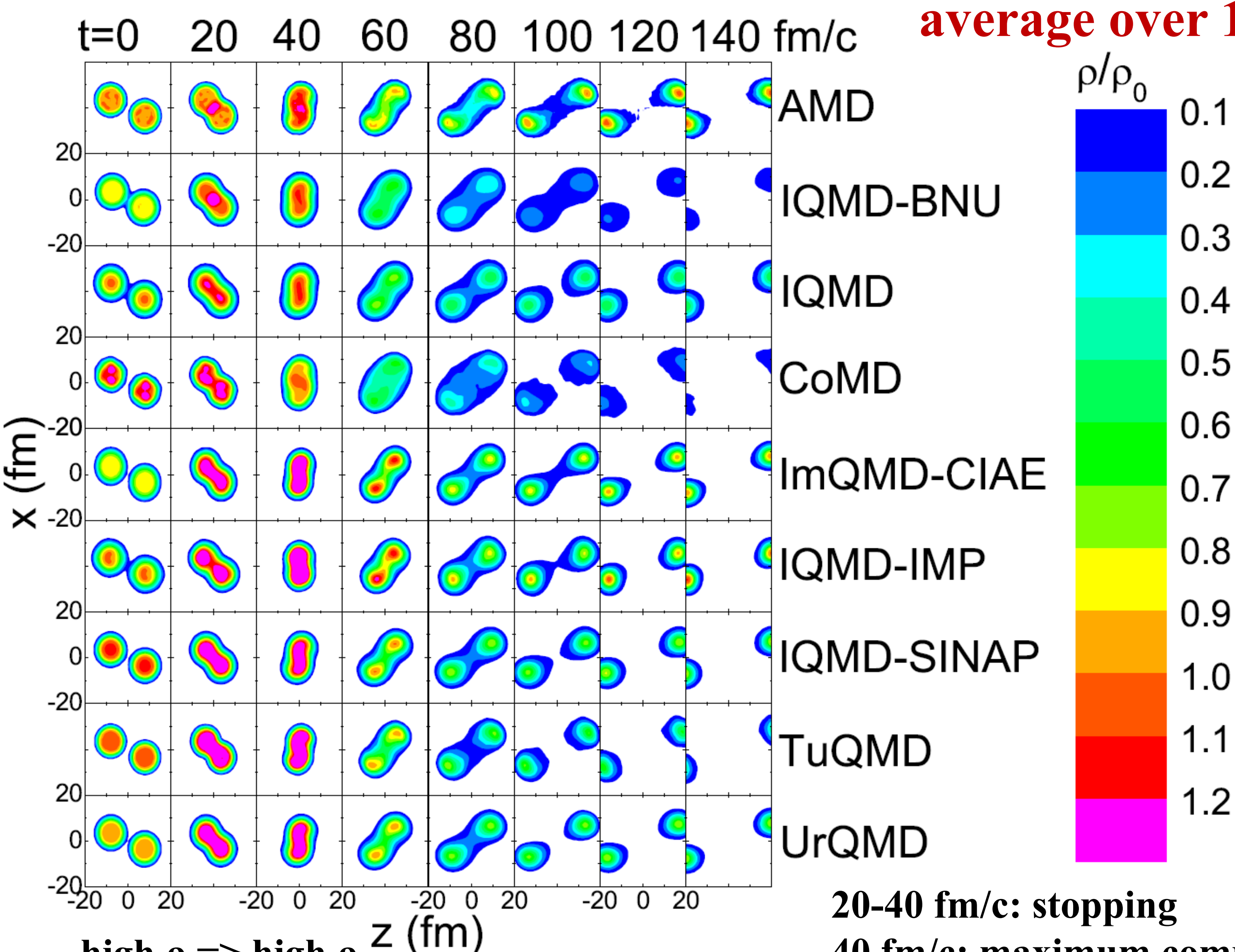

high ρ => high ρ

20-40 fm/c: stopping
40 fm/c: maximum compression
60-80 fm/c: sideward flow developed
Around 100 fm/c: neck

Fluctuation in BUU and QMD

4 runs with 100 TPs per nucleon

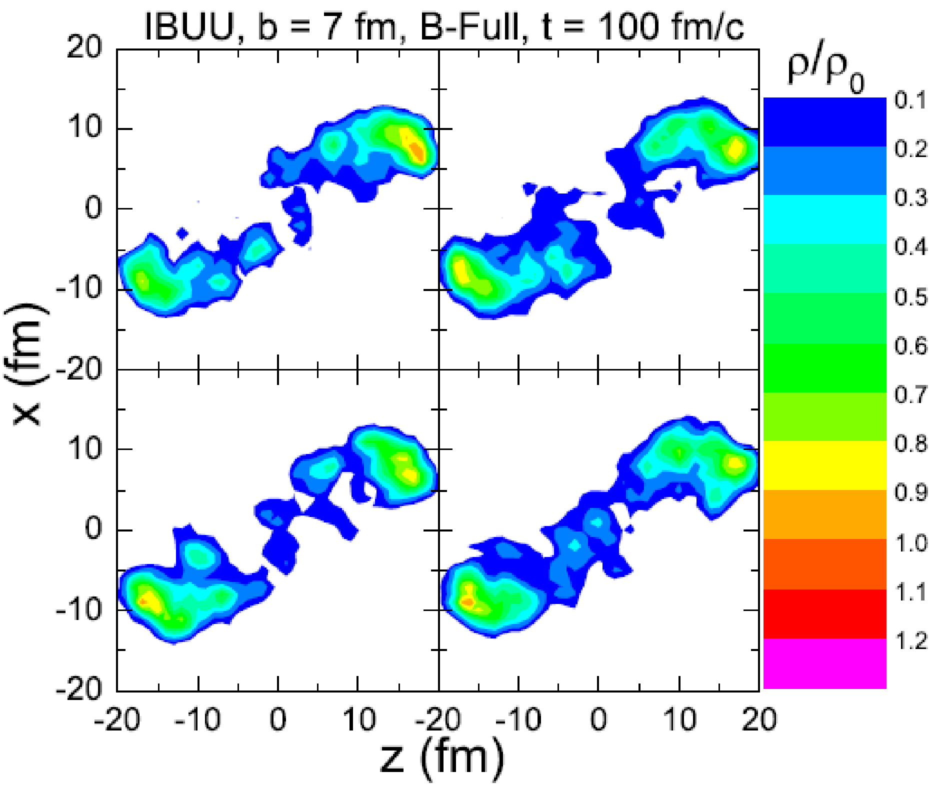

Deterministic nature

4 individual events

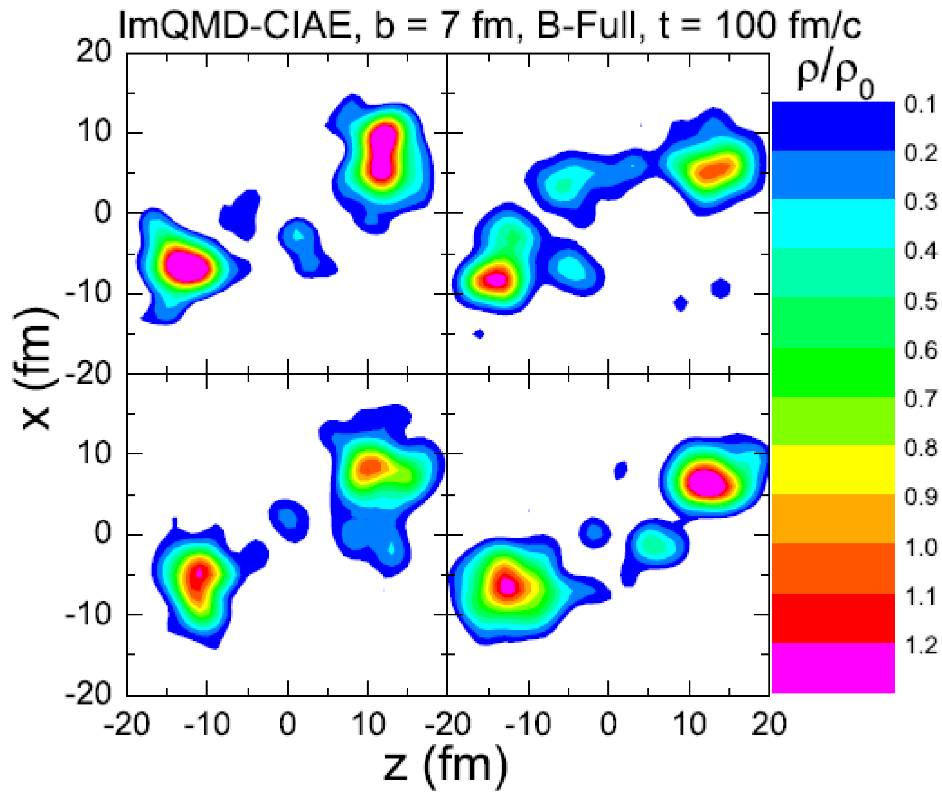

larger fluctuation
stronger fragmentation

NN scattering & Pauli blocking - BUU

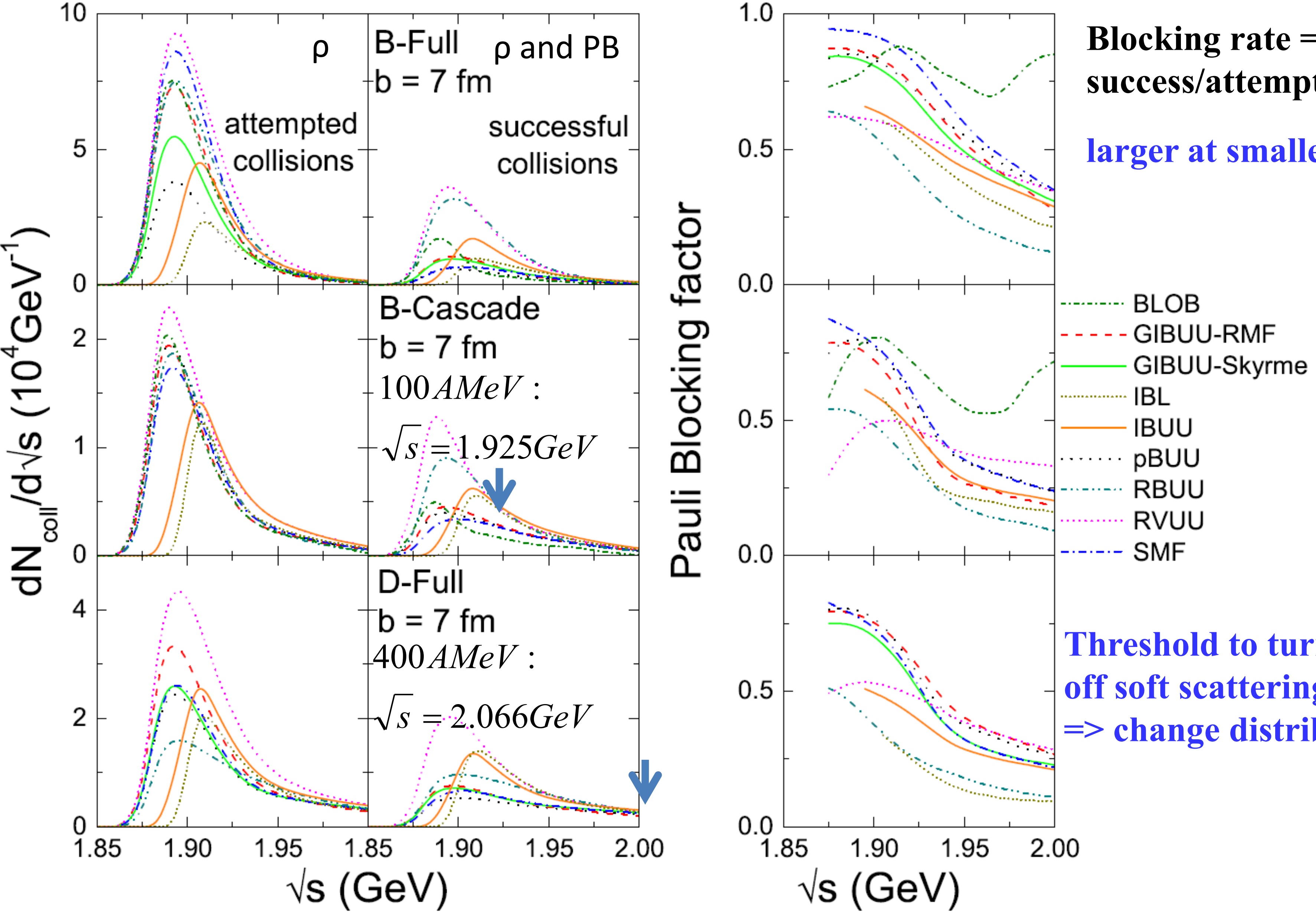

Blocking rate = 1-success/attempted

larger at smaller √s

Threshold to turn off soft scatterings => change distribution

NN scattering & Pauli Blocking - QMD

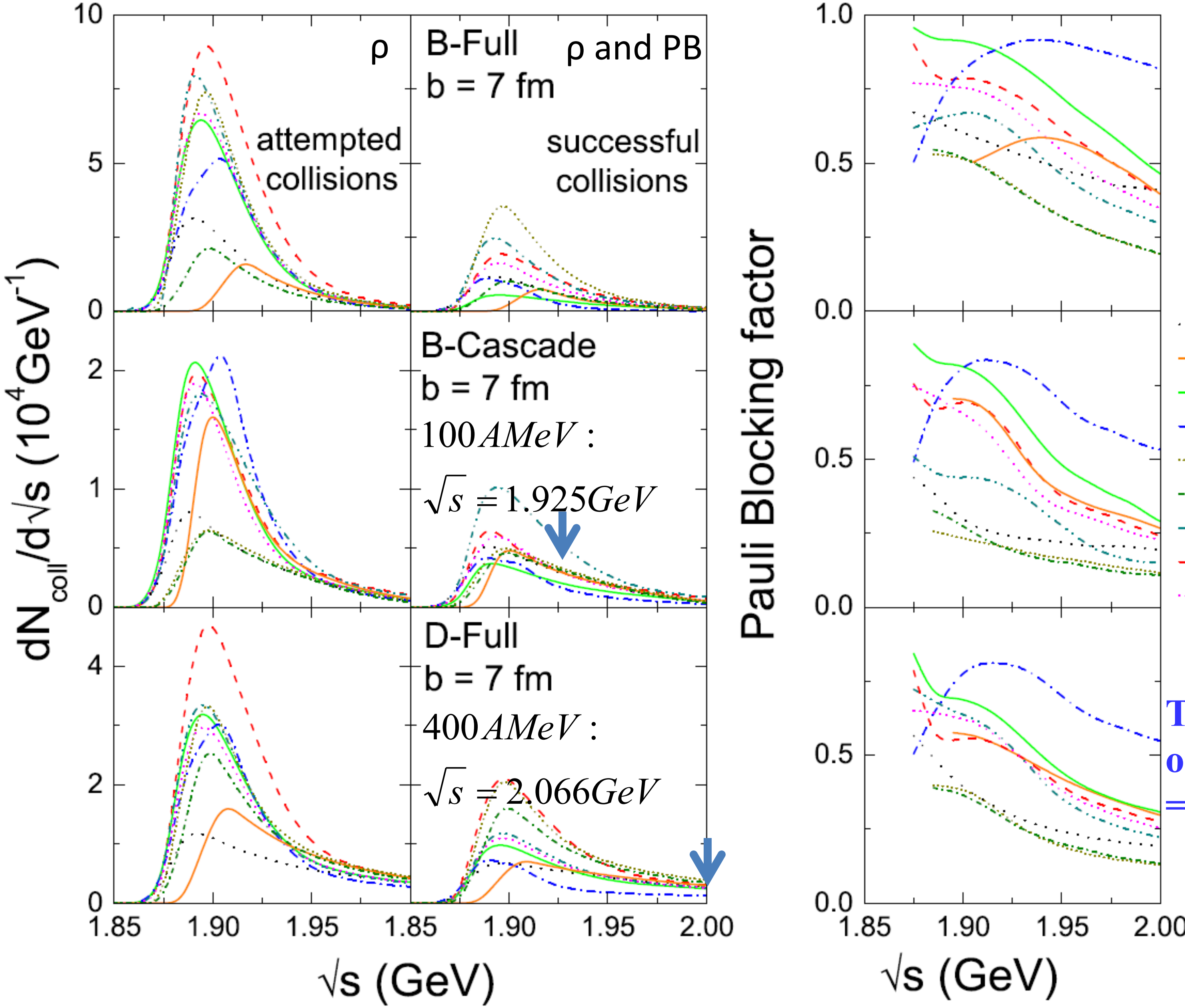

Blocking rate = 1-success/attempted

larger at smaller √s

Threshold to turn off soft scatterings => change distribution

Rapidity distribution (B-mode)

Au+Au, b = 7 fm

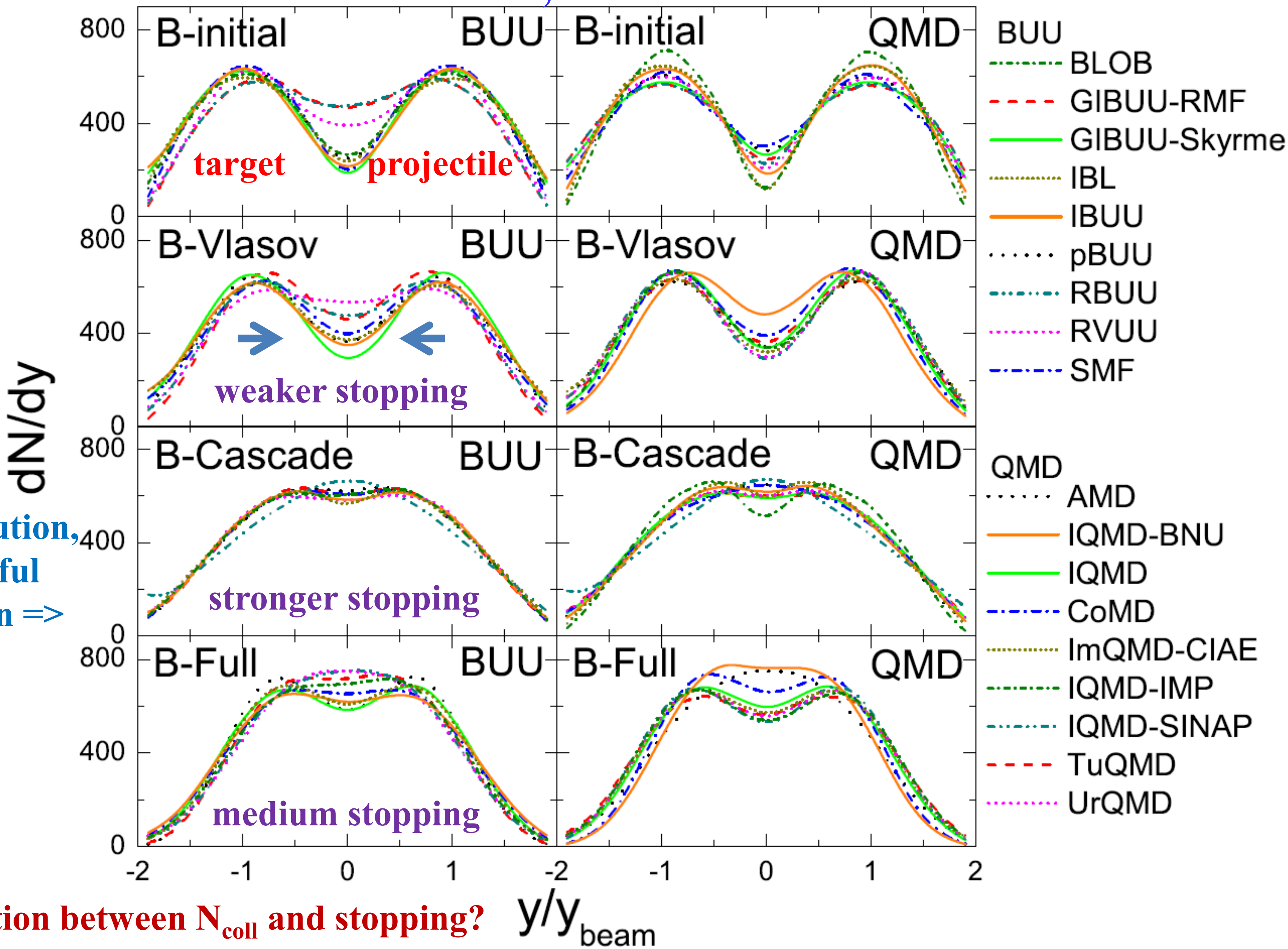

Initial distribution, successful collision =>

Correlation between N_{coll} and stopping?

Rapidity distribution (Full mode)

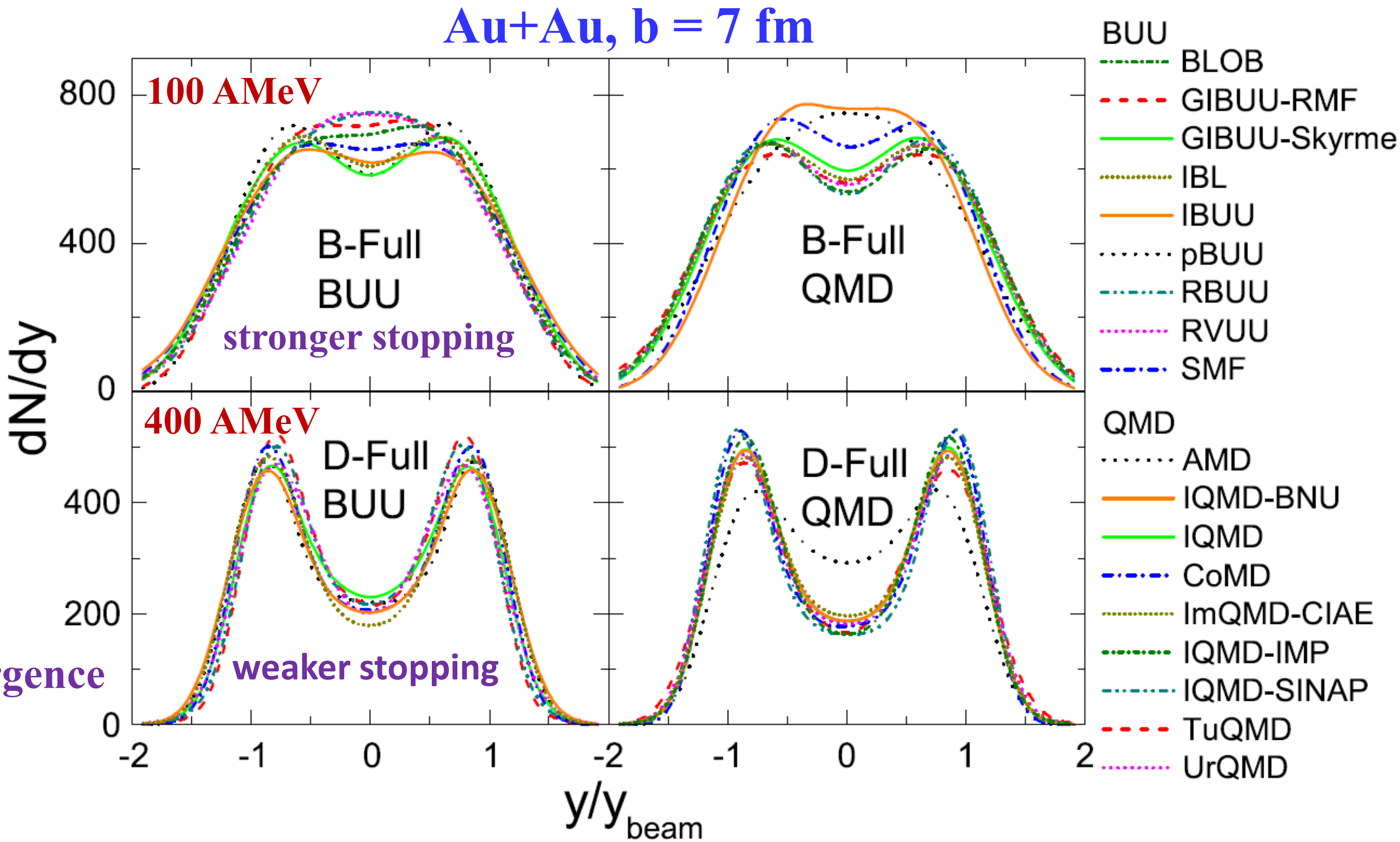

Good convergence

400AMeV: weaker Pauli blocking, less sensitive to initialization, good convergence of N_{coll} at larger $\sqrt{s}$

Transverse flow (B-mode)

Au+Au, b = 7 fm

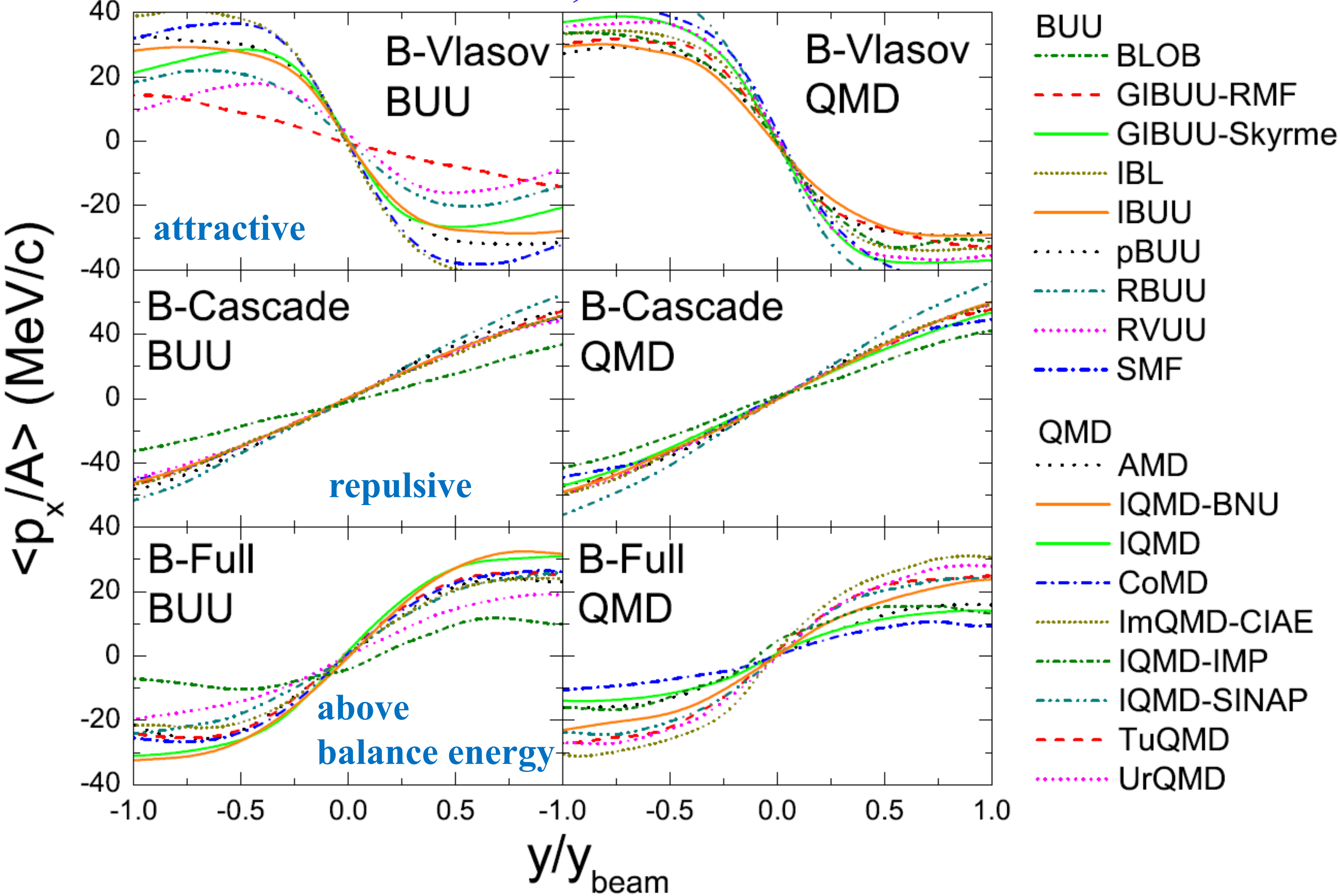

Correlation between stopping and flow?

Transverse flow (Full-mode)

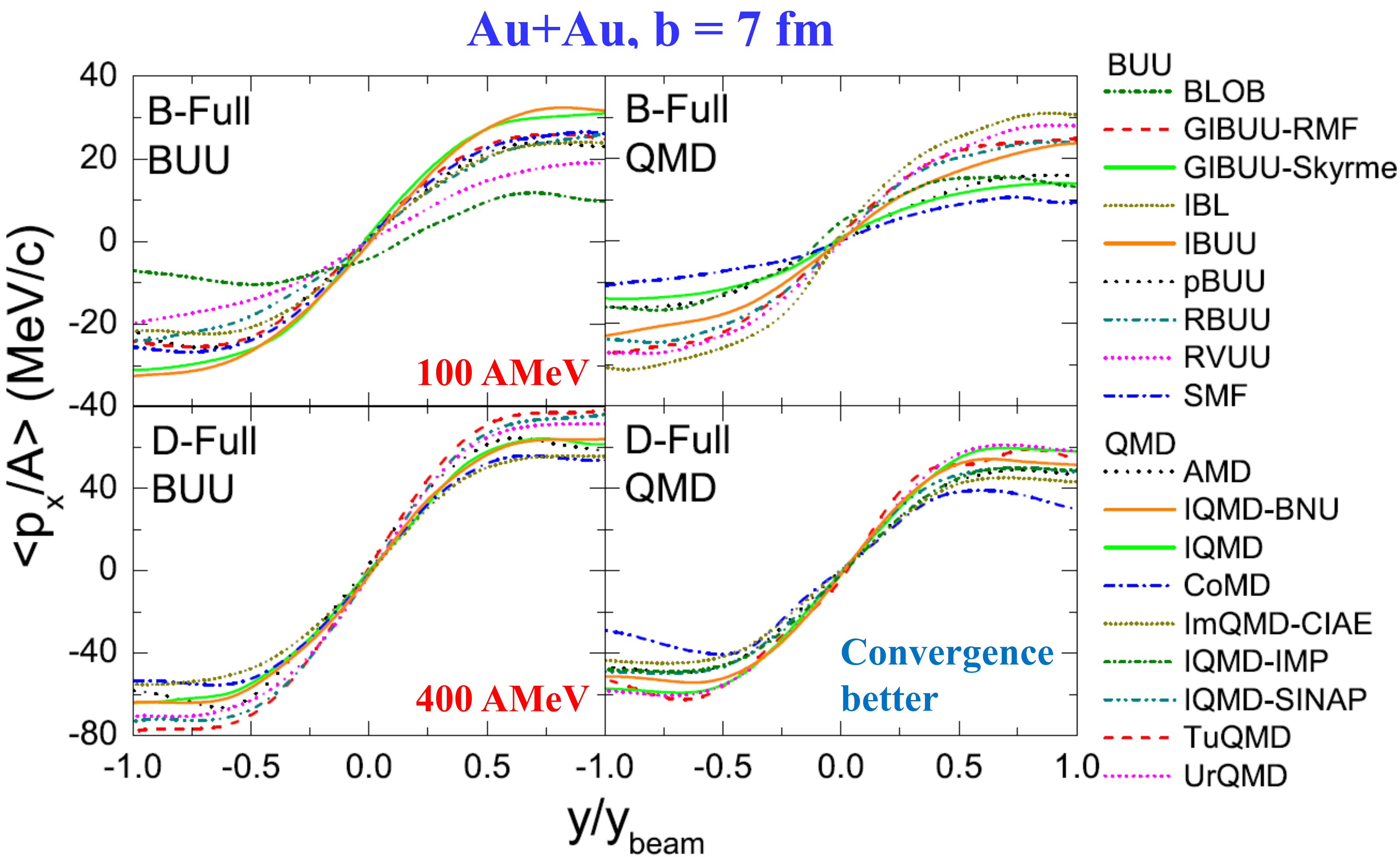

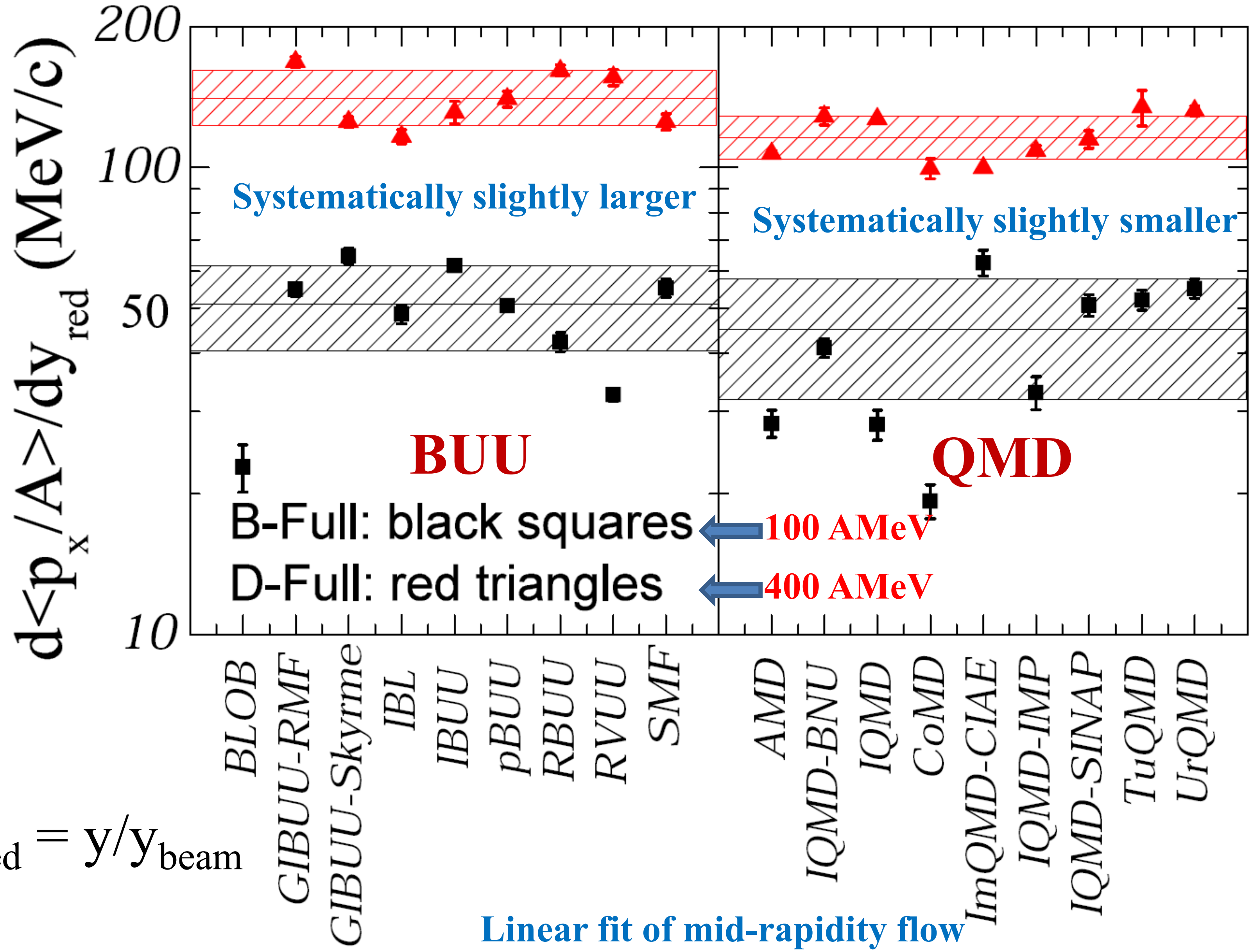

$y_{red} = y/y_{beam}$

Linear fit of mid-rapidity flow

Theoretical uncertainties of flow parameter:

about 30% at 100 AMeV, 13% at 400 AMeV

Transport2017 at MSU

More photos of Transport2017

Box calculations with periodic boundary conditions

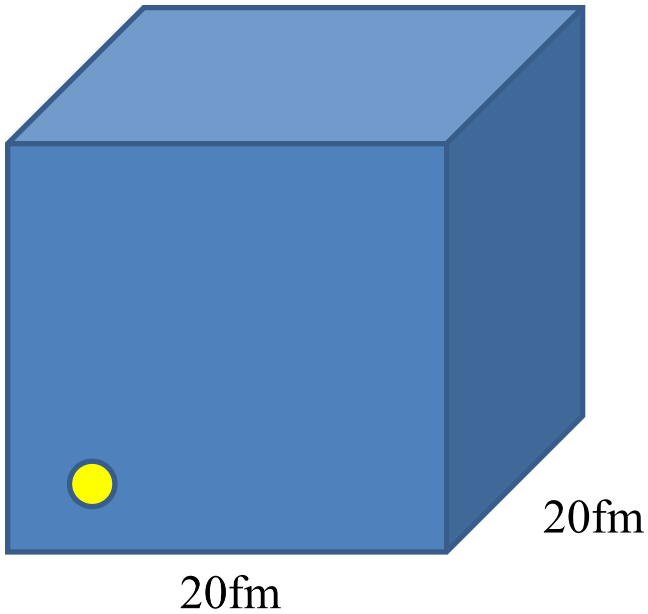

•Details of periodic boundary conditions

1. a box of volume $V = L_1*L_2*L_3$, where the system is confined.
2. The position of the center of box is $(L_1/2, L_2/2, L_3/2)$.
3. In order to keep all particles inside the box, a particle leaving the box has to enter it on the opposite side, keeping the same momentum.

•Initialization:

Uniform density ρ_0=0.16 fm^{-3}, with isospin asymmetry equal to zero. With the above size of the box this corresponds to 1280 nucleons, 640 neutrons and 640 protons. Particle positions are initialized randomly from 0 to L_k.

Homework 1 (Cascade mode) requirements

- **Particles interact only through two-body collisions, i.e. the mean-field interaction and Coulomb force are suppressed.**
- **constant isotropic elastic cross section of σ=40 mb without any artificial threshold**
- The simulation should be followed until **t=140 fm/c**, with a recommended step of Δt=0.5 or 1.0 fm/c.

•Initialization:

Particle momenta are initialized randomly in a sphere with Fermi momentum p_F=265 MeV/c (T=0 case) or with the Fermi distribution at T=5MeV.

•Modes

CT0, CT5: Cascade without Pauli blocking

CBOP1T0, CBOP1T5: Cascade with default Pauli blocking

CBOP2T0, CBOP2T5: Cascade with ideal Pauli blocking (test purpose)

Participating codes

Type	Acronym	Code correspondents	Rel./nonrel.
	BUU-VM[a]	S. Mallik	Rel.
	GiBUU	J. Weil	Rel.
	IBUU	J. Xu, L. W. Chen, B. A. Li	Rel.
BUU	pBUU	P. Danielewicz	Rel.
	RVUU	T. Song, Z. Zhang, C. M. Ko	Rel.
	SMASH	D. Oliinychenko, H. Petersen	Rel.
	SMF	M. Colonna	Nonrel.
	CoMD	M. Papa	Nonrel.
	ImQMD[b]	Y. X. Zhang, Z. X. Li	Rel,
	IQMD-BNU	J. Su, F. S. Zhang	Rel.
	IQMD-IMP[c]	Z. Q. Feng	Rel.
QMD	JAM	A. Ono, N. Ikeno, Y. Nara	Rel.
	JQMD	T. Ogawa	Rel.
	TuQMD	D. Cozma	Rel.
	UrQMD	Y. J. Wang, Q. F. Li	Rel.

7 BUU codes and 8 QMD codes

Theoretical collision rate in CT0

$$\frac{4}{\rho}\int_0^{p_F}\frac{p^2}{2m}\frac{d^3p}{(2\pi)^3}=\frac{3}{5}\varepsilon_F$$

Fermi-Dirac distribution

Energy conservation

Maxwell-Boltzmann distribution

$$\frac{4}{\rho}\int\exp\left(-\frac{p^2}{2mT}\right)\frac{p^2}{2m}\frac{d^3p}{(2\pi)^3}=\frac{3}{2}T$$

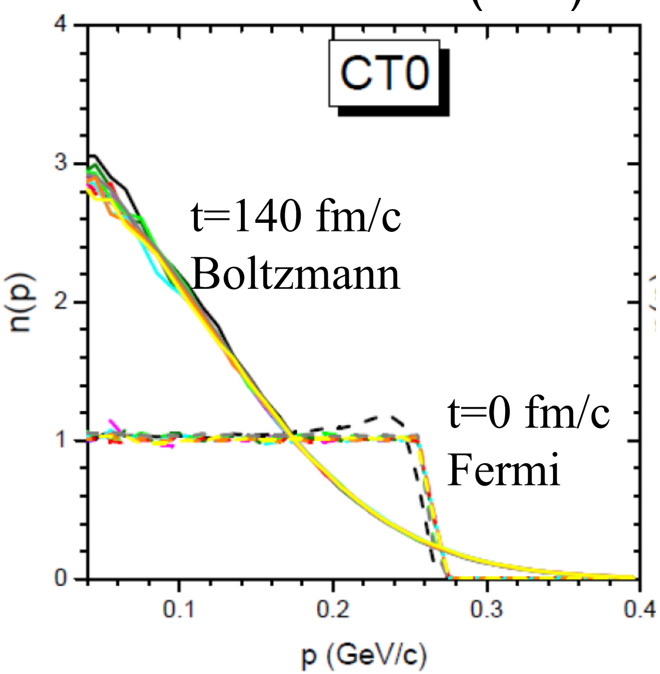

$$T=\frac{2}{5}\varepsilon_F\approx 14.7MeV$$

$$\frac{dN_{coll}}{dt}=\frac{1}{2}\langle\sigma v\rangle\rho^2L^3\approx\begin{cases}119(FD)\\112(MB)\end{cases}$$

Time evolution of momentum distribution

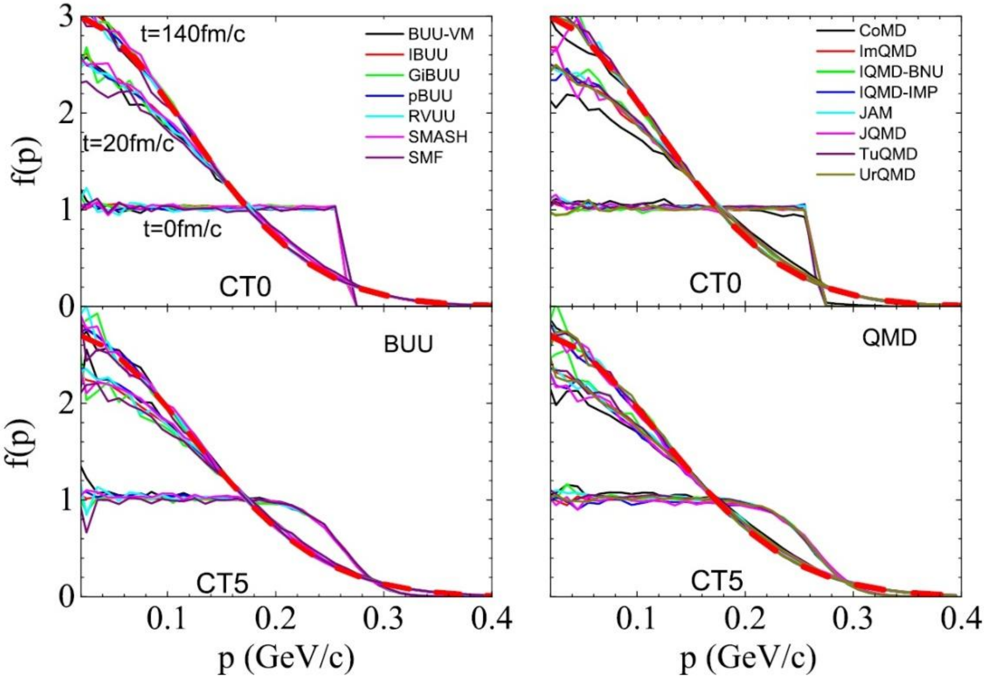

Time evolution of collision rate

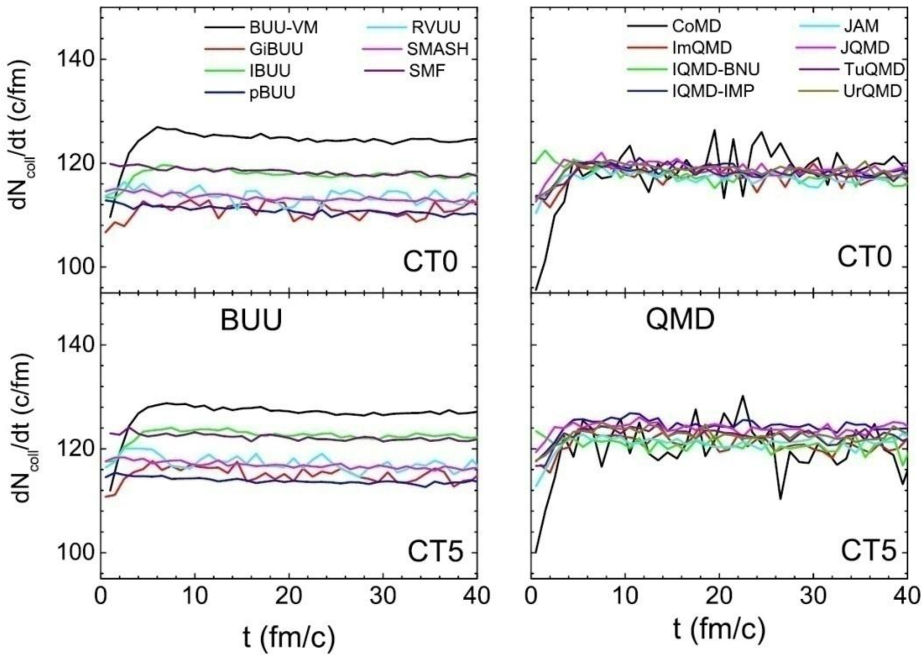

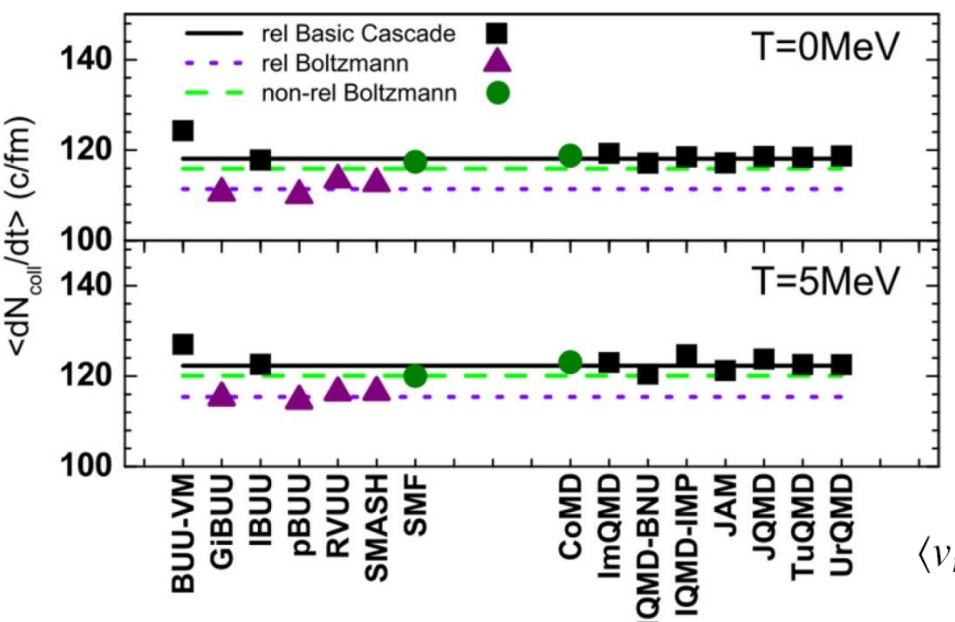

$$\frac{dN_{coll}}{dt} = \frac{1}{2} A\rho\sigma\langle v_{rel}\rangle$$

non-relativisitic Boltzmann

$$\langle v_{rel}\rangle = (4/\sqrt{5\pi})(p_F/m)$$

Relativistic Boltzmann

$$\langle v_{rel}\rangle = \frac{1}{4m^4 T_B K_2^2(m/T_B)} \int_{2m}^{\infty} d\sqrt{s}\, s(s-4m^2) K_1(\sqrt{s}/T_B)$$

Taken from Akira Ono

Bertsch prescription (nonrelativistic version)

Two nucleons may collide

- when the relative distance is minimum during a time step, $2|\mathbf{r}\cdot\mathbf{v}| < \mathbf{v}^2\Delta t$,
- and when the minimum distance is $\mathbf{r}^2 - (\mathbf{r}\cdot\mathbf{v})^2/\mathbf{v}^2 < \sigma/\pi$,

where $\mathbf{r}$ and $\mathbf{v}$ are the relative coordinate and velocity, respectively, at the current time t. There is not anything more.

Then the same pair of two particles can collide more than once, as in the second example.

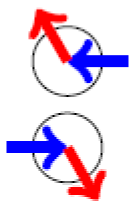

- By the collision, the momenta are changed from the blue to the red arrows. After the collision, the particles are moving away from each other ($\mathbf{r}\cdot\mathbf{v} > 0$), so they will never collide again.

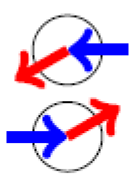

- After the collision (red arrows), the particles are again approaching to each other ($\mathbf{r}\cdot\mathbf{v} < 0$) and the distance is $|\mathbf{r}| < \sqrt{\sigma/\pi}$, so they will collide again at a later time.

Repeated/spurious scatterings

Avoid repeated spurious scatterings

Principle

After a collision happened for a pair of particles (i, j), the same pair should not collide again until one of i and j collides with some other particle.

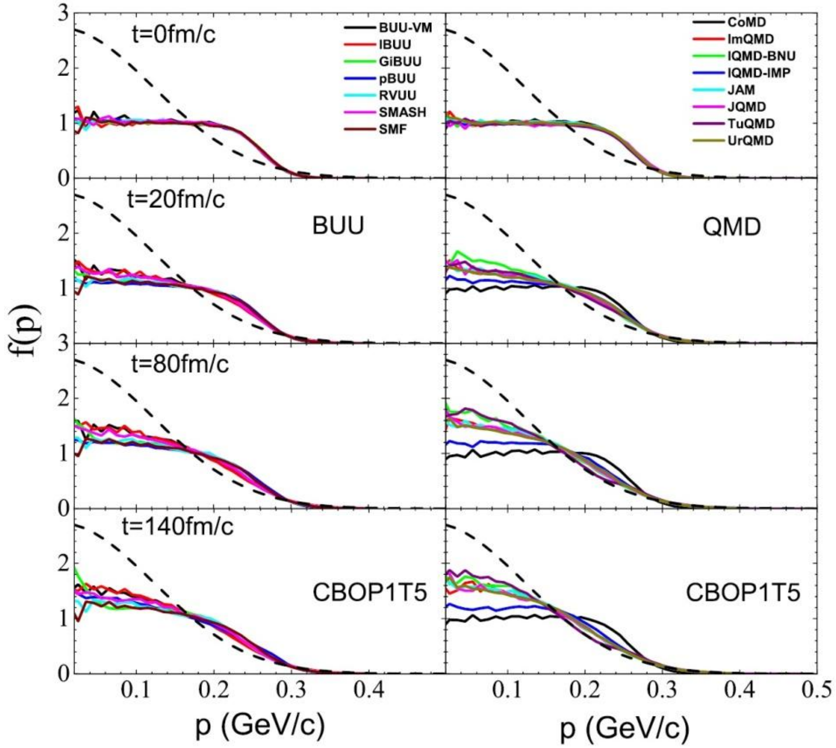

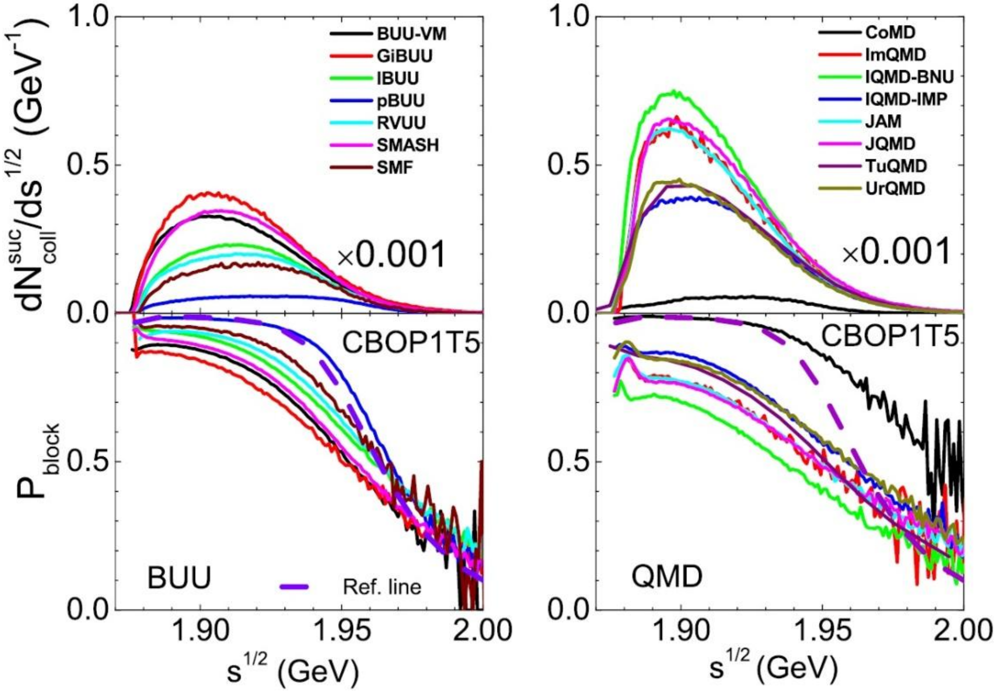

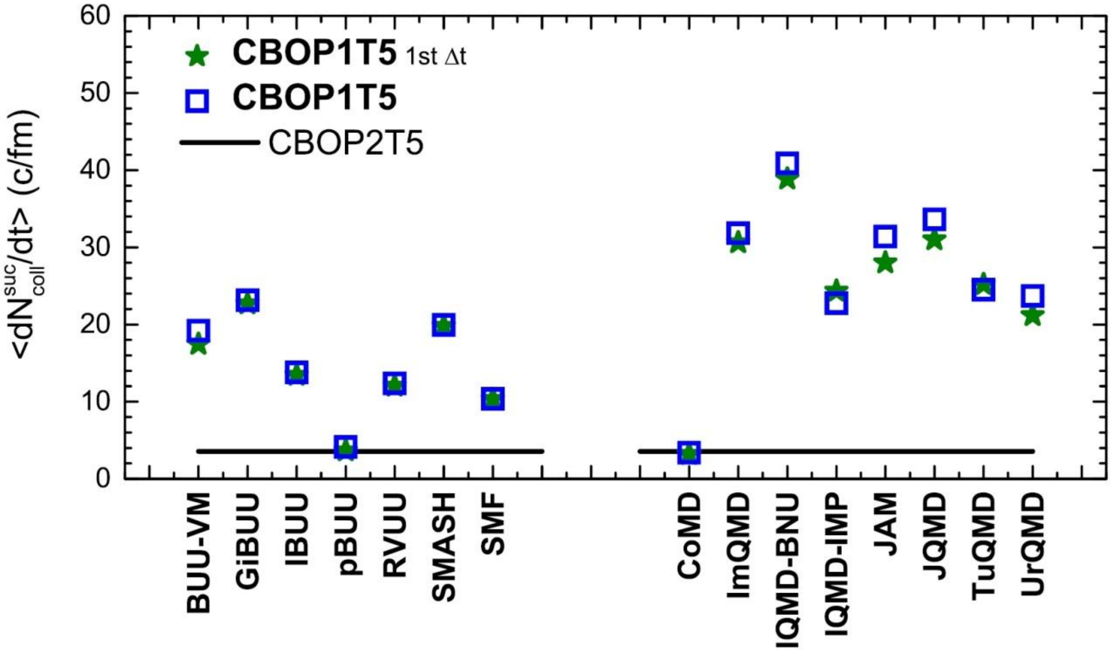

With Pauli blocking,
the successful collision rates
are much overestimated
in QMD codes than in BUU codes.

Momentum occupation in the final state of the collision in the first time step

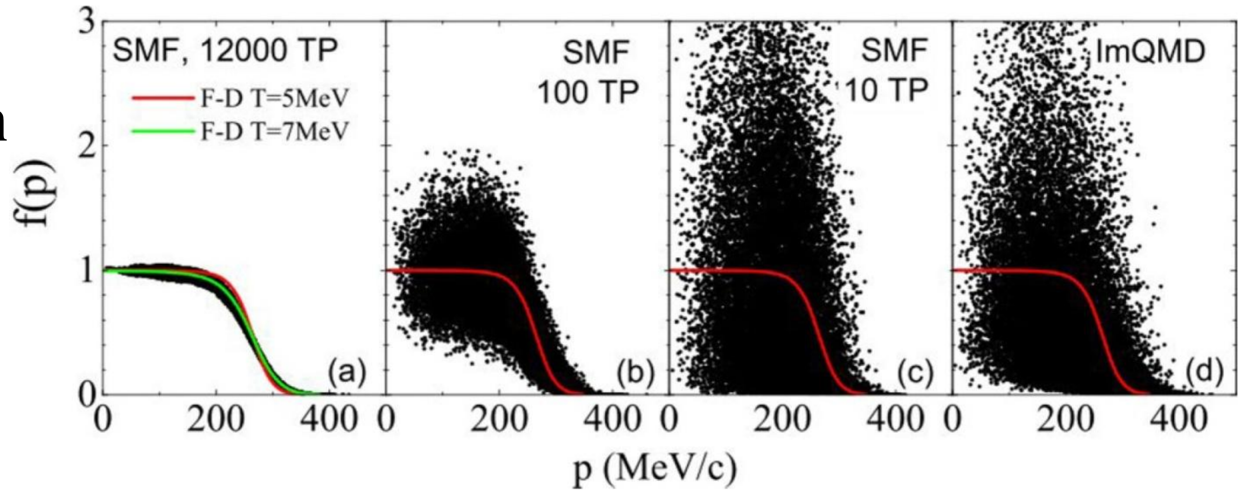

Fluctuations in BUU codes decrease with increasing TP number, but always exist in QMD codes.

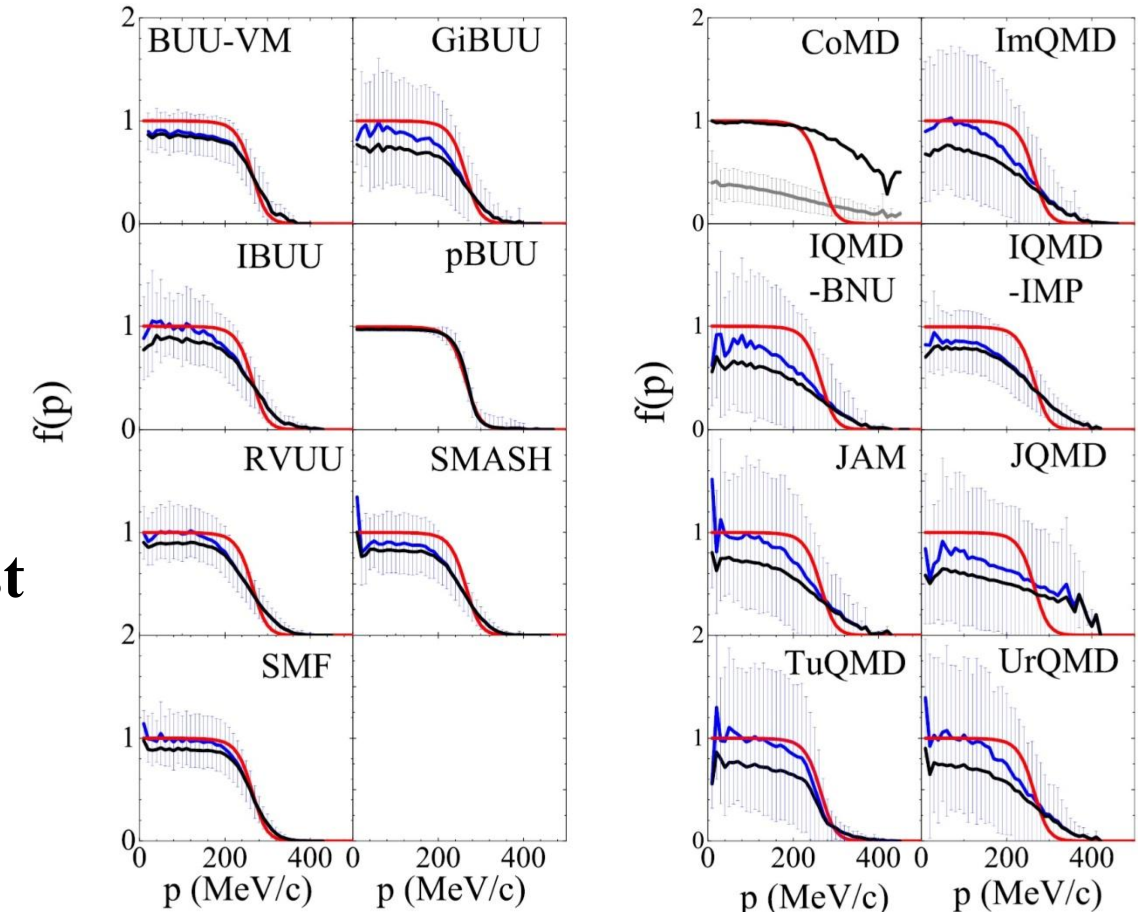

Box-pion calculation

pion production, N+N↔N+Δ, Δ↔N+π

One-way Δ production or two-way Δ production (detailed balance)
Fixed Δ mass or a Breit-Wigner form
Turn on isospin asymmetry π^-/π^+

Theoretical limit of kinetic equation (N+N↔N+Δ only):

$$\frac{d\rho_N(t)}{dt} = -\frac{1}{2}\lambda_{NN}\left(\rho_N(t)\right)^2 + \lambda_{N\Delta}\rho_N(t)\rho_\Delta(t)$$

$$\frac{d\rho_\Delta(t)}{dt} = \frac{1}{2}\lambda_{NN}\left(\rho_N(t)\right)^2 - \lambda_{N\Delta}\rho_N(t)\rho_\Delta(t)$$

Further:
Δ↔N+π
isospin

$$\rho_N(t=0) = \rho_0 \qquad \rho_\Delta(t=0) = 0$$

$$\lambda_{AB} = \left\langle \sigma_{AB\to CD} v_{AB} \right\rangle = \frac{\int f_A(p_A) f_B(p_B) \sigma_{AB\to CD} v_{AB} d^3p_A d^3p_B}{\int f_A(p_A) f_B(p_B) d^3p_A d^3p_B}$$

Box-pion calculation

N+N→N+Δ and elastic B+B↔B+B

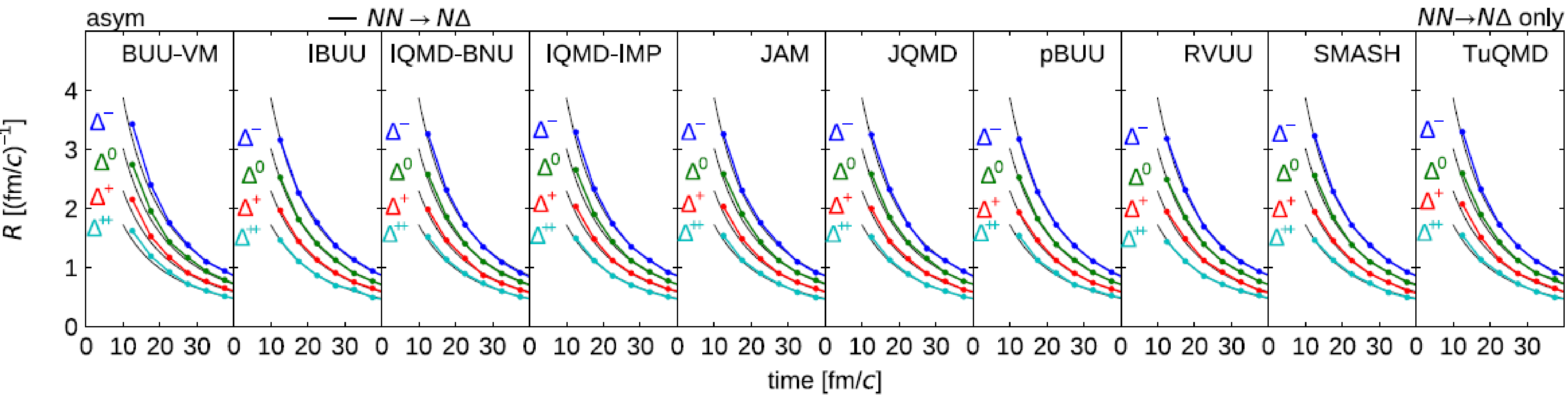

N+N↔N+Δ and elastic B+B↔B+B

detailed balance

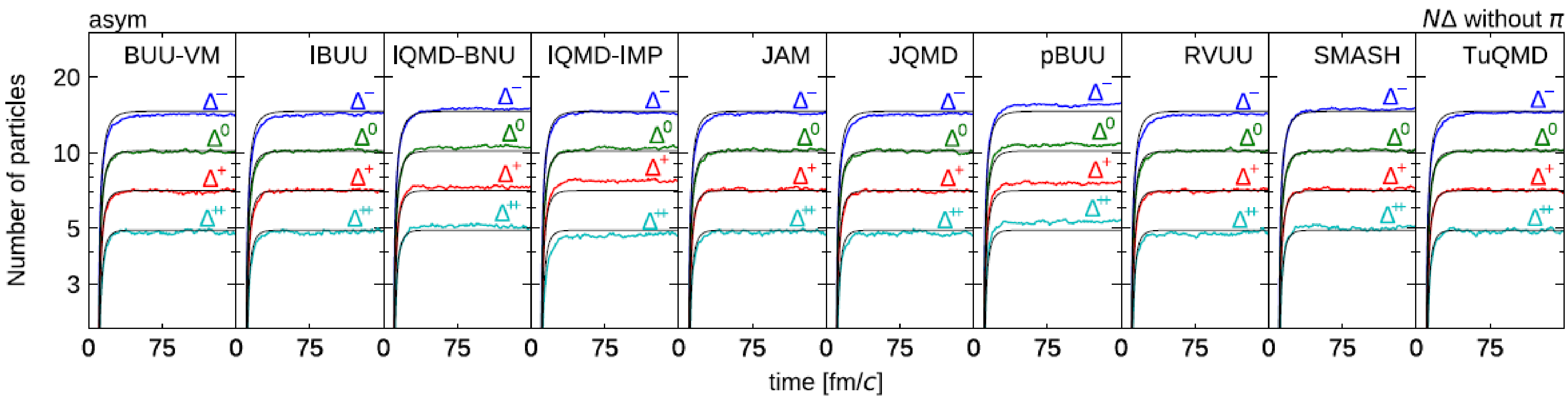

Blacking solid lines: theoretical limits from reaction rate equations/statistical model

Sequence of collisions and decays

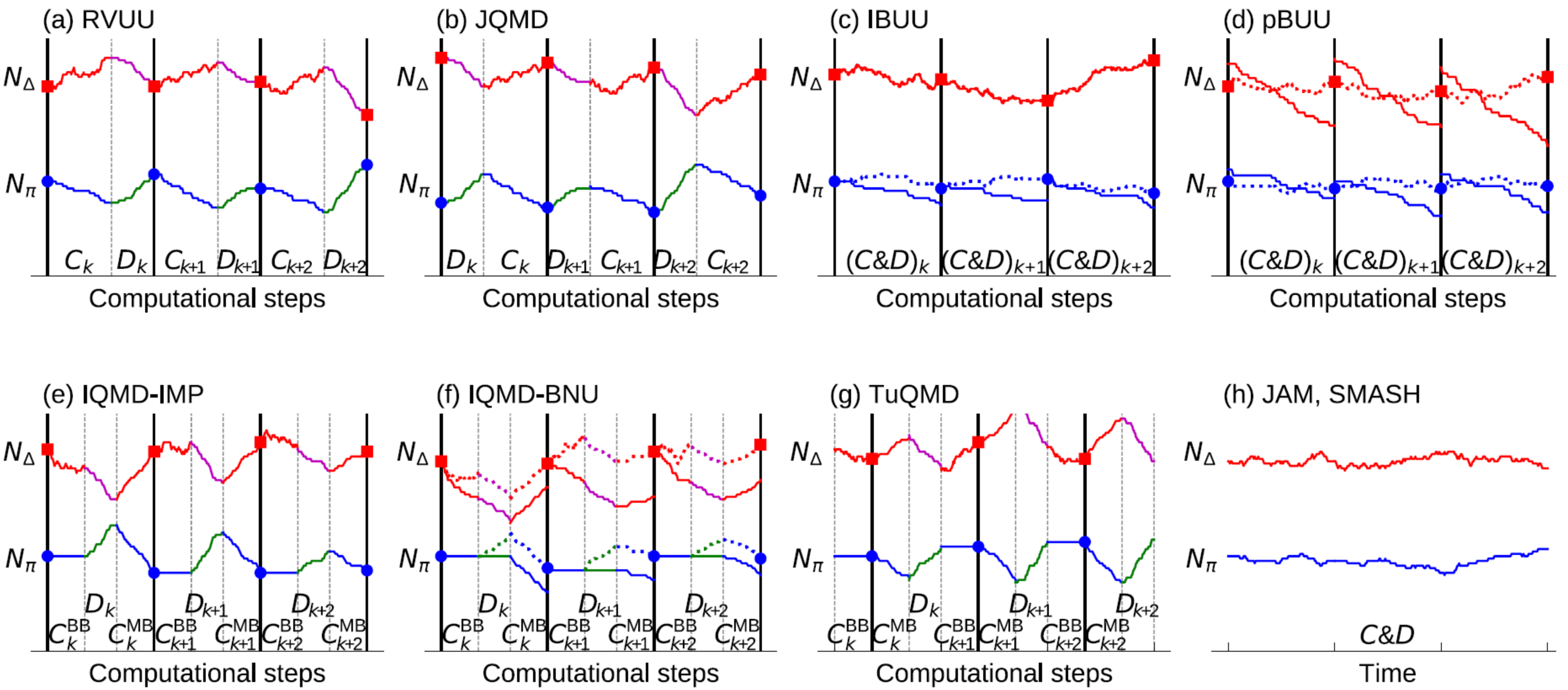

$N+N \leftrightarrow N+\Delta$, $N+\pi \rightarrow \Delta$ **$\Delta \rightarrow N+\pi$**

C: collisions, increase N_Δ and decrease N_π **D: decay: decrease N_Δ and increase N_π**

Different sequences of collisions and decays affect N_Δ and N_π at the time boundary

Higher-order correlations induced by collisions

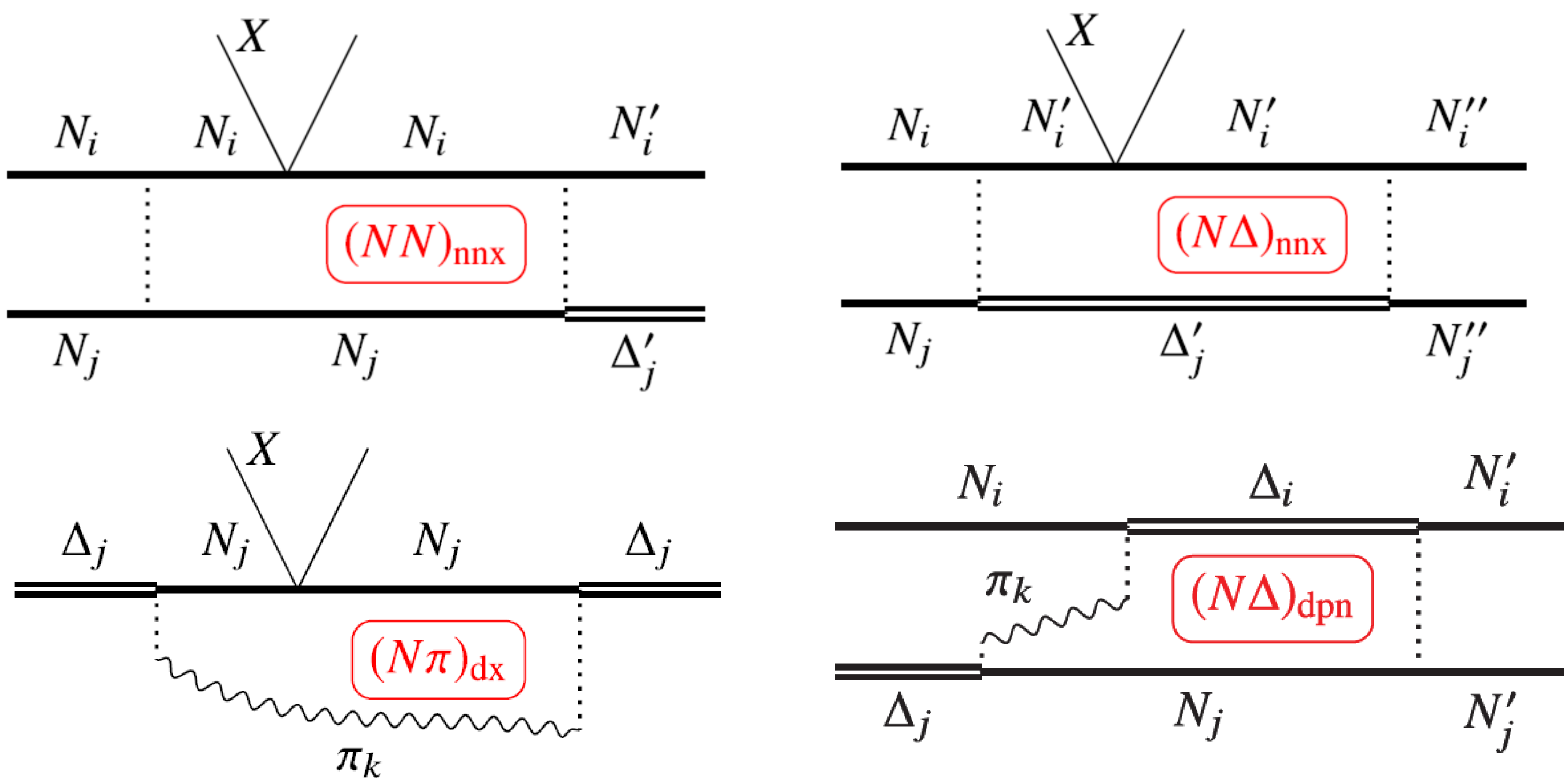

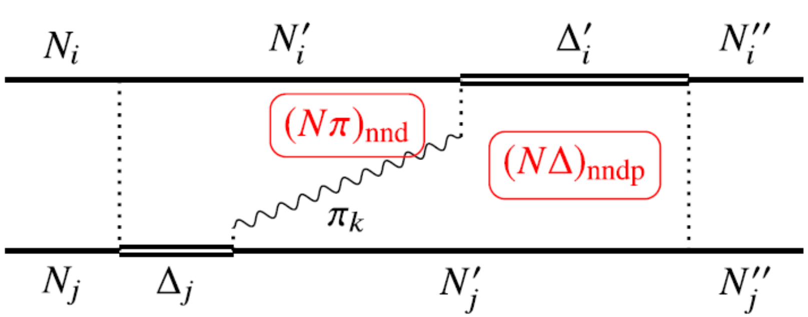

$$n_i n_j \leftrightarrow p_i \Delta_j^- \quad \sigma_{\rm tot}[p\Delta^-]$$

$$\vee$$

$$n_i n_j \leftrightarrow n_i \Delta_j^0 \quad \sigma_{\rm tot}[n_i \Delta_j^0]$$

Box-pion calculation

N+N↔N+Δ, and Δ↔N+π, and elastic B+B↔B+B

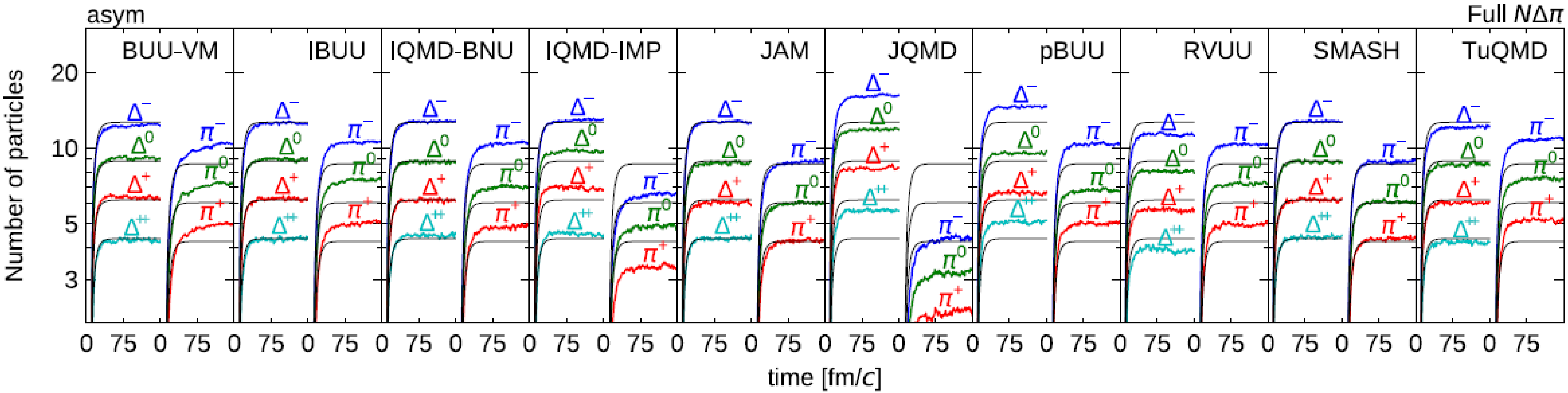

Situation becomes worse with pions.

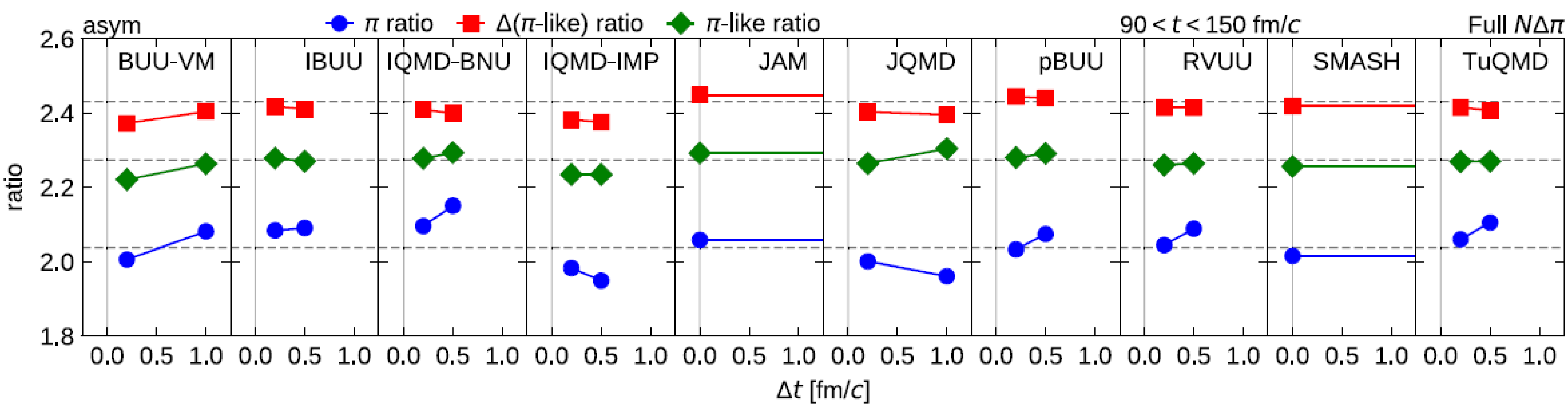

Sequence of N+N↔N+Δ and Δ↔N+π affects pion multiplicity (weak when Δt→0); Higher-order correlations lead to isospin violation in geometrical collision treatment (full ensemble method (mix N_{TP}, σ→σ/N_{TP}) as a cure).

e.g. leading to $\Delta^0\Delta^+/\Delta^-\Delta^{++}>1$

Box-pion calculation: summary

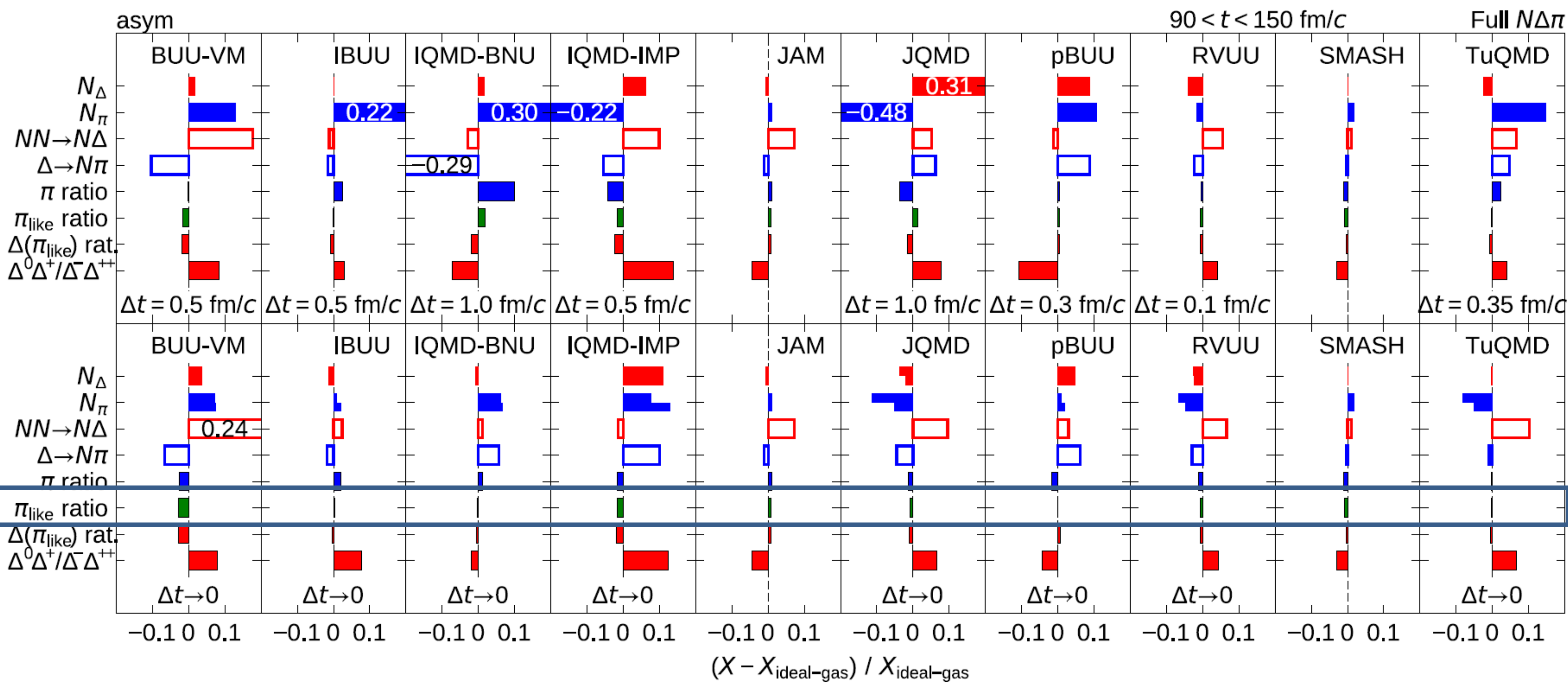

Extrapolation to Δt → 0 can be helpful (or time-step free code).
π_{like} ratio is OK due to cancellation of different effects.

Box-Vlasov calculation

$\rho(z,t=t_0) = \rho_0 + a_\rho \sin(k_i z)$ $\quad k_i = n_i\, 2\pi/L \quad a_\rho = 0.2\,\rho_0$

Momentum sampled within local Fermi sphere determined by local density

Study the time evolution of ρ(z)

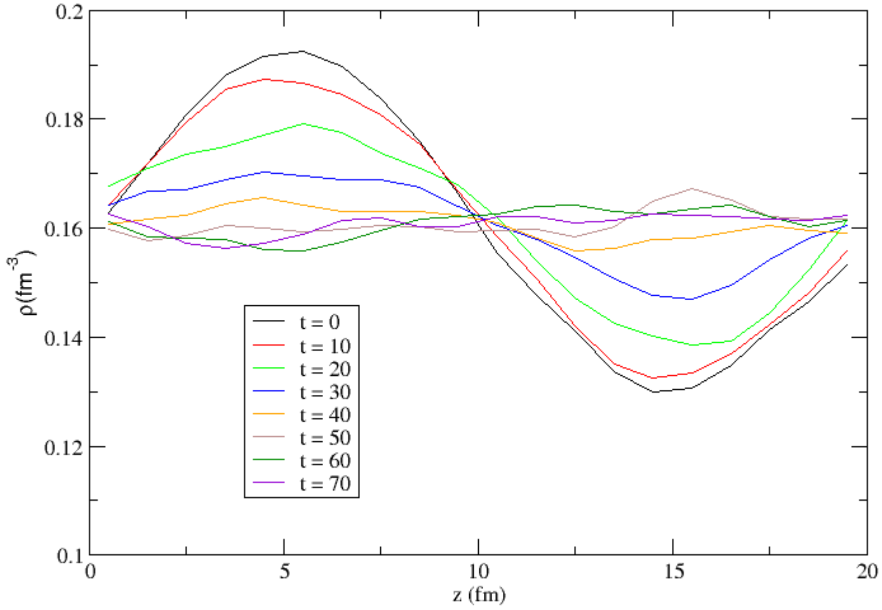

Isospin symmetric nuclear matter

Only momentum-independent mean-field potential
a) Skyrme-like
b) σ-ω coupling

No surface or Coulomb potential

No NN collision due to large fluctuations and dissipations in QMD models

Incompressibility K_0=240 MeV → K_0=500 MeV

Damping sources:

1) **Landau damping: mixing modes**
2) **Numerical damping: fluctuations**
   a) **Decreases with increasing TP numbers**
   b) **Decreases with increasing particle size**

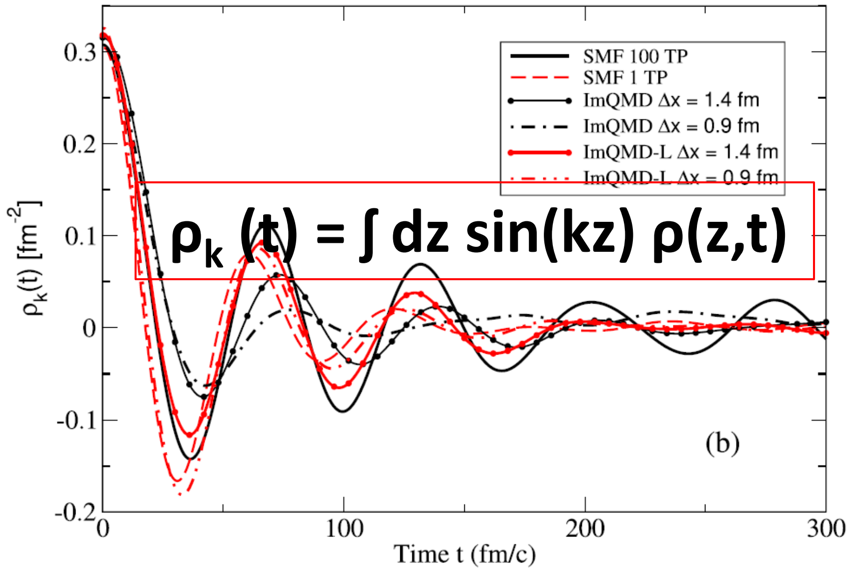

$$-F = \frac{\partial U}{\partial Z_i} \approx \int d^3r\, U(\rho)\, \frac{\partial G(\vec{r}-\vec{R}_i)}{\partial Z_i} = \frac{\partial H_{\text{pot}}}{\partial Z_i}$$

$$H_{\text{pot}} = \int d^3r \left[\frac{a}{2}\left(\rho^2/\rho_0\right) + \frac{b}{\sigma+1}\left(\rho^{\sigma+1}/\rho_0^{\sigma}\right)\right]$$

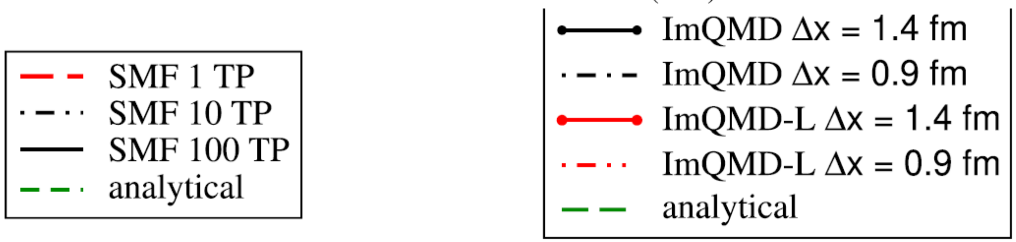

$$H_{\text{pot}}^{\text{2body,QMD}} = \frac{a}{2\rho_0}\sum_i \tilde{\rho}_i$$

$$H_{\text{pot}}^{\text{3body,QMD}} = \frac{b}{(\sigma+1)\rho_0^{\sigma}}\sum_i \tilde{\rho}_i^{\sigma}$$

$\langle\rho^{\sigma}\rangle \approx \langle\rho\rangle^{\sigma}$

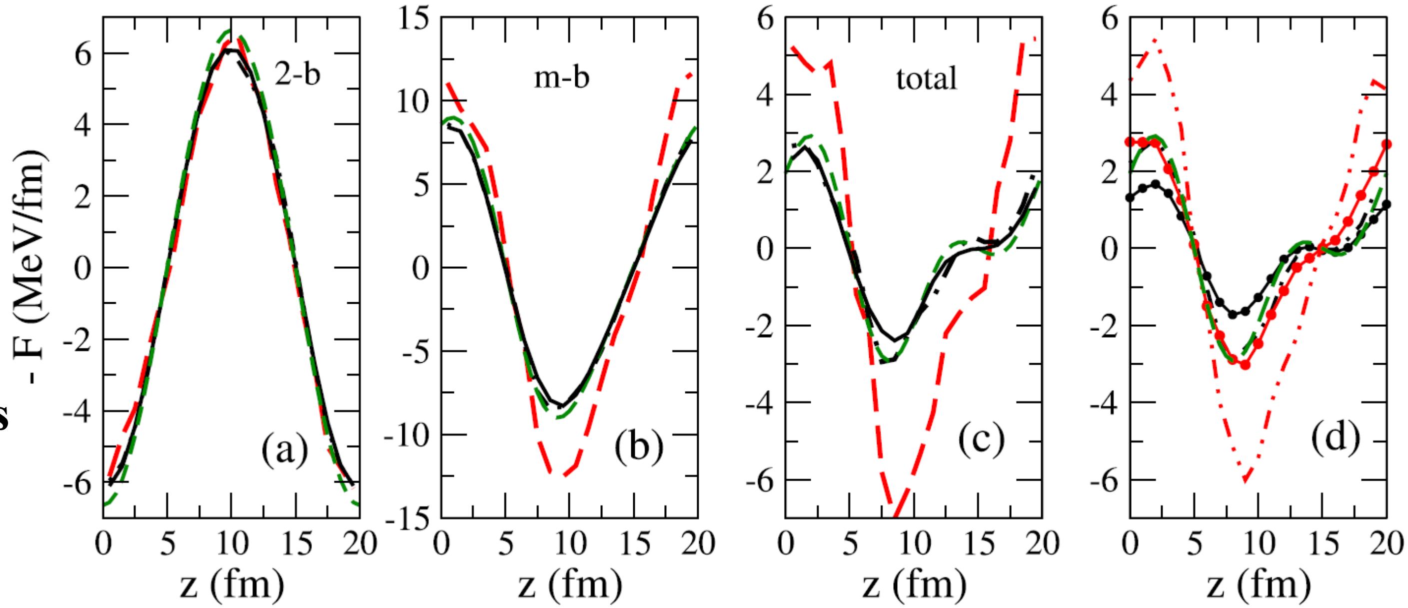

Inaccurate 3-body force calculation with few TPs (or in QMD);
Suitable size of particle

Time Fourier transformation

$$\rho_k(t) = \int dz \sin(kz)\, \rho(z,t)$$

$$\rho_k(\omega) = \int dt \cos(\omega t)\, a_k(t)$$

Nonrel: v = p/m

Rel: v = p/E

Cov: depends on m*

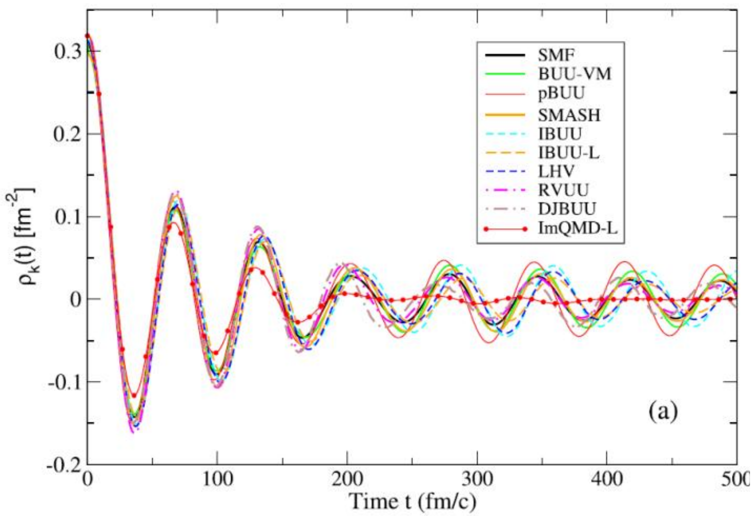

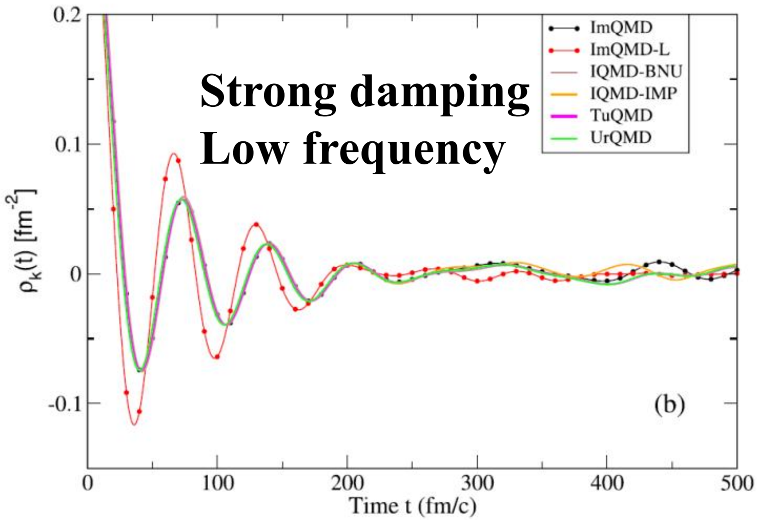

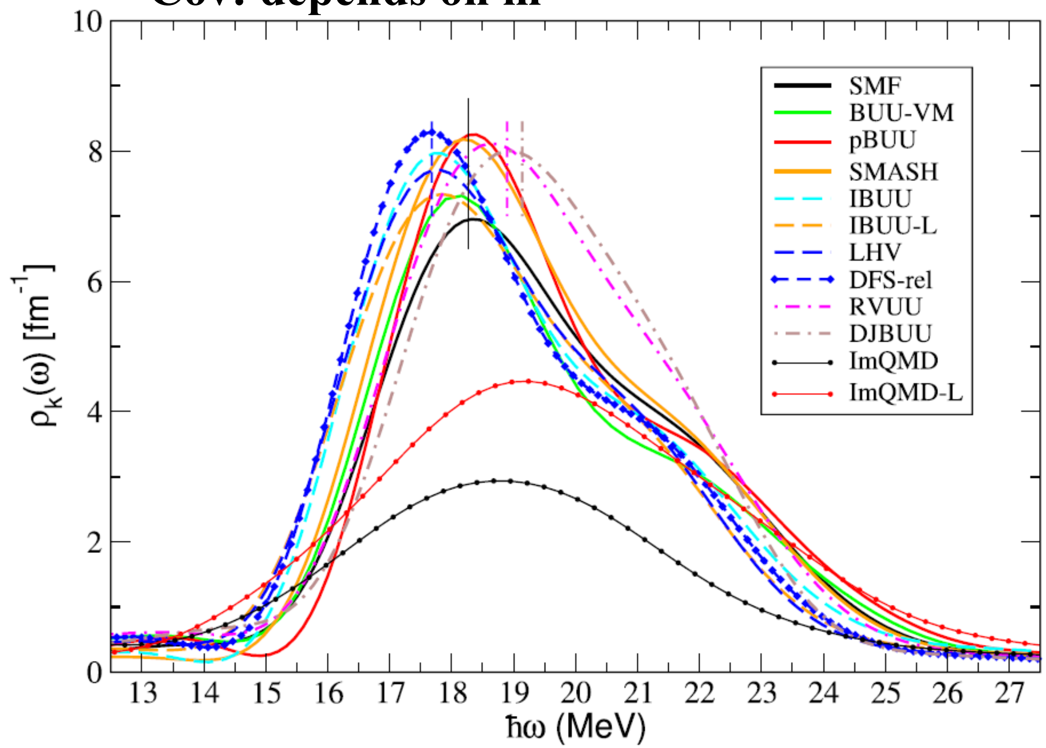

Peak of $\rho_k(\omega)$ ⇔ zero-sound

Landau parameter

Transport2019 at ECT*

HIC-pion calculation with realistic setups by code authors

Compared with SπRIT data without first knowing the data

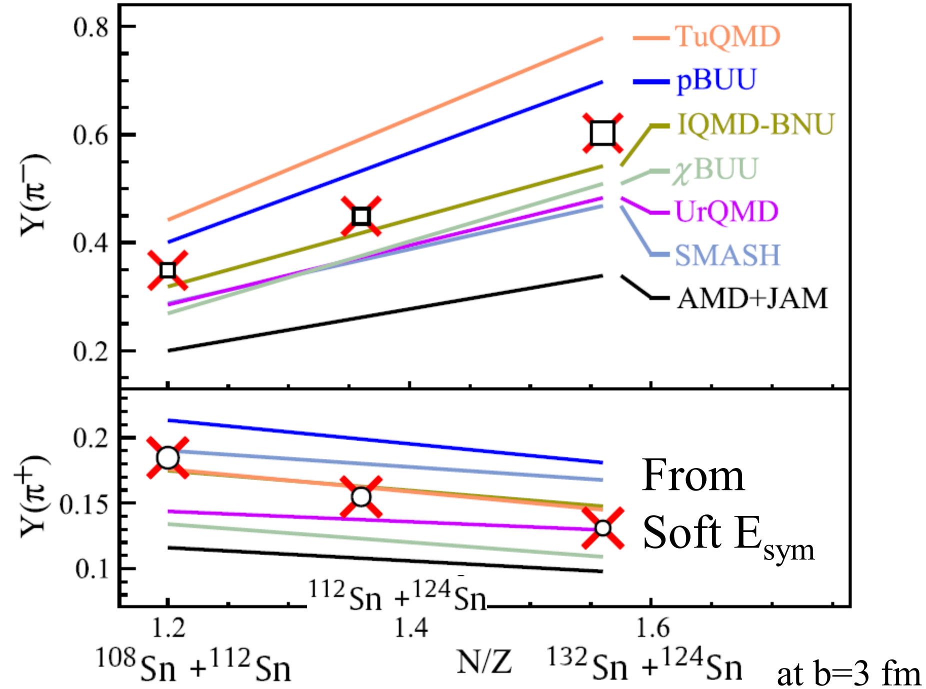

Deviations among code predictions on π^-/π^+ are larger than the E_{sym} effect.

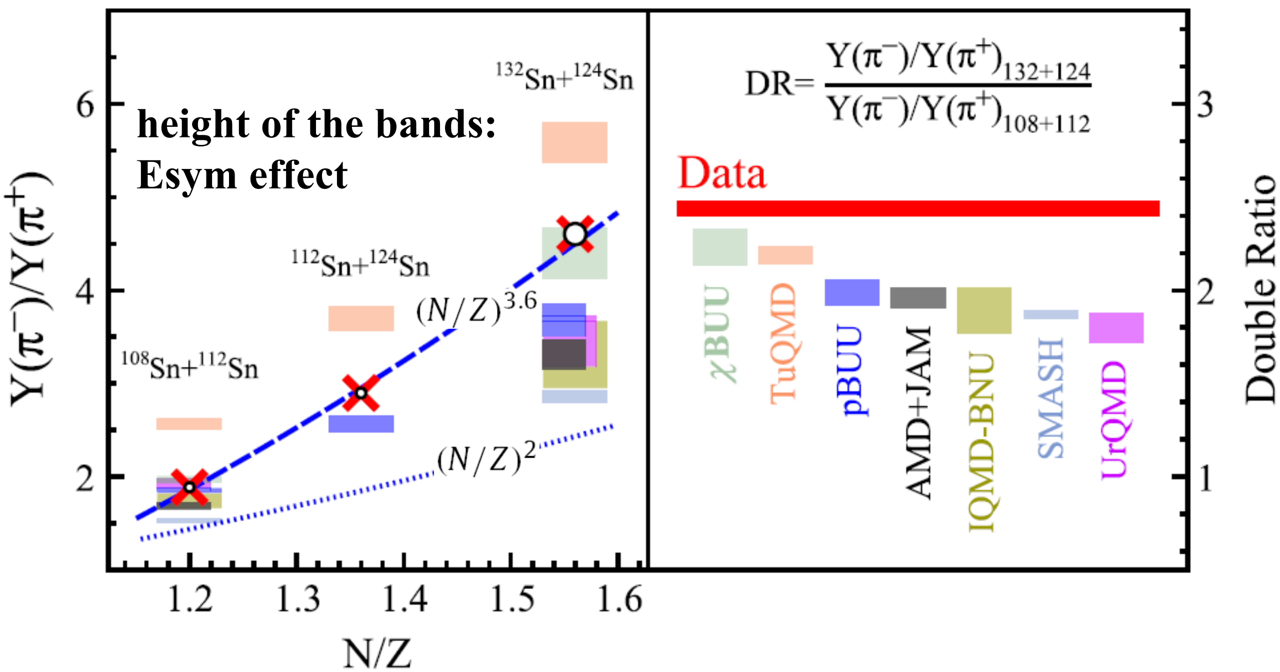

Uncertainties of different physics
+
Uncertainties of their different incorporations

G. Jhang et al., PLB (2021)

Comparisons of SπRIT data with TuQMD results

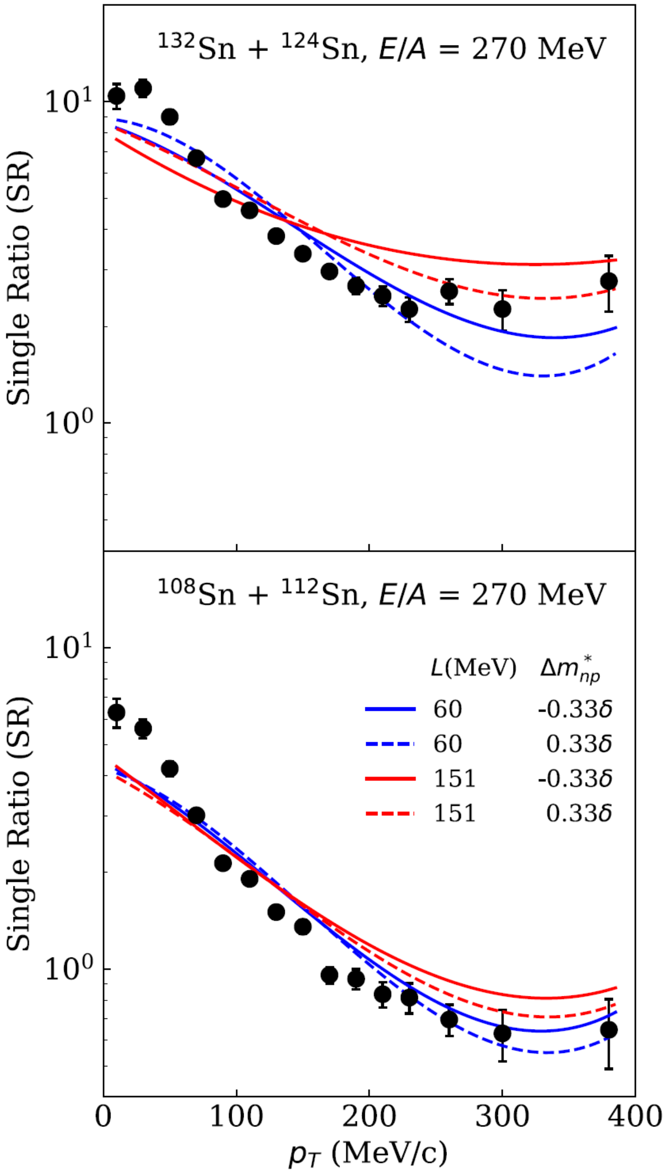

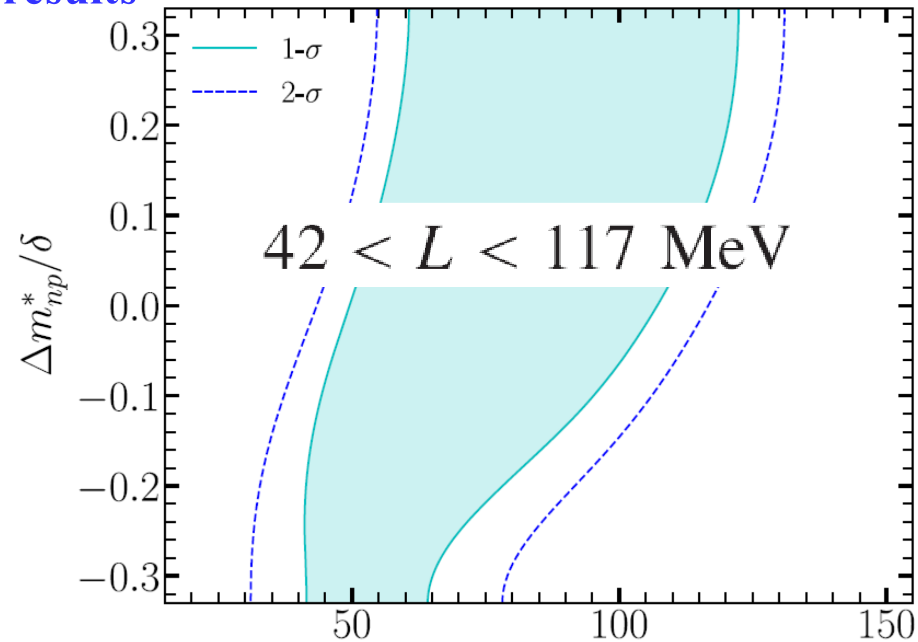

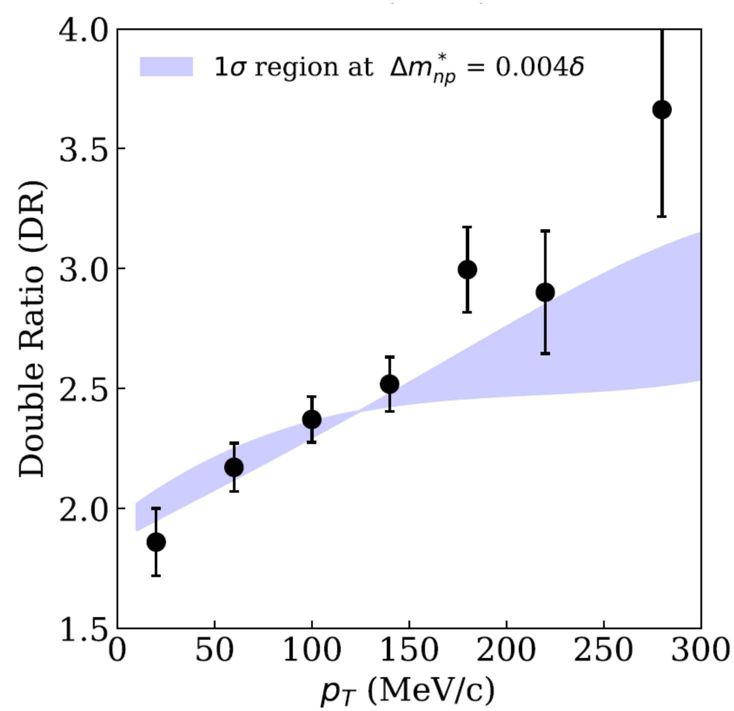

J. Estee et al., PRL (2021)

Comparing pion production in transport simulations of heavy-ion collisions at 270A MeV under controlled conditions

Jun Xu,[1,2,*] Hermann Wolter,[3,†] Maria Colonna,[4,‡] Dan Cozma,[5,§] Pawel Danielewicz,[6,7,¶] Che Ming Ko,[8,**] Akira Ono,[9,††] ManYee Betty Tsang,[6,7,‡‡] Ying-Xun Zhang,[10,11,§§] Hui-Gan Cheng,[12] Natsumi Ikeno,[13,14] Rohit Kumar,[6] Jun Su,[15] Hua Zheng,[16] Zhen Zhang,[15] Lie-Wen Chen,[17] Zhao-Qing Feng,[12] Christoph Hartnack,[18] Arnaud Le Fèvre,[19] Bao-An Li,[20] Yasushi Nara,[21] Akira Ohnishi¶¶,[22] and Feng-Shou Zhang[23,24]

(TMEP Collaboration)

TABLE I: Code names, authors and correspondents, and representative references of 4 BUU-type and 6 QMD-type codes participating in the present study. SMF and ImQMD-L only participate in the comparison of nucleon observables and are therefore listed separately in the last row.

BUU-type	code correspondents	reference	QMD-type	code correspondents	reference
IBUU[a]	J. Xu, L.W. Chen, B.A. Li	[14, 38, 39]	IQMD-BNU	J. Su, F.S. Zhang	[44]
pBUU	P. Danielewicz	[40, 41]	IQMD-IMP[b]	H.G. Cheng, Z.Q. Feng	[45]
RVUU	Z. Zhang, C.M. Ko	[42]	IQMD	R. Kumar, Ch. Hartnack, A. Le Fèvre	[46]
			JAM	N. Ikeno, A. Ono, Y. Nara, A. Ohnishi	[26, 47]
			TuQMD[c]	D. Cozma	[48]
SMF	M. Colonna, H. Zheng	[43]	ImQMD-L[d]	Y.X. Zhang	[49, 50]

[a] A new version using the lattice Hamiltonian framework, recently developed in Ref. [39], is mainly used in the present study. The original version (called IBUU-O here) is described in Refs. [14, 38].

[b] Also known as LQMD in literature.

[c] This code provides both traditional and accurate calculations of the non-linear density-dependent term in the mean-field potential, with the latter dubbed "TuQMD-L" in the present study. The dcQMD model, used in Ref. [37] to describe the pion spectra from the SπRIT experiment, is a recent offspring of the TuQMD transport code.

[d] A lattice version of ImQMD with a more accurate calculation of the non-linear density-dependent term in the mean-field potential recently developed in Ref. [50] is used in the present study. The original version is described in Ref. [49].

JX et al., Phys. Rev. C 109, 044609 (2024)

HIC-pion homework description

SπRIT condition: $^{132}Sn+^{124}Sn$@270A MeV, $^{112}Sn+^{108}Sn$@270A MeV, b = 4 fm

Summary of treatments in different codes

	TP shape/size	Coulomb potential	Pauli blocking	Δt (fm/c)
IBUU	$n = 2$, $l = 1$ fm	$N_m = 1$, $r_c = 1$ fm	cubic cell, $\Delta r = 2$ fm, $\Delta p = 100$ MeV/c, 100 TPs	0.2
pBUU	modified g, $l = 0.92$ fm	Poisson equation	fit with a superposition of two FD distributions	0.2
RVUU	point	$N_m = 10$, $r_c = 0.1$ fm	spherical cell, $\Delta r = 1$ fm, $\Delta p = 150$ MeV/c, 1000 TPs	0.2
SMF	$n = 2$, $l = 1$ fm	Poisson equation	spherical cell, $\Delta r = 2.53$ fm, $\sigma_p = 29$ MeV/c, 100 TPs	0.5
IQMD-BNU	L = 2 fm^2	standard	overlap of wave packets	1
IQMD-IMP	L = 2 fm^2	standard	overlap of wave packets	0.2
IQMD	L = 2 fm^2	standard	$\Delta r = 3$ fm, $\Delta p = 100$ MeV/c, surface correction	0.2
JAM	L = 2 fm^2	EB fields with $r_c = 2$ fm	overlap of wave packets	0
TuQMD	L = 2 fm^2	standard	$\Delta r = 3$ fm, $\Delta p = 100$ MeV/c, surface correction	0.2
ImQMD-L	L = 2 fm^2	standard	overlap of wave packets	0.2

Different simulation modes

	Coulomb potential	Pauli blocking	Mean-field potential
Cascade-nopb	off	off	off
Cascade-nopb-cou	on	off	off
Cascade	off	on	off
Cascade-cou	on	on	off
Full-nopb	off	off	on
Full-nopb-cou	on	off	on
Full	off	on	on
Full-cou	on	on	on

Nucleon evolution

BUU and lattice QMD have a lower density (ρ^{γ} term) → Less pions → Larger π^-/π^+

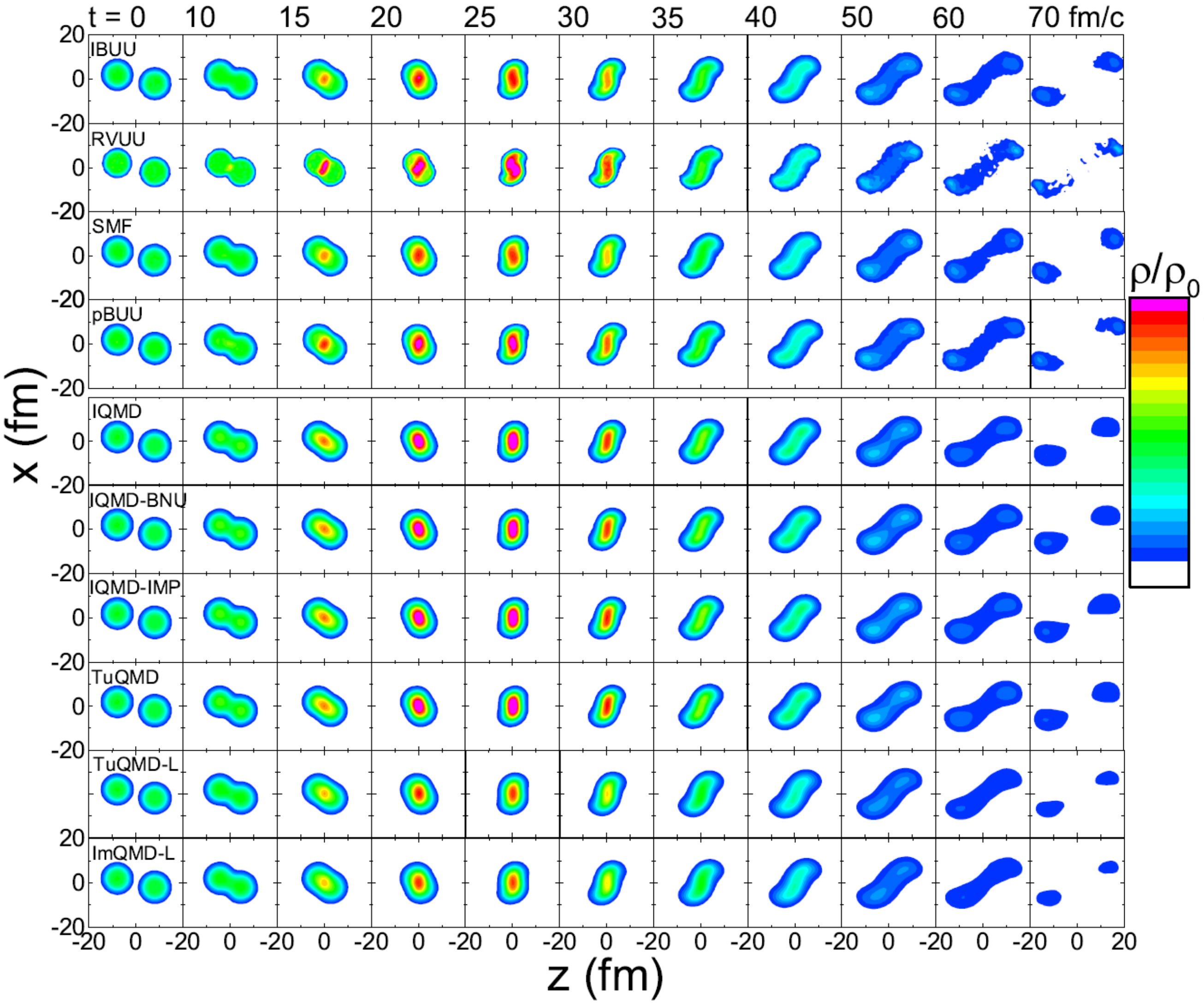

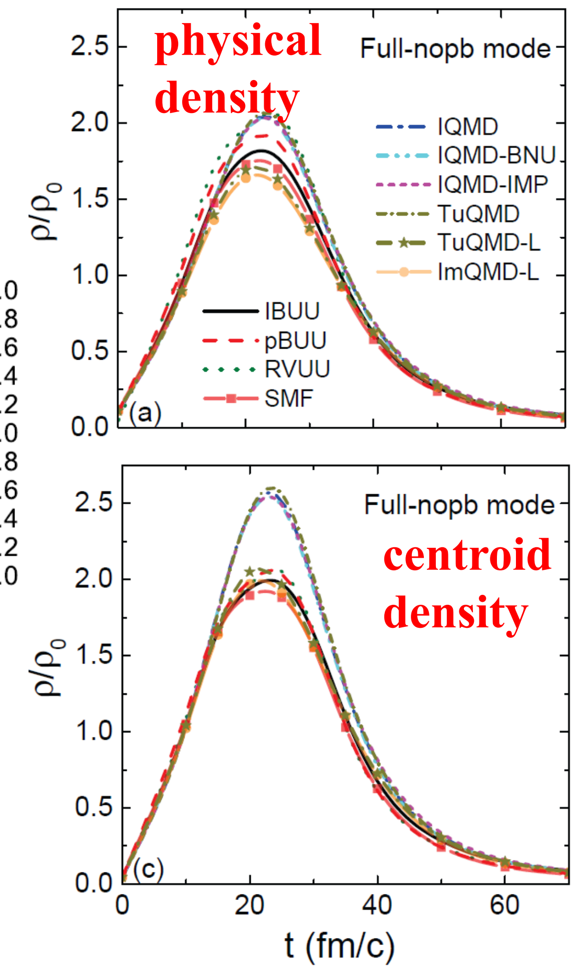

Time evolution of pion production

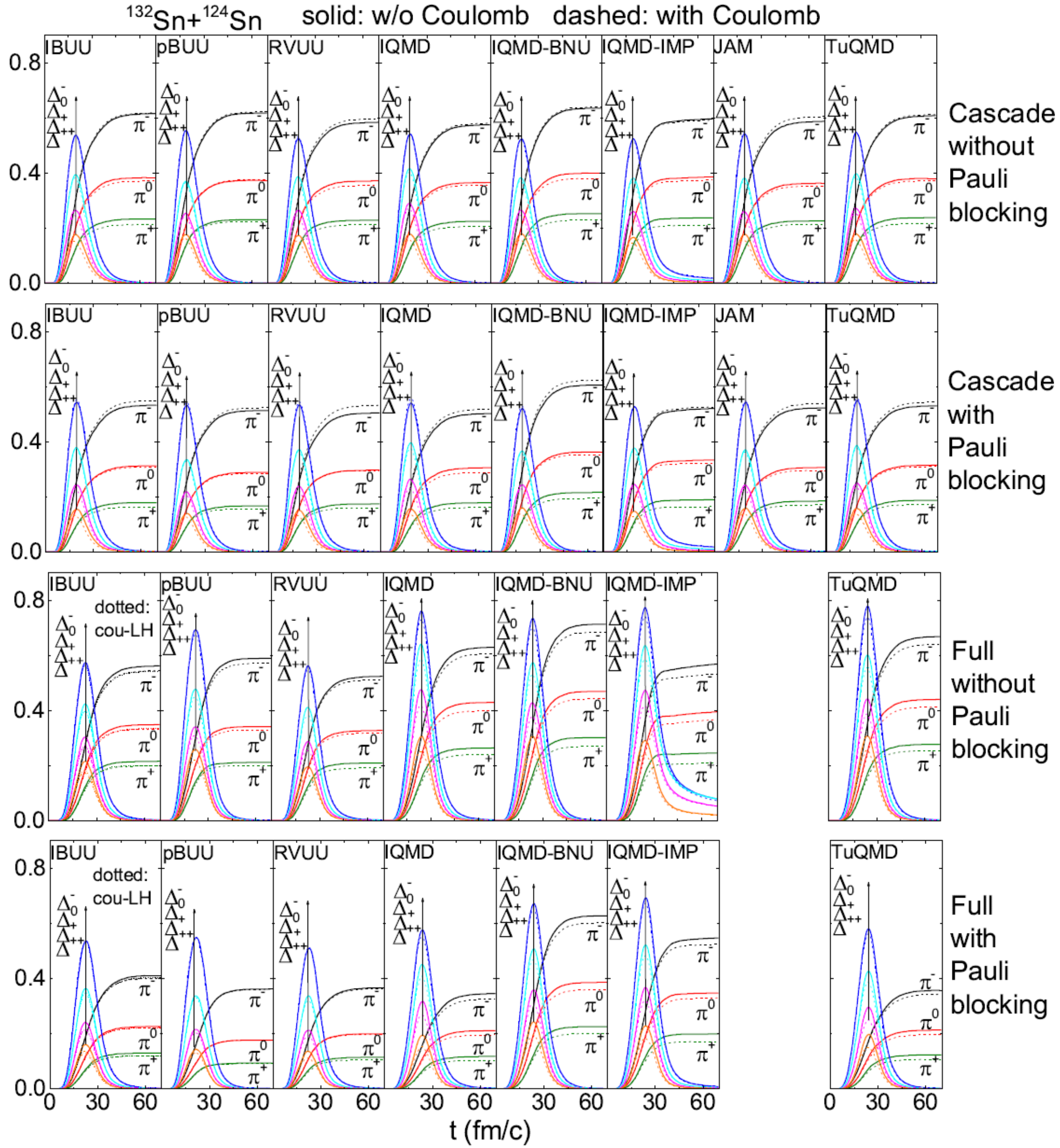

Pauli blocking

Pauli blocking:

1) Suppress more NN → NΔ than NΔ →NN, suppress Δ(π) production

2) Suppress more pp → nΔ^{++} than nn → pΔ^{-}, enhance π^{-}/π^{+} yield ratio

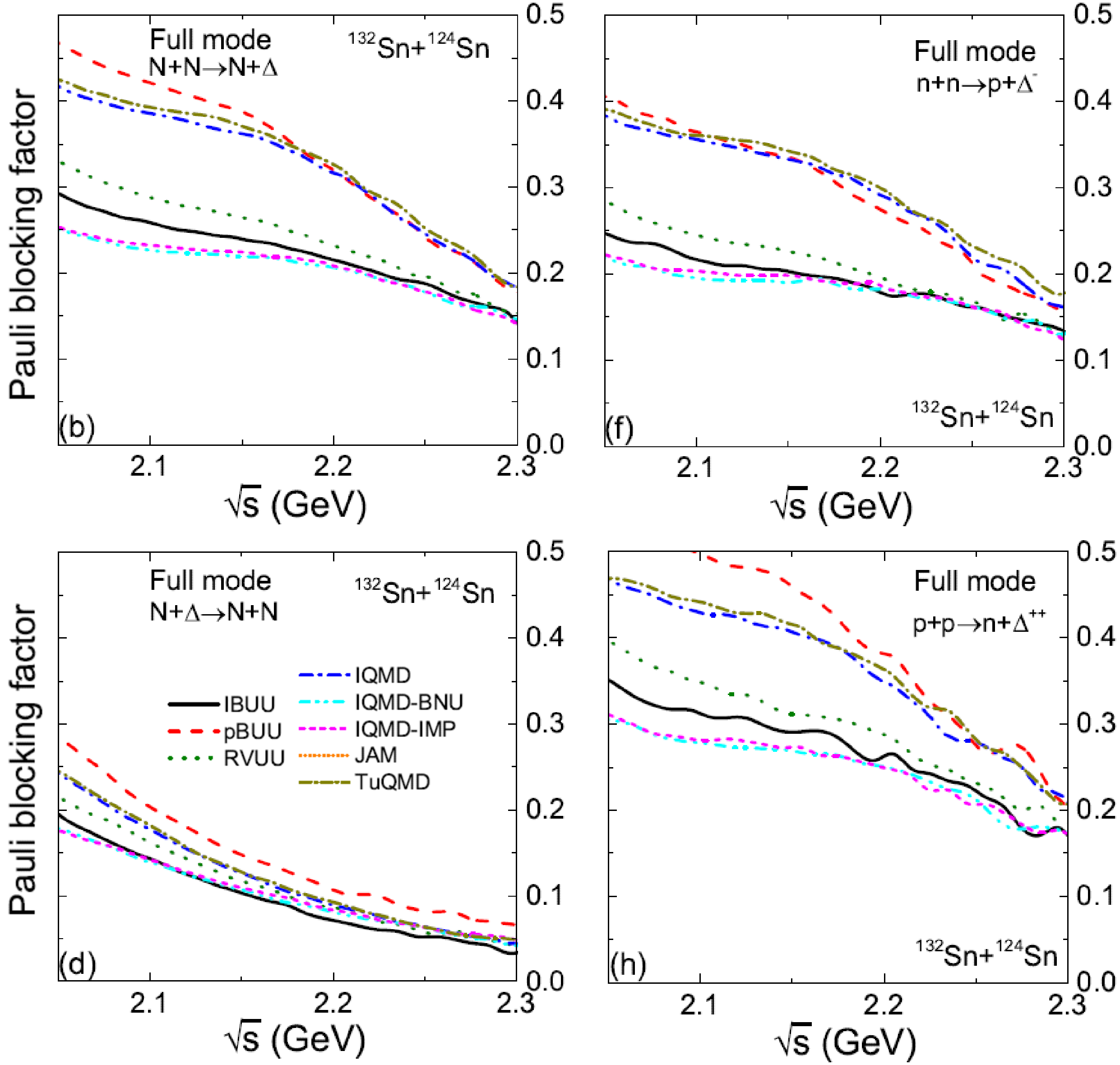

stronger Pauli blocking with local statistic method in pBUU

stronger Pauli blocking with surface correction in IQMD and TuQMD

Pion yield and ratio I

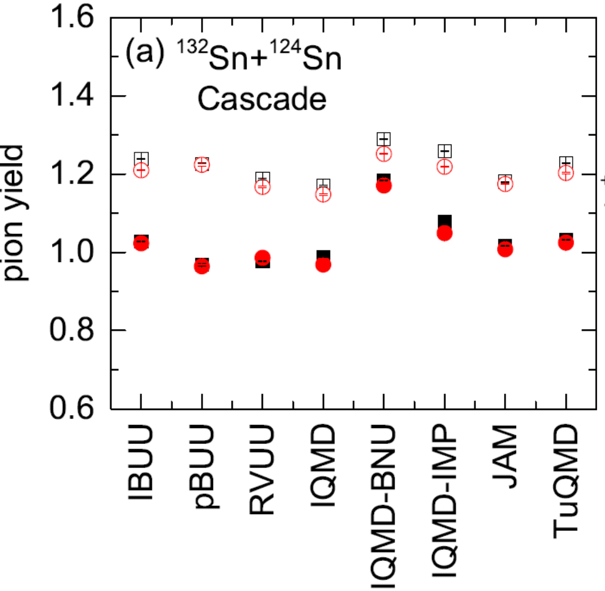

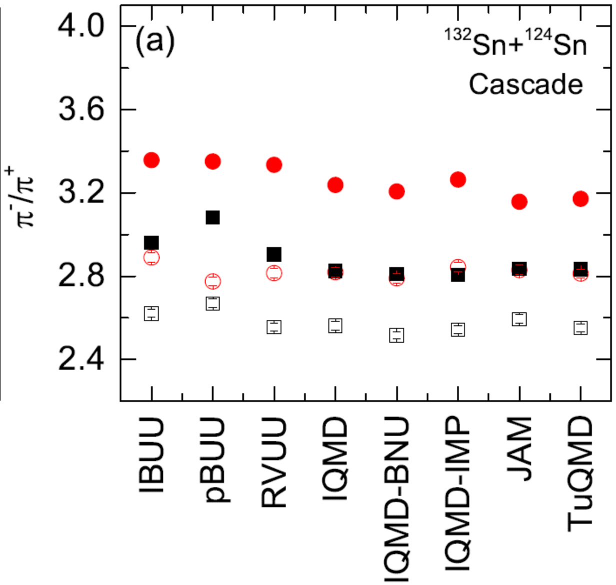

Cascade results mostly OK

Coulomb potential:

1) Suppress slightly the total $\Delta(\pi)$ production

2) Affect isospin asymmetry in the high-density phase and thus π^-/π^+ yield ratio (not exactly cancel when taking double ratio)

3) Affect high-momentum pion spectra

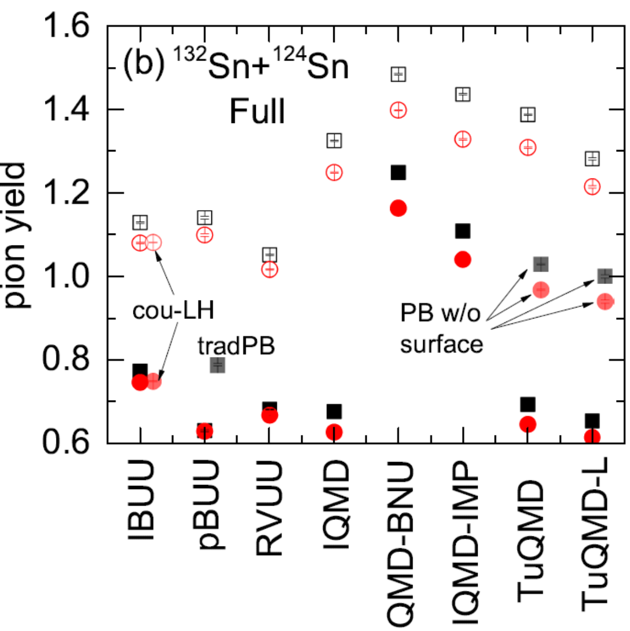

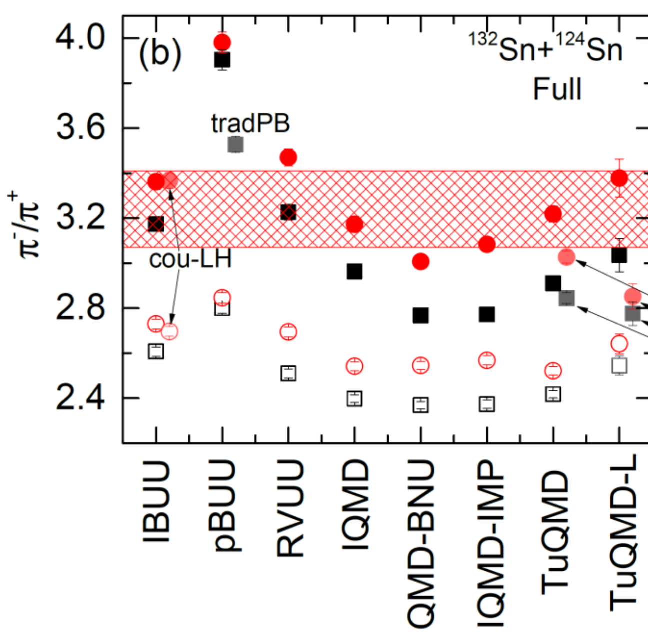

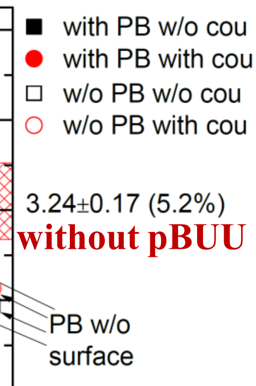

With mean-field potential, discrepancies become larger:

1) ρ^γ term

2) Stronger Pauli blocking

pBUU: with Δ and π potential, not comparable in Full mode

Pion yield and ratio II

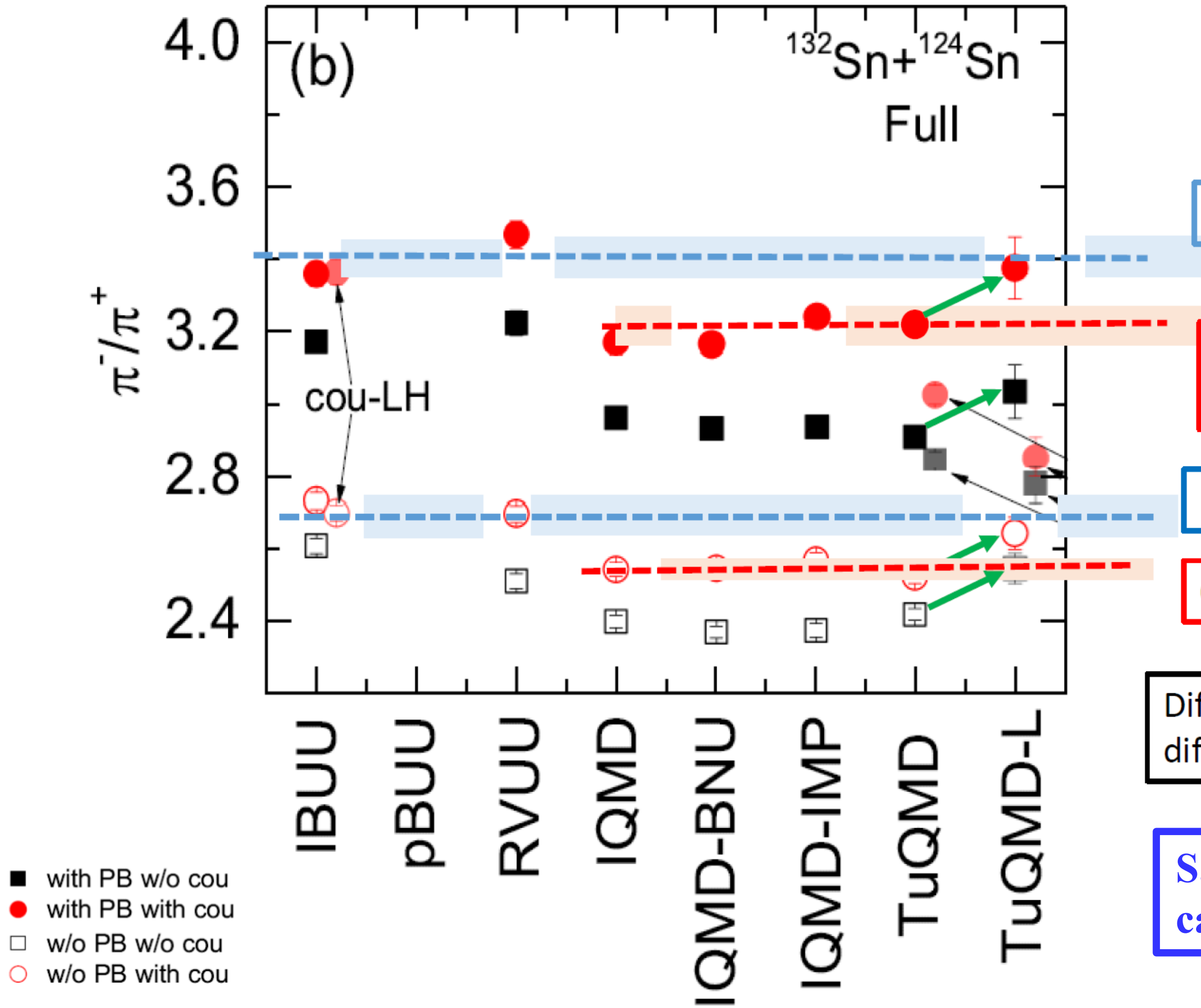

PB effect correction (6.3%)

Key results, neglect pBUU

BUU-type codes, **3.40±0.06 (1.7%)**

ρ^γ term effect correction (4.8%)

QMD-codes with surface corr **3.22±0.05 (1.8%)**

IQMD-BNU
IQMD-IMP

BUU-like codes (w/o PB) 2.69±0.04

QMD codes (w/o PB) 2.54±0.02

Difference between BUU and QMD-T **0.18**
difference TuQMD-T and TuQMD-L **0.16**

Same Pauli blocking and ρ^γ term calculation (after corrections)

π^-/π^+ ratios converge within 1.6%

Reduce uncertainty of transport simulation (TMEP)

Transport simulation
- **initialization**
- **collision**
  - **elastic**
  - **inelastic**
  - **Pauli blocking**
- **mean-field**

14 Boltzmann-Uehling-Uhlenbeck
12 Quantum Molecular Dynamics

Model dependence

HIC simulation

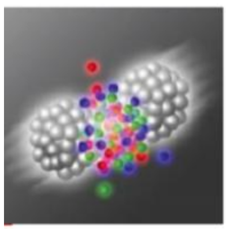

box simulation (theoretical limit)

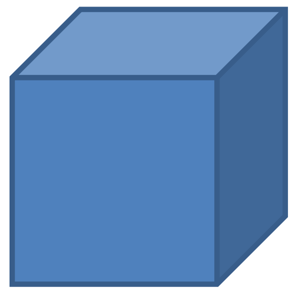

HIC simulation

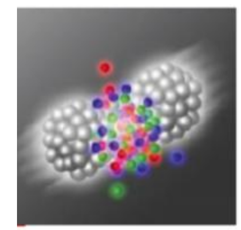

JX, et al., PRC (2016)

initialization; theoretical error of directed flow

Y.X. Zhang, et al., PRC (2018)
elastic collisions, Pauli blocking

A. Ono, JX, et al., PRC (2019)
inelastic collisions, π production

M. Colonna, et al., PRC (2021)
mean-field evolution

JX, et al., PRC (2024)

reduce uncertainty of π^-/π^+ from 5.2% to 1.6%

main uncertainties:
mean-field, Pauli blocking

Research papers published

J. Phys. G: Nucl. Part. Phys. **31** (2005) S741–S757

Transport theories for heavy-ion collisions in the 1 *A* GeV regime

E E Kolomeitsev[1,2], C Hartnack[3], H W Barz[4], M Bleicher[5], E Bratkovskaya[5], W Cassing[6], L W Chen[7,8], P Danielewicz[9], C Fuchs[10], T Gaitanos[11], C M Ko[7], A Larionov[6,13], M Reiter[5], Gy Wolf[12] and J Aichelin[3,14]

PHYSICAL REVIEW C **93**, 044609 (2016)

Understanding transport simulations of heavy-ion collisions at 100*A* and 400*A* MeV: Comparison of heavy-ion transport codes under controlled conditions

Jun Xu,[1,*] Lie-Wen Chen,[2,†] ManYee Betty Tsang,[3,‡] Hermann Wolter,[4,§] Ying-Xun Zhang,[5,‖] Joerg Aichelin,[6] Maria Colonna,[7] Dan Cozma,[8] Pawel Danielewicz,[3] Zhao-Qing Feng,[9] Arnaud Le Fèvre,[10] Theodoros Gaitanos,[11] Christoph Hartnack,[6] Kyungil Kim,[12] Youngman Kim,[12] Che-Ming Ko,[13] Bao-An Li,[14] Qing-Feng Li,[15] Zhu-Xia Li,[5] Paolo Napolitani,[16] Akira Ono,[17] Massimo Papa,[18] Taesoo Song,[19] Jun Su,[20] Jun-Long Tian,[21] Ning Wang,[22] Yong-Jia Wang,[15] Janus Weil,[19] Wen-Jie Xie,[23] Feng-Shou Zhang,[24] and Guo-Qiang Zhang[1]

PHYSICAL REVIEW C **97**, 034625 (2018)

Comparison of heavy-ion transport simulations: Collision integral in a box

Ying-Xun Zhang,[1,2,*] Yong-Jia Wang,[3,†] Maria Colonna,[4,‡] Pawel Danielewicz,[5,§] Akira Ono,[6,‖] Manyee Betty Tsang,[5,¶] Hermann Wolter,[7,#] Jun Xu,[8,**] Lie-Wen Chen,[9] Dan Cozma,[10] Zhao-Qing Feng,[11] Subal Das Gupta,[12] Natsumi Ikeno,[13] Che-Ming Ko,[14] Bao-An Li,[15] Qing-Feng Li,[3,11] Zhu-Xia Li,[1] Swagata Mallik,[16] Yasushi Nara,[17] Tatsuhiko Ogawa,[18] Akira Ohnishi,[19] Dmytro Oliinychenko,[20] Massimo Papa,[4] Hannah Petersen,[20,21,22] Jun Su,[23] Taesoo Song,[20,21] Janus Weil,[20] Ning Wang,[24] Feng-Shou Zhang,[25,26] and Zhen Zhang[14]

PHYSICAL REVIEW C **100**, 044617 (2019)

Comparison of heavy-ion transport simulations: Collision integral with pions and Δ resonances in a box

Akira Ono,[1,*] Jun Xu,[2,3,†] Maria Colonna,[4] Pawel Danielewicz,[5] Che Ming Ko,[6] Manyee Betty Tsang,[5] Yong-Jia Wang,[7] Hermann Wolter,[8] Ying-Xun Zhang,[9,10] Lie-Wen Chen,[11] Dan Cozma,[12] Hannah Elfner,[13,14,15] Zhao-Qing Feng,[16] Natsumi Ikeno,[17,18] Bao-An Li,[19] Swagata Mallik,[20] Yasushi Nara,[21] Tatsuhiko Ogawa,[22] Akira Ohnishi,[23] Dmytro Oliinychenko,[24] Jun Su,[25] Taesoo Song,[13] Feng-Shou Zhang,[26,27] and Zhen Zhang[25]

PHYSICAL REVIEW C **104**, 024603 (2021)

Comparison of heavy-ion transport simulations: Mean-field dynamics in a box

Maria Colonna,[1,*] Ying-Xun Zhang,[2,3,†] Yong-Jia Wang,[4,‡] Dan Cozma,[5] Pawel Danielewicz,[6,§] Che Ming Ko,[7] Akira Ono,[8,‖] Manyee Betty Tsang,[6,¶] Rui Wang,[9,10] Hermann Wolter,[11,#] Jun Xu,[12,9,**] Zhen Zhang,[13] Lie-Wen Chen,[14] Hui-Gan Cheng,[15] Hannah Elfner,[16,17,18] Zhao-Qing Feng,[15] Myungkuk Kim,[19] Youngman Kim,[20] Sangyong Jeon,[21] Chang-Hwan Lee,[22] Bao-An Li,[23] Qing-Feng Li,[4,24] Zhu-Xia Li,[2] Swagata Mallik,[25] Dmytro Oliinychenko,[26,27] Jun Su,[13] Taesoo Song,[16,28] Agnieszka Sorensen,[29] and Feng-Shou Zhang[30,31]

PHYSICAL REVIEW C **109**, 044609 (2024)

Comparing pion production in transport simulations of heavy-ion collisions at 270*A* MeV under controlled conditions

Jun Xu,[1,*] Hermann Wolter,[2,†] Maria Colonna,[3,‡] Mircea Dan Cozma,[4,§] Pawel Danielewicz,[5,6,‖] Che Ming Ko,[7,¶] Akira Ono,[8,#] ManYee Betty Tsang,[5,6,**] Ying-Xun Zhang,[9,10,††] Hui-Gan Cheng,[11] Natsumi Ikeno,[12,13] Rohit Kumar,[5] Jun Su,[14] Hua Zheng,[15] Zhen Zhang,[14] Lie-Wen Chen,[16] Zhao-Qing Feng,[11] Christoph Hartnack,[17] Arnaud Le Fèvre,[18] Bao-An Li,[19] Yasushi Nara,[20] Akira Ohnishi,[21,‡‡] and Feng-Shou Zhang[22,23]
(TMEP Collaboration)

Compare model calculations with exp data

Symmetry energy investigation with pion production from Sn+Sn systems

Physics Letters B 813 (2021) 136016

G. Jhang, et al. (SπRIT Collaboration and TMEP Collaboration)

A few review papers related to TMEP

Dynamics of clusters and fragments in heavy-ion collisions

Akira Ono

Progress in Particle and Nuclear Physics 105 (2019) 139-179

Transport approaches for the description of intermediate-energy heavy-ion collisions

Jun Xu *

Progress in Particle and Nuclear Physics 106 (2019) 312–359

Collision dynamics at medium and relativistic energies

M. Colonna

Progress in Particle and Nuclear Physics 113 (2020) 103775

Transport models for intermediate-energy heavy-ion studies

Hermann Wolter, et al.

Progress in Particle and Nuclear Physics 125 (2022) 103962

Concluding remarks

Accurate knowledge of nuclear force/EOS extracted from intermediate-energy HIC needs well calibrated transport approaches.

Strategies
- **HIC comparison among models, simple physics input**
- **Box comparison among models, theoretical limits available**
- **HIC comparison with exp data, realistic physics input**

Transport models that (partially) participated in transport model evaluation project

Boltzmann-Uehling-Uhlenbeck approach	Quantum Molecular Dynamics approach
Boltzmann-Langevin One Body (BLOB)	Antisymmetrized Molecular Dynamics (AMD)
BUU by Budapest/Rossendorf group (BUU-BR)	Constrained Molecular Dynamics (CoMD)
BUU by VECC and McGill University (BUU-VM)	Improved QMD at CIAE (ImQMD-CIAE)
Daejeon BUU (DJBUU)	Improved QMD at GXNU (ImQMD-GXNU)
BUU by Giessen group (GiBUU)	Isospin-dependent QMD (IQMD)
Hadron String Dynamics (HSD)	Isospin-dependent QMD at BNU (IQMD-BNU)
Isospin-dependent Boltzmann-Langevin (IBL)	Isospin-dependent QMD at IMP (IQMD-IMP)
Isospin-dependent BUU (IBUU)	Isospin-dependent QMD at SINAP (IQMD-SINAP)
Lattice BUU (LBUU or LHV)	jet AA microscopic (JAM) & sJAM
Pawel's BUU (pBUU)	QMD at Japan Atomic Energy Research Institute (JQMD)
Relativistic BUU (RBUU)	Tübingen QMD(TuQMD)
Relativistic Vlasov-Uehling-Uhlenbeck (RVUU)	Ultra-relativistic QMD (UrQMD)
Simulating Many Accelerated Strongly-interacting Hadron (SMASH)	
Stochastic Mean-Field (SMF)	
BUU based on MF from χEFT (χBUU)	

What we learned

- **Initialization:** ground-state distribution - stable
- **Mean-field potential:** size of particles
  - BUU: Lattice Hamiltonian method, more test particles
  - QMD: accurate calculation of $<\rho^\gamma>$

$\Delta t \rightarrow 0$

- **NN collisions:**
  - Attempted: γ factor, remove spurious collisions, reduce higher-order correlations, prefer full-ensemble method, prefer stochastic method
  - Pauli blocking:
    - BUU: more test particles, effective temperature fit
    - QMD: antisymmetrized wave function (?), surface correction (?)
  - Inelastic: prefer time-step free or full-ensemble method, reduce higher-order correlations, randomize collision order list
  - Coulomb(?): independent of distance cut, TP size, …

- **Main ingredients affecting π^-/π^+:**
  - **Pauli blocking**
  - **ρ^γ term (QMD)**
  - **Coulomb potential**
  - **…**

Acknowledgements

ManYee Betty Tsang, Hermann Wolter, Ying-Xun Zhang, Akira Ono, Maria Colonna, Mircea Dan Cozma, Che Ming Ko, Pawel Danielewicz, Zhen Zhang, Rui Wang, Yong-Jia Wang, Qing-Feng Li, ...

junxu@tongji.edu.cn

From Schrödinger equation to Vlasov equation

Wigner function (phase-space distribution function):

$$f(r,p,t) = \alpha \sum_i \int \phi_i(r-s,t)\phi_i^*(r+s,t)e^{2ips}d^3s$$

$$i\frac{\partial}{\partial t}f(r,p,t) = \alpha \sum_i \int [h\phi_i(r-s,t)\phi_i^*(r+s,t) - \phi_i(r-s,t)h\phi_i^*(r+s,t)]e^{2ips}d^3s$$

$$h = -\nabla \cdot \left(\frac{1}{2m}\nabla\right) + V(r)$$

Schrödinger equation $i\frac{\partial}{\partial t}\phi_i = h\phi_i$ **(TDHF)**

Kinetic contribution: $i\frac{\partial}{\partial t}f^k(r,p,t) = -i\frac{p}{m}\nabla_r f(r,p,t)$

Potential contribution: $i\frac{\partial}{\partial t}f^p(r,p,t) \approx i\nabla_r V \cdot \nabla_p f(r,p,t) - \frac{i}{24}\nabla_r^3 V \cdot \nabla_p^3 f(r,p,t) + \ldots$

Boltzmann-Vlasov equation: $\frac{\partial}{\partial t}f(r,p,t) \approx -\frac{p}{m}\nabla_r f(r,p,t) + \nabla_r V \cdot \nabla_p f(r,p,t)$

or $\frac{2}{\hbar}\sin\left(\frac{\hbar}{2}\nabla_r \cdot \nabla_p\right)$

Equations of motion for solving Boltzmann equation

Substitute

$$f(rp,t) = \int \frac{\mathrm{d}r_0\,\mathrm{d}p_0\,\mathrm{d}s}{(2\pi\hbar)^3} \exp\{\mathrm{i}s\cdot[p - P(r_0p_0s,t)]/\hbar\}\,\delta[r - R(r_0p_0s,t)]\,f(r_0p_0,t_0)$$

into the Boltzmann-Vlasov equation

$$\frac{\partial f(rp,t)}{\mathrm{d}t} + \frac{p}{m}\cdot\nabla_r f(rp,t) - \frac{2}{\hbar}\sin\left\{\frac{\hbar}{2}\nabla_r^V\cdot\nabla_p^f\right\}V(r,t)\,f(rp,t) = 0$$

First term:

$$\begin{aligned}\frac{\partial f(rp,t)}{\partial t} = \int \frac{\mathrm{d}r_0\,\mathrm{d}p_0\,\mathrm{d}s}{(2\pi\hbar)^3} f(r_0p_0,t_0)\Bigg[&\frac{(-\mathrm{i}s)}{\hbar}\cdot\frac{\partial P}{\partial t}\\ &\times \exp\{\mathrm{i}s\cdot[p - P(r_0p_0s,t)]/\hbar\}\delta[r - R(r_0p_0s,t)]\\ &+ \exp\{\mathrm{i}s\cdot[p - P(r_0p_0s,t)]/\hbar\}\\ &\times (\nabla_R\delta[r - R(r_0p_0s,t)])\cdot\partial R(r_0p_0s,t)/\partial t\Bigg].\end{aligned}$$

C. Y. Wong, PRC (1982)

Noting that

$$\nabla_R \delta[r - R(r_0 p_0 s, t)] = -\nabla_r \delta[r - R(r_0 p_0 s, t)]$$

So

$$\int \frac{\mathrm{d}r_0\,\mathrm{d}p_0\,\mathrm{d}s}{(2\pi\hbar)^3} f(r_0 p_0, t_0) \exp\{\mathrm{i}s \cdot [p - P(r_0 p_0 s, t)]/\hbar\} \times (-\nabla_r \delta[r - R(r_0 p_0 s, t)]) \cdot \partial R(r_0 p_0 s, t)/\partial t$$
$$= -\frac{\partial R(r_0 p_0 s, t)}{\partial t} \cdot \nabla_r f(rp, t),$$

The potential term:

$$\frac{2}{\hbar} \sin\left\{\frac{\hbar}{2} \nabla_r^V \cdot \nabla_p^f\right\} V(r, t) f(rp, t)$$
$$= \frac{1}{\hbar} \int \frac{\mathrm{d}r_0\,\mathrm{d}p_0\,\mathrm{d}s}{(2\pi\hbar)^3} f(r_0 p_0, t_0)$$
$$\times \exp\{\mathrm{i}s \cdot [p - P(r_0 p_0 s, t)]/\hbar\} \delta[r - R(r_0 p_0 s, t)]$$
$$\times \frac{[V(r - \frac{s}{2}, t) - V(r + \frac{s}{2}, t)]}{\mathrm{i}}.$$

C. Y. Wong, PRC (1982)

Put everything together:

$$\begin{aligned}&\left[-\frac{\partial R(r_0 p_0 s,t)}{\partial t}+\frac{p}{m}\right]\cdot\nabla_r f(rp,t)\\&\quad+\int\frac{\mathrm{d}r_0\,\mathrm{d}p_0\,\mathrm{d}s}{(2\pi\hbar)^3}f(r_0p_0,t_0)\left[\frac{(-\mathrm{i}s)}{\hbar}\cdot\frac{\partial P}{\partial t}\right.\\&\quad\left.-\frac{[V(r-\frac{s}{2},t)-V(r+\frac{s}{2},t)]}{\mathrm{i}\hbar}\right]\\&\quad\times\exp\{\mathrm{i}s\cdot[p-P(r_0p_0s,t)]/\hbar\}\\&\quad\times\delta[r-R(r_0p_0s,t)]=0.\end{aligned}$$

C. Y. Wong, PRC (1982)

Momentum-dependent potential:
One more term in BV equation

$$+\frac{2}{\hbar}\sin\left(\frac{\hbar}{2}\nabla_p^V\cdot\nabla_r^f\right)V(R,P,t)f(R,P,t)$$

Equations of motion:

$$\frac{\partial R}{\partial t}=\frac{p}{m},$$

$$\frac{\partial R}{\partial t}=\frac{p}{m}+\nabla_p V$$

$$s\cdot\frac{\partial P}{\partial t}=V\left(R-\frac{s}{2},t\right)-V\left(R+\frac{s}{2},t\right).$$

$$\frac{\partial P}{\partial t}\approx-\nabla_R V(R,t)$$

Brief discussions on fluctuation and clusters in transport model simulation

Fluctuation in BUU and QMD

Ordinary BUU: finite TPs => statistical fluctuation
infinite TPs => exact solution of BUU equation

IBL, SMF, BLOB

$$\left(\frac{\partial}{\partial t}+\frac{\vec{p}}{m}\cdot\nabla_r-\nabla_r U\left(\hat{f}\right)\cdot\nabla_p\right)\hat{f}\left(\vec{r},\vec{p},t\right)=K\left(\hat{f}\right)$$

$$+\delta K\left(\vec{r},\vec{p},t\right)$$

SMF: fluctuations are projected on the coordinate space
BLOB: fluctuations are implemented in full phase space

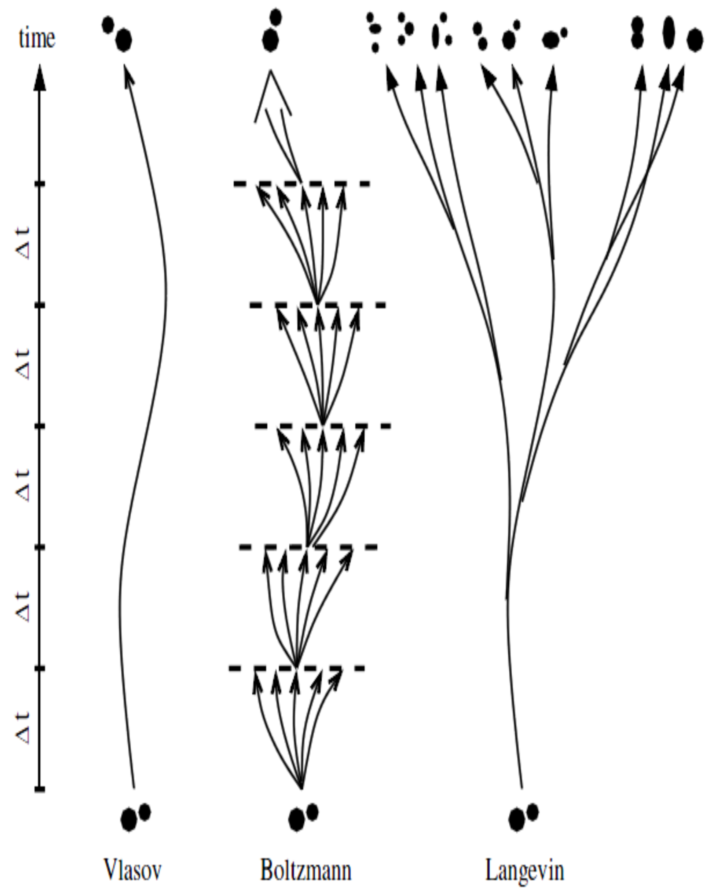

Ordinary QMD:

fluctuation related to the Gaussian width
larger width => smaller fluctuation

Cluster production in BUU and QMD

For freeze-out phase-space distribution

Naïve coalescence:

$$|\vec{r}_i - \vec{r}_j| < R_0 \qquad |\vec{p}_i - \vec{p}_j| < P_0$$

Dynamical coalescence:

The multiplicity of a M-nucleon cluster

$$\frac{dN_M}{d^3K} = G \binom{A}{M} \binom{M}{Z} \frac{1}{A^M} \int \left[\prod_{i=1}^{Z} f_p(\mathbf{r}_i, \mathbf{k}_i) \right] \left[\prod_{i=Z+1}^{M} f_n(\mathbf{r}_i, \mathbf{k}_i) \right]$$

R. Mattiello et al.,
Phys. Rev. Lett 1995
Phys. Rev. C 1997.

$$\times \rho^W(\mathbf{r}_{i_1}, \mathbf{k}_{i_1}, \ldots, \mathbf{r}_{i_{M-1}}, \mathbf{k}_{i_{M-1}})\, \delta\big(\mathbf{K} - (\mathbf{k}_1 + \cdots + \mathbf{k}_M)\big)\, d\mathbf{r}_1\, d\mathbf{k}_1 \cdots d\mathbf{r}_M\, d\mathbf{k}_M$$

ρ^W the Wigner phase-space density of the M-nucleon cluster

Wigner phase-space density

deuteron

$$\rho_d^W(\mathbf{r},\mathbf{k}) = \int \phi\left(\mathbf{r}+\frac{\mathbf{R}}{2}\right)\phi^*\left(\mathbf{r}-\frac{\mathbf{R}}{2}\right)\exp(-i\mathbf{k}\cdot\mathbf{R})\,d\mathbf{R},$$

$$\mathbf{k} = (\mathbf{k}_1 - \mathbf{k}_2)/2 \qquad \mathbf{r} = (\mathbf{r}_1 - \mathbf{r}_2)$$

Internal wave function $\phi(r)$ ⇨ root-mean-square radius of 1.96 fm

Triton or Helium3

$$\rho^W_{\mathrm{t}(^3\mathrm{He})}(\rho,\lambda,\mathbf{k}_\rho,\mathbf{k}_\lambda) = \int \psi\left(\rho+\frac{\mathbf{R}_1}{2},\lambda+\frac{\mathbf{R}_2}{2}\right)\psi^*\left(\rho-\frac{\mathbf{R}_1}{2},\lambda-\frac{\mathbf{R}_2}{2}\right) \times \exp(-i\mathbf{k}_\rho\cdot\mathbf{R}_1)\exp(-i\mathbf{k}_\lambda\cdot\mathbf{R}_2)3^{3/2}\,d\mathbf{R}_1\,d\mathbf{R}_2$$

$$\begin{pmatrix}\mathbf{R}\\ \rho\\ \lambda\end{pmatrix} = J\begin{pmatrix}\mathbf{r}_1\\ \mathbf{r}_2\\ \mathbf{r}_3\end{pmatrix} \quad J = \begin{pmatrix}\frac{1}{3} & \frac{1}{3} & \frac{1}{3}\\ \frac{1}{\sqrt{2}} & -\frac{1}{\sqrt{2}} & 0\\ \frac{1}{\sqrt{6}} & \frac{1}{\sqrt{6}} & -\frac{2}{\sqrt{6}}\end{pmatrix} \quad \begin{pmatrix}\mathbf{K}\\ \mathbf{k}_\rho\\ \mathbf{k}_\lambda\end{pmatrix} = J^{-,+}\begin{pmatrix}\mathbf{k}_1\\ \mathbf{k}_2\\ \mathbf{k}_3\end{pmatrix} \quad J^{-,+} = \begin{pmatrix}1 & 1 & 1\\ \frac{1}{\sqrt{2}} & -\frac{1}{\sqrt{2}} & 0\\ \frac{1}{\sqrt{6}} & \frac{1}{\sqrt{6}} & -\frac{2}{\sqrt{6}}\end{pmatrix}$$

Internal wave function $\psi(\mathbf{r}_1,\mathbf{r}_2,\mathbf{r}_3)$ ⇨ RMS radius 1.61 and 1.74 fm for triton and ^{3}He.

Multifragmentation in intermediate and high energy nuclear reactions

Experimentally established: 1) few stages of reactions leading to multifragmentation, 2) short time ~100fm/c for primary fragment production, 3) freeze-out density is around $0.1\rho_0$, 4) high degree of equilibration at the freeze-out, 5) primary fragments are hot.

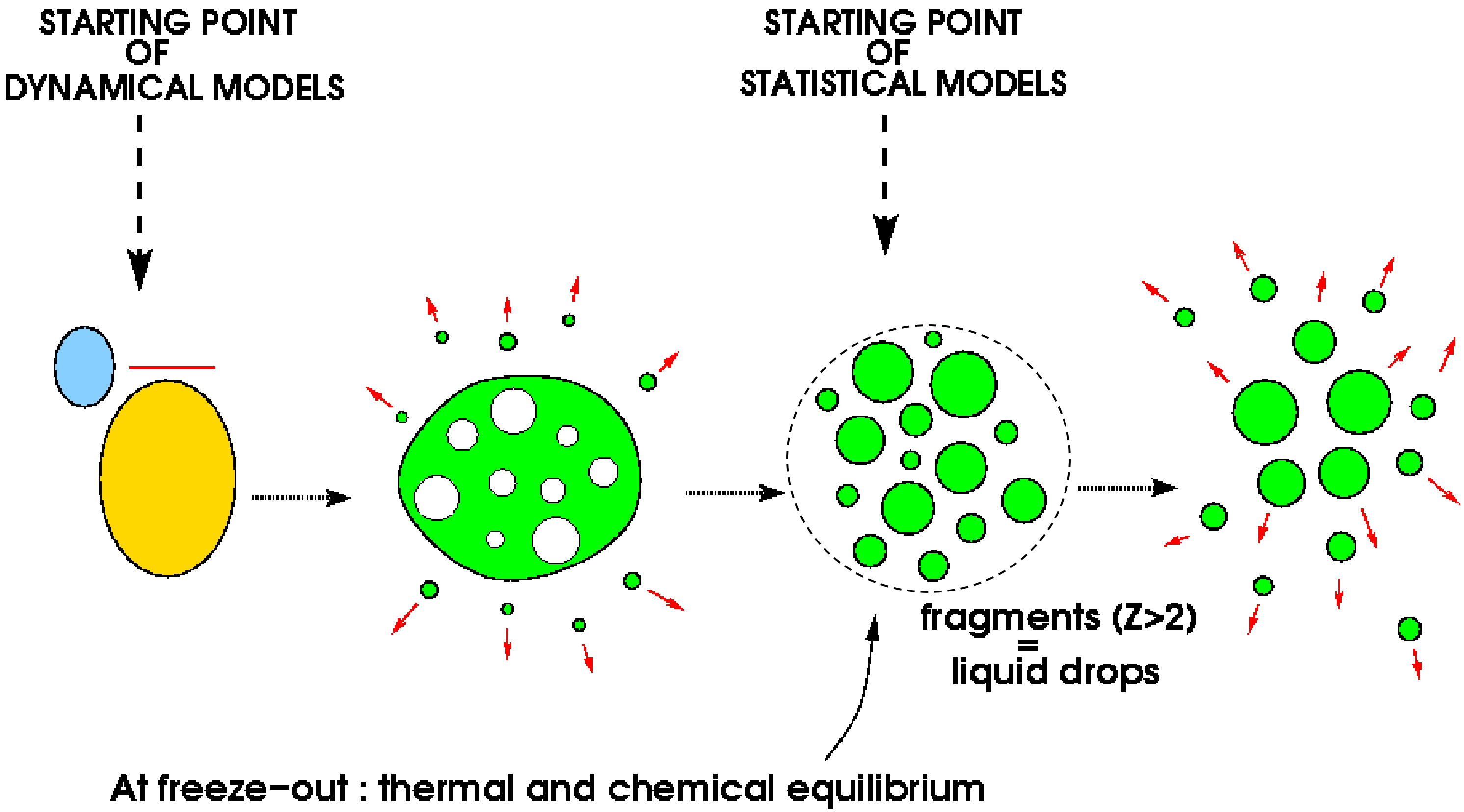

Multifragmentation as afterburner of transport simulation

Code	Evaporation	User	Author	Ref.
Statistical Multifragmentati				
ISMM-c	MSU-decay	Tsang	Das Gupta	[2]
ISMM-m	MSU-decay	Souza	Souza	[13, 14]
SMM95	own code	Bougault	Botvina	[4,9]
MMM1	own code	AH Raduta	AH Raduta	[15]
MMM2	own code	AR Raduta	AR Raduta	[15]
MMMC	own code	Le Fèvre	Gross	[5, 16]
LGM	N/A	Regnard	Gulminelli	[17]
QSM	own code	Trautmann	Stöcker	[18]
EES	EES	Friedman	Friedman	[7,8]
BNV-box	N/A	Colonna	Colonna	[24]
Evaporation codes				
Gemini		Charity	Charity	[25]
Gemini-w		Wada	Wada	[25–28]
SIMON		Durand	Durand	[29]
EES		Friedman	Friedman	[7,8]
MSU-decay		Tsang	Tan *et al.*	[14]

Different statistical multifragmentation models and evaporation codes

Different approaches for multifragmentation and cluster deexictation

M.B. Tsang et al., EPJA (2006)

Cluster dynamics in BUU and QMD

pBUU:

$$\overline{|\mathcal{M}^{npN\to Nd}|^2} = \overline{|\mathcal{M}^{Nd\to Nnp}|^2} \propto d\sigma^{Nd\to Nnp}$$

3-body collision forms a deuteron

4-body collision forms a triton or ^{3}He

P. Danielewicz and G.F. Bertsch, NPA 533, 712 (1991)

AMD:

$$N_1 + B_1 + N_2 + B_2 \to C_1 + C_2$$

- N_1, N_2 : Colliding nucleons
- B_1, B_2 : Spectator nucleons/clusters
- C_1, C_2 : N, $(2N)$, $(3N)$, $(4N)$ (up to α cluster)

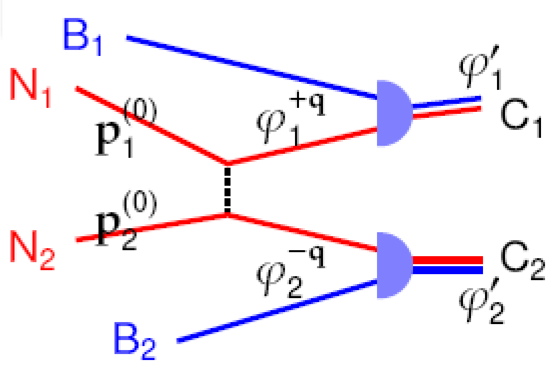

Fluctuation in BUU and QMD

Central Collisions of $^{112}Sn + ^{112}Sn$ at 50 MeV/nucleon

BUU-type (Stochastical Mean-Field)

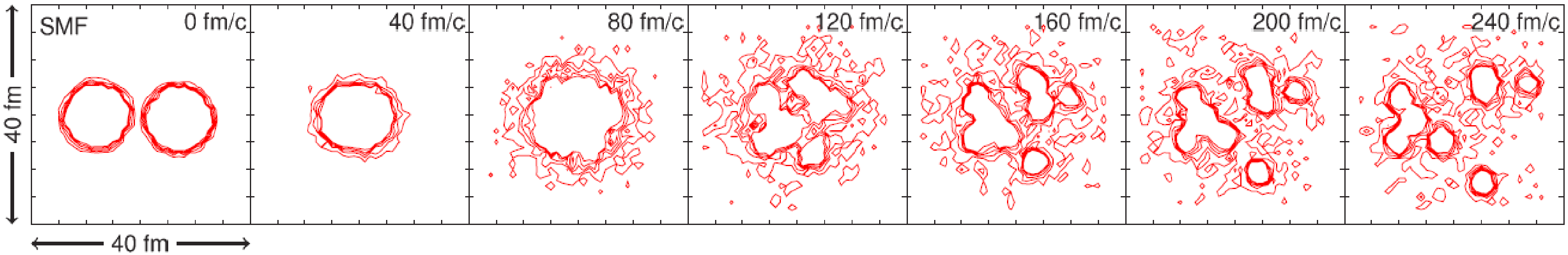

QMD-type (Antisymmetrized Molecular Dynamics)

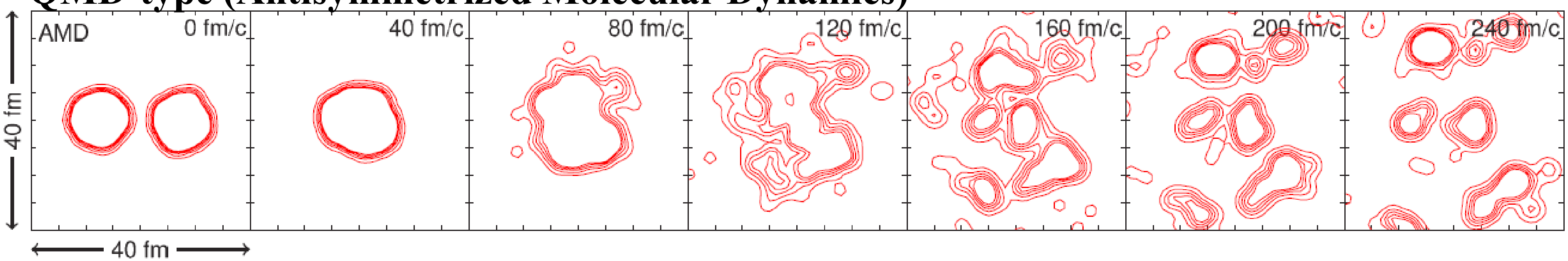

M. Colonna, A. Ono, and J. Rizzo, PRC 82, 054613 (2010)

SMF: more emitted nucleons
AMD: expansion faster